

Development of Pyruvate:ferredoxin Oxidoreductase Inhibitors for the Treatment of
Clostridium difficile Infection

Alexandra Marie Marshall
Batavia, New York

B.A. Chemistry, Colgate University, 2011

A Thesis Presented to the Graduate Faculty
of the University of Virginia in Candidacy for the Degree of
Master of Science

Department of Chemistry

University of Virginia
December, 2013

Abstract

Clostridium difficile is an anaerobic, Gram-positive bacillus that can be found in normal human intestinal flora. Toxigenic strains of *C. difficile* can lead to *C. difficile* infection (CDI), which has recently overtaken Methicillin-resistant *Staphylococcus aureus* (MRSA) as the most frequently diagnosed hospital-acquired infection (HAI). The expense of drug development and looming threat of microbial resistance has stifled the introduction of novel antibiotics and current modes of treatment have little success in reducing recurrence of infection.

Nitazoxanide (NTZ) is an FDA-approved antibiotic that is effective at treating and preventing the recurrence of CDI. NTZ inhibits bacterial growth by targeting pyruvate:ferredoxin oxidoreductase (PFOR), a metabolic enzyme in anaerobic bacteria that is responsible for the oxidative decarboxylation of pyruvate to form acetyl coenzyme A. It has been proposed that thiamine pyrophosphate (TPP), a coenzyme of PFOR, is inhibited by NTZ, presenting a novel therapeutic mechanism that could circumvent common modes of bacterial resistance. While effective against CDI, NTZ is not selective and lends itself to preventing complete recovery from infection.

The development of NTZ-based PFOR inhibitors is presented here, including the initial elucidation of the mechanism of action of NTZ in PFOR and the optimization of the nitrothiazolide scaffold to the lead inhibitor amixicile (AMX) that inspired subsequent scaffold modifications. A variety of structure activity relationship (SAR) studies of nitrothiazolides were performed and used in the design of AMX which was more soluble, potent and non-toxic than NTZ. A series of second-generation inhibitors was proposed using the favorable properties of AMX and docking studies using a

homology model based on the solved crystal structure of PFOR from *Desulfovibrio africanus* and the proposed mechanism of action of NTZ. The homology model was trained with PFOR inhibitors to predict the activity of additional NTZ derivatives.

The library of PFOR inhibitors presented here represents a promising breakthrough in an otherwise dismal field of drug discovery. Although nitrothiazolide antibiotics are more active at the PFOR enzyme, they still do not perform as well as NTZ in whole cells, indicating that further structural modifications must be made to the scaffold of AMX in order to achieve an optimal lead compound for *in vivo* testing.

To Mom and Dad, for all of the four-leaf clovers and lucky pennies

and

To Andy, for his patience, love and rationality

Contents

| | |
|------------------------|------|
| Abstract..... | i |
| Acknowledgements | iii |
| Contents | iv |
| Figures | vi |
| Schemes | viii |
| Tables..... | ix |
| Abbreviations..... | x |

Chapter 1: Antibiotics and Nitroreductive Compounds..... 1

| | |
|---|----|
| 1.1. Antibiotic Classes, their Benefits and Pitfalls | 1 |
| 1.1.1 Antibiotic Classes and Targets | 2 |
| 1.1.2 Antibiotic Resistance and the Emergence of Superbugs..... | 5 |
| 1.2 Nitroreductive Compounds | 8 |
| 1.2.1 Metronidazole | 9 |
| 1.2.2 DNA Damage from Nitroreduction | 10 |
| 1.2.3 Resistance to MTZ | 11 |
| 1.3 Conclusion..... | 12 |
| References | 14 |

Chapter 2: Nitazoxanide 16

| | |
|---|----|
| 2.1 Nitazoxanide Uses and Relevancy | 16 |
| 2.2 <i>Clostridium difficile</i> | 17 |
| 2.2.1 Pathogenesis of CDI | 19 |
| 2.2.2 Change in Epidemiology | 20 |
| 2.3 Nitazoxanide and <i>C. difficile</i> Infection..... | 21 |
| 2.4 Nitroreduction in Nitazoxanide | 23 |
| 2.5 Pyruvate:ferredoxin Oxidoreductase | 23 |
| 2.5.1 Overview of PFOR Function | 24 |
| 2.5.2 Thiamine Pyrophosphate | 26 |
| 2.6 Nitazoxanide Mechanism of Action | 27 |
| 2.7 Conclusion | 32 |
| References | 33 |

Chapter 3: Nitazoxanide Derivative Design and Discovery 37

| | |
|--|----|
| 3.1 Nitazoxanide-Based Inhibitor Discovery | 37 |
| 3.2 Head Region Analysis | 39 |
| 3.3 Tail Region Analysis | 43 |
| 3.3.1 Benzene Ring Substitution | 44 |

| | |
|---|----|
| 3.3.2 Heteroaromatic Tail Groups | 47 |
| 3.3.3 Full Biological Evaluation of Select Tail Region Analogues..... | 47 |
| 3.3.4 Solubilizing Moieties..... | 49 |
| 3.4 Amixicile | 52 |
| 3.4.1 <i>In vivo</i> Evaluation | 53 |
| 3.4.2 <i>In silico</i> Evaluation | 54 |
| 3.5 Conclusion | 55 |
| References | 58 |

Chapter 4: Pyruvate:ferredoxin Oxidoreductase Homology Models and Rational Design of Amixicile Analogues 59

| | |
|--|----|
| 4.1 Pyruvate:ferredoxin Oxidoreductase Homology Model..... | 59 |
| 4.2 Tail Length Analysis | 60 |
| 4.3 Linker Region Analysis | 63 |
| 4.4 Hybrid Molecules | 69 |
| 4.5 Conclusion | 70 |
| References | 73 |

Chapter 5: Experimentals..... 74

| | |
|-----------------------------|-----|
| 5.1 Biological Methods..... | 74 |
| 5.2 Chemical Synthesis..... | 75 |
| References | 131 |

Figures

| | | |
|--------------|---|----|
| 1.1. | Representative antibiotic structures and classes | 5 |
| 1.2. | Resistance acquisition mechanisms | 7 |
| 1.3. | Representative nitro drugs | 8 |
| 1.4. | Reduction of the NO ₂ group in MTZ by the PFOR enzyme system | 10 |
| 2.1. | Chemical structures of MTZ, NTZ and its active metabolite TZ | 17 |
| 2.2. | The risk of CDI after treatment with antibiotics..... | 18 |
| 2.3. | Pathogenesis of <i>C. difficile</i> and clinical outcome of CDI..... | 20 |
| 2.4. | Therapies for the treatment of CDI..... | 22 |
| 2.5. | Ribbon drawing of <i>Desulfovibrio africanus</i> PFOR (2.3 Å) | 24 |
| 2.6. | Pyruvate:ferredoxin oxidoreductase enzymatic reaction..... | 25 |
| 2.7. | Evolution of carbon dioxide from the PFOR enzymatic reaction | 28 |
| 2.8. | Remaining pyruvate in PFOR reaction with NTZ..... | 29 |
| 2.9. | Absorbance properties during pH titration of NTZ | 30 |
| 2.10. | NTZ mechanism of action | 31 |
| 3.1. | Inhibitor design from NTZ | 38 |
| 3.2. | Composition of library head groups and tail groups | 39 |
| 3.3. | Interaction between TPP and TZ anion | 40 |
| 3.4. | <i>C. difficile</i> infected mouse survival curves..... | 53 |
| 3.5. | NTZ docked in PFOR crystal structure | 54 |
| 3.6. | AMX presentation in the PFOR pocket..... | 55 |
| 4.1. | Inhibitor design from AMX..... | 61 |
| 4.2. | Proposed AMX analogues with benzene ring substitution..... | 64 |

| | | |
|-------------|--|----|
| 4.3. | <i>In silico</i> docking image of AMX in the PFOR pocket | 68 |
| 4.4. | Hybrid AMX analogues..... | 69 |

Schemes

| | | |
|-------------|---|----|
| 1.1. | Evolution of mutagenic nitro compounds | 11 |
| 2.1. | Mechanism of acetyl-CoA production at PFOR..... | 26 |
| 2.2. | Activation of thiamine pyrophosphate | 27 |
| 3.1. | Representative synthesis of compound library with varied head groups | 40 |
| 3.2. | Synthetic routes towards modified tail regions | 44 |
| 3.3. | Representative synthesis towards NTZ derivatives with solubilizing groups | 50 |
| 4.1. | Synthetic routes towards proposed AMX tail analogues..... | 62 |
| 4.2. | General synthetic plan towards AMX derivatives..... | 65 |
| 4.3. | Synthesis towards AMX hybrid molecules 4.18 and 4.19 | 70 |

Tables

| | | |
|-------------|---|----|
| 1.1. | Common antibiotic classes and their modes of action | 3 |
| 3.1. | MIC and percent PFOR inhibition values for head region analogues 3.3 and 3.4 compared to NTZ..... | 42 |
| 3.2. | Biological evaluation of mono- and di-substituted benzene ring analogues | 46 |
| 3.3. | Furan and thiophene analogues of NTZ and evaluation against <i>H. pylori</i> and <i>C.</i> <i>jejuni</i> | 47 |
| 3.4. | Evaluation of selected analogues against human foreskin cells and a summary of biological data..... | 48 |
| 3.5. | Biological evaluation of NTZ derivatives with solubilizing ether and aliphatic amine moieties in place of the 2-acetoxy group of NTZ | 51 |
| 3.6. | Summary of <i>in vitro</i> data for NTZ versus AMX | 53 |
| 4.1. | Percent direct enzyme inhibition of PFOR by tail region analogues | 63 |
| 4.2. | Biological evaluation of AMX analogues with EDG and EWG additions to the benzene linker region..... | 67 |

Abbreviations

| | |
|------------|--|
| 2AT | 2-amino-5-nitrothiazole |
| 9-BBN | 9-borabicyclo[3.3.1]nonane |
| AcOH | acetic acid |
| AMX | amixicile |
| Boc | <i>tert</i> -butyl carbamate |
| BV | benzyl viologen |
| CDAD | <i>Clostridium difficile</i> associated diarrhea |
| CDI | <i>Clostridium difficile</i> infection |
| CoA | coenzyme-A |
| DMAP | 4-dimethylaminopyridine |
| DMF | dimethylformamide |
| DMSO | dimethyl sulfoxide |
| dppf | 1,1'-bis(diphenylphosphino)ferrocene |
| EDC | 1-Ethyl-3-(3-dimethylaminopropyl)carbodiimide |
| EDG | electron donating group |
| Et | ethyl |
| EtOAc | ethyl acetate |
| EWG | electron withdrawing group |
| Fd | ferredoxin |
| HAI | hospital-acquired infection |
| HGT | horizontal gene transfer |
| HOBt | N-hydroxybenzotriazole |
| i-Pr | isopropyl |
| LDH | lactate dehydrogenase |
| <i>m</i> - | <i>meta</i> - |
| MDR | multi-drug resistant |
| Me | methyl |
| MIC | minimum inhibitory concentration |
| MOE | molecular operating environment |
| MRSA | methicillin-resistant <i>Staphylococcus aureus</i> |
| MTZ | metronidazole |
| NAD | nicotinamide adenine dinucleotide |
| NADPH | nicotinamide adenine dinucleotide phosphate |
| NAP1 | North American pulsed-field type 1 |
| NTZ | nitazoxanide |
| <i>o</i> - | <i>ortho</i> - |
| <i>p</i> - | <i>para</i> - |
| PDH | pyruvate dehydrogenase |
| PFOR | pyruvate:ferredoxin oxidoreductase |
| PyBOP | benzotriazol-1-yl-oxytripyrrolidinophosphonium hexafluorophosphate |
| SAR | structure-activity relationship |
| t-Bu | <i>tert</i> -butyl |
| TcdA | <i>C. difficile</i> cytotoxin A |
| TcdB | <i>C. difficile</i> cytotoxin B |

| | |
|-----|----------------------------------|
| TEA | triethylamine |
| TFA | trifluoroacetic acid |
| THF | tetrahydrofuran |
| TPP | thiamine pyrophosphate |
| TZ | tizoxanide |
| VRE | vancomycin resistant enterococci |
| XDR | extensively drug-resistant |

Development of Pyruvate:ferredoxin Oxidoreductase Inhibitors for the Treatment of *Clostridium difficile* Infection

Alexandra Marshall

1

Antibiotics and Nitroreductive Compounds

The propensity of any organism to endure environmental stress is a vital factor of survival. Therapeutics are designed with this in mind. In the case of antibiotics, the medicinal chemist is challenged with the task of creating a drug that is tolerated by the host but lethal to the organism living within it. This unique scenario is made even more difficult by the threat of antibiotic resistance. There are a select few popular targets for antibacterials, all of which are susceptible to resistance mechanisms. By placing evolutionary pressure on microorganisms through human administration of antibiotics, the rate of resistance is growing by the day, threatening the advancements of modern medicine.

1.1 Antibiotic Classes, their Benefits and Pitfalls

The birth of antibiotic chemotherapy in the 20th century revolutionized modern medicine, creating a strategic method to combat invading organisms in the human body. The concept of a “magic bullet,” wherein a poison is selectively delivered to a target organism, spawned a new era of drug discovery that started with the rapid development of antimicrobials. The decades following the dawn of antibiotics brought about a

“Golden Age” that spawned many of the families of therapeutics still used today. Between 1955 and 1985, 100 drugs went into clinical trials, producing 60 new approved antibiotics.¹

Like all other organisms, bacteria adjust to their surroundings to survive. As a result, antibiotic resistance is inevitable. The first cases of penicillin resistance were reported within a decade of its introduction to the marketplace, generating a new need for a drug that treated the same indication.² This trend has been consistent with all major classes of antibiotics. Bacterial infections are a major world health concern, and antimicrobials are becoming more widely dispersed and strains more resistant. The expense of drug development and looming threat of swift resistance has stifled the introduction of novel antibiotics to combat this emerging dilemma.²⁻⁵

1.1.1 Antibiotic Classes and Targets

The development of antibiotics dates back to as early as the 1400s when heavy metals were used to treat syphilis (*Treponema palladium*). Salvarsan, an arsenic compound developed by Paul Ehrlich, was the first “bullet” of its kind, transforming how medicine was developed and administered around the world. The first nonmetal antibiotics came from excretions of other microbes. Drugs were identified based on their ability to inhibit bacterial growth until target-based screening was developed in the 1960s.⁶ Since then, there have only been a few new classes of antibiotics developed. All other drugs on the market today are known as “me too” compounds based on the same chemical scaffolds introduced in the early development of antibiotics.⁵

Antibiotics are a unique class of medicine, targeting those biochemical processes that are not in common with humans. As a result the drugs have to withstand different biological barriers than a typical therapeutic. Most drugs or compounds in screening libraries are intended for targets in humans and follow the typical rules of small molecule drug discovery. Thus there is limited chemical diversity available to discover new antimicrobials, which do not need to follow these rules. Furthermore, antibiotics should target pathways or mechanisms that are unsusceptible to resistance, adding to the challenge of drug discovery and development.

| Antibiotic Class | Example | Target |
|-------------------------|------------------|----------------------------|
| β -Lactams | Penicillins | Peptidoglycan biosynthesis |
| Aminoglycosides | Gentamicin | Translation |
| Glycopeptides | Vancomycin | Peptidoglycan biosynthesis |
| Tetracyclines | Minocycline | Translation |
| Macrolides | Erythromycin | Translation |
| Lincosamides | Clindamycin | Translation |
| Streptogramins | Synercid | Translation |
| Oxazolidinones | Linezolid | Translation |
| Phenicol | Chloramphenicol | Translation |
| Quinolones | Ciprofloxacin | DNA replication |
| Pyrimidines | Trimethoprim | C ₁ metabolism |
| Sulfonamides | Sulfamethoxazole | C ₁ metabolism |
| Rifamycins | Rifampin | Transcription |
| Lipopeptides | Daptomycin | Cell membrane |
| Cationic peptides | Colistin | Cell membrane |

Table 1.1. Common antibiotic classes and their modes of action.⁴

The major classes of antibiotics, as well as their uses and targets are listed in Table 1.1.⁴ Antibiotic targets differ based on the characteristics of the bacterial cell. A common therapeutic target is the peptidoglycan layer, a protective polymer that resides outside of the bacterial cell wall. Gram-positive bacteria have a thick peptidoglycan layer that maintains the Gram stain.^{7,8} Additionally, antibiotics can interfere with different aspects of protein biosynthesis in bacteria by binding to the ribosome and inhibiting translation or disrupting communication between DNA and RNA.⁹⁻¹²

Drugs like β -lactams (penicillins) and glycopeptides (vancomycin) interfere with the synthesis of the peptidoglycan layer, making cells unable to reproduce or withstand osmotic pressure in the cytoplasm (Figure 1.1). Specifically, β -lactams disrupt catalytic cycles at the end of peptidoglycan biosynthesis, preventing glycan cross-linking.^{7,8} Vancomycin and other glycopeptides inhibit polymerization and cross-linking by binding to substrates of enzymes like transglycosylases and transpeptidases.⁸

Antimicrobials like aminoglycosides, macrolides and oxazolidinones all target different aspects of protein biosynthesis in bacteria. Macrolides and oxazolidinones do this by inhibiting the bacterial ribosome from carrying out translation (Figure 1.1).^{9,10} Quinolones and rifamycins interfere with communication between DNA and RNA. Fluoroquinolones like ciprofloxacin form complexes with DNA and bacterial topoisomerases, crucial enzymes for maintaining the proper DNA topology that is required for protein biosynthesis and DNA repair and replication.¹¹ Furthermore, rifamycins inhibit DNA-dependent RNA polymerase by binding to the enzyme in the initiation phase of RNA synthesis.¹² Although these are successful mechanisms of bacterial cytotoxicity, they are also easily evaded by bacteria.

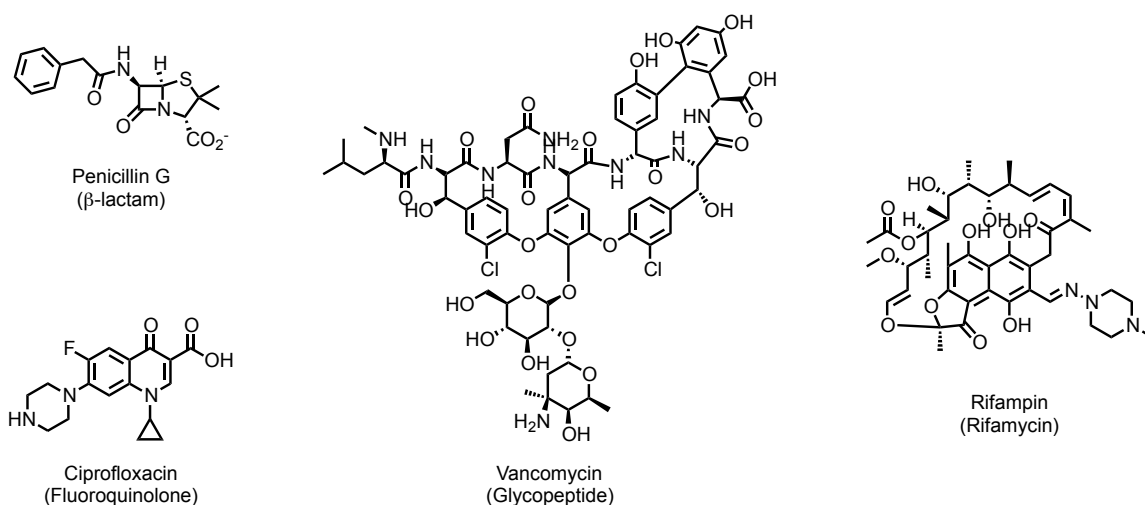


Figure 1.1. Representative antibiotic structures and classes.

1.1.2 Antibiotic Resistance and the Emergence of Superbugs

Antibiotics inherently lend themselves to resistance as a result of their selectivity. By targeting susceptible organisms, less susceptible bacteria that were once the minority in a population become the dominant group as the drug kills the weaker cells. Simply put, the use of antibiotics breeds resistance.

The threat of a post-antibiotic era, wherein society is left to deal with infections as though antibiotics never existed, is very real. A 2012 report by Dr. Margaret Chan of the World Health Organization describes the severity of this issue: “A post-antibiotic era means, in effect, an end to modern medicine as we know it. Things as common as strep throat or a child’s scratched knee could once again kill.”³ Multi-drug resistant (MDR) and extensively drug-resistant (XDR) strains have been dubbed “superbugs,” possessing multiple mutations that lead to increased morbidity and mortality.⁴ A majority of U.S. hospital-acquired infections (HAIs) are caused by the ESKAPE pathogens: *Enterococcus faecium*, *Staphylococcus aureus*, *Klebsiella pneumonia*, *Acinetobacter baumannii*,

Pseudomonas aeruginosa and *Enterobacter* species, as they are able to circumvent the effects of most antibiotics.¹³ One of the more notorious pathogens, methicillin-resistant *S. aureus* (MRSA), causes ~19,000 U.S. deaths every year – more than HIV/AIDS and tuberculosis combined.^{1,13} Antibiotic resistance costs U.S. hospitals over \$20 billion per year, suggesting a growing and lucrative market for pharmaceutical companies.¹⁴ Unfortunately, most companies have eliminated antibiotic programs altogether due to rapid drug resistance.

Bacteria utilize three major mechanisms of resistance to stave off antibiotics: enzyme modification of the antibiotic, efflux through transmembrane pumps and alteration of drug targets.^{6,15,16} The rate of antibiotic resistance is dependent upon the rates of mutation and horizontal gene transfer (HGT), wherein resistance determinants can be transferred by cell-to-cell conjugation, transformation by DNA released by dead cells, or transduction (Figure 1.2).¹⁶ Most mechanisms of resistance that are of major concern are the result of these events.⁶ Overuse of antibiotics allows for these resistant traits to be transferred rapidly without containment, leading to the epidemics seen in many healthcare facilities today.

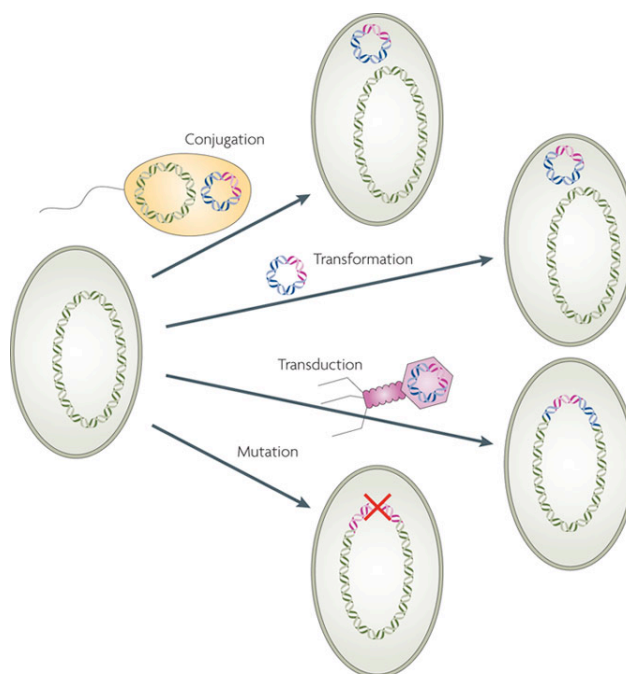


Figure 1.2. Resistance acquisition mechanisms. DNA containing an antibiotic resistance gene (pink) can be transferred to other bacteria cells via HGT through three paths: cell-to-cell conjugation, transformation, or transduction. *De novo* mutations (red cross) can also lead to antimicrobial resistance. Reused from reference 16 with permission of the publisher.

Resistance plagues most major classes of antibiotics (Table 1.1). In the case of penicillins, β -lactamase enzymes hydrolyze the drug, making it ineffective.⁷ Vancomycin resistant enterococci (VRE) avoid antibiotics by lowering the target susceptibility through reprogramming.⁸ Erythromycin resistance arises from reduced drug binding due to ribosome modifications and efflux of antibiotic.⁹ The ability of microorganisms to curtail the effects of antimicrobials quickly extinguishes the usefulness of common targets, creating a constant need for new avenues to disrupt bacterial biological pathways.

1.2 Nitroreductive Compounds

In the case of the research presented here, nitro-drugs are of utmost interest. Nitro antibiotics include a variety of compounds with nitro-substituted heterocycles as displayed in Figure 1.3. The most common antimicrobial of this kind is metronidazole (MTZ), a 5-nitroimidazole compound that acts as a prodrug to treat a wide therapeutic spectrum spanning from protozoa to Gram-positive and Gram-negative bacteria.¹⁷ The main aspects of these compounds that are responsible for their therapeutic activity are their selectivity and cytotoxicity for anaerobic organisms.¹⁸ The mechanism by which these agents kill pathogens is closely related to their common nitro substituent.

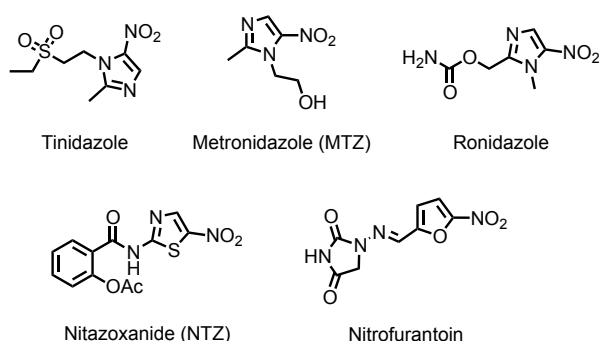


Figure 1.3. Representative nitro drugs.

5-nitroimidazoles like MTZ are redox-active prodrugs, meaning that they are inactive in the body until they undergo reduction in drug metabolism.¹⁹ Redox-active enzymes in anaerobes like pyruvate/ketoacid oxidoreductases and hydrogenase reduce the nitro group, producing mutagenic compounds that have cytotoxic effects.^{19,20} The rapid reduction of nitro drugs in anaerobes decreases intracellular concentration of the unreduced compound, pushing the concentration gradient to favor drug uptake.¹⁸

1.2.1 Metronidazole

Metronidazole (Flagyl; 1-(2-hydroxyethyl)-2-methyl-5-nitroimidazole, MTZ, Figure 1.3) has broad-spectrum activity against Gram-positive and Gram-negative bacteria as well as protozoa. It is specific to anaerobic or microaerophilic organisms, making MTZ a versatile antibiotic with the ability to selectively kill anaerobic, non-host cells. It was first developed to treat *Trichomonas vaginalis* infections but has since been used for a variety of indications. MTZ is used against *Helicobacter pylori*, a microaerophilic bacteria that is the major cause of peptic ulcer disease.¹⁹ It is also the first line of therapy to treat *Clostridium difficile* associated diarrhea (CDAD).²¹ The cytotoxic properties of MTZ originate from the nitro group.

Nitroimidazoles like MTZ are activated through reduction of the nitro moiety. In the case of MTZ, the prodrug is believed to be activated to its toxic state by accepting electrons from ferredoxin (Fd), an iron-sulfur protein responsible for electron transfer in metabolic reactions. Compounds like nitrofurans (nitrofurazone, nitrofurantoin and furazolidone) have high redox potentials, meaning that they are easily activated by a number of enzymes such as the NAD(P)H reductases in enteric bacteria.²² The selectivity of MTZ for anaerobic organisms is due to the relatively low redox potential of the 5-nitro group that can only be reduced by anaerobic enzymes like pyruvate:ferredoxin oxidoreductases (PFOR) and hydrogenases (Figure 1.4).²² This initial activation step is the beginning of a series of reduction steps that produce toxic radical compounds.

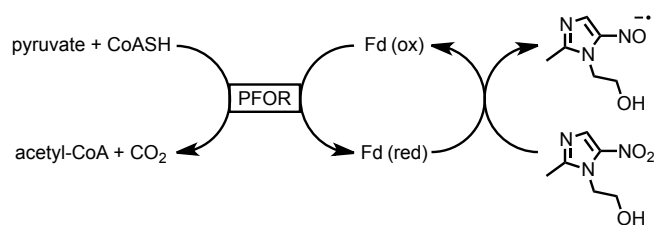
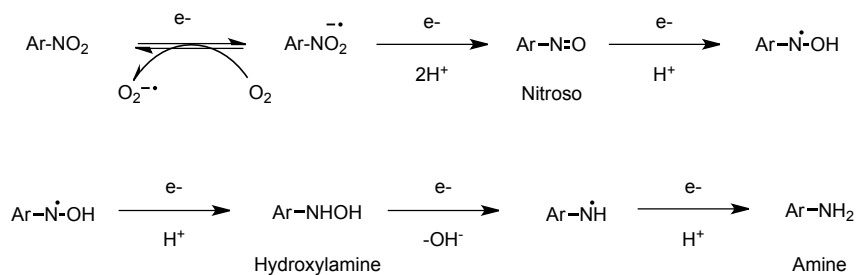


Figure 1.4. Reduction of the NO_2 group in MTZ by the PFOR enzyme system. Acetyl-CoA and CO_2 are the products of the PFOR metabolic reaction, wherein ferredoxin (Fd) acts as an electron acceptor. Normally, NADP oxidases or hydrogenases oxidize the reduced Fd at the end of the enzymatic cycle, however nitroimidazoles like MTZ interrupt this reaction by accepting electrons from the reduced Fd. This electron transfer reduces the nitro group of MTZ to the cytotoxic nitroso radical (right).²²

It is believed that the corresponding nitroso radical is responsible for the cytotoxicity of MTZ (Figure 1.4). This can be produced via several different pathways. The PFOR enzyme found in anaerobic bacteria, which carries out oxidative pyruvate decarboxylation, can transfer electrons to MTZ via ferredoxins as shown in Figure 1.4. Additionally, as is the case in *H. pylori*, nitroreductase enzymes like RdxA can reduce the nitro group and form toxic radicals.^{19,22} The RdxA-catalyzed reduction of MTZ takes place through a two-step, four-electron reduction to first the nitroso and then hydroxylamine products.¹⁹ Regardless of the process by which MTZ is reduced, the active products have damaging effects on DNA.

1.2.2 DNA Damage from Nitroreduction

The target of nitroimidazole antibiotics is DNA. The products of nitro reduction are notorious compounds that are known for their mutagenic effects on DNA. For this reason, nitro substituents are “alarm groups” to medicinal chemists.^{23,24} Aromatic nitro groups follow common mechanisms that lead to mutagenicity. A simplified version of this route is shown in Scheme 1.1.²³



Scheme 1.1. Evolution of mutagenic nitro compounds.²³

Arylamines, nitroarenes, and nitrosoarenes can become aryl hydroxylamines, which are known to conjugate with acetate or sulfate and decompose to the aryl nitrenium ion. This ion can interact with DNA in humans, causing mutagenicity (Scheme 1.1).²³ For this reason, nitro groups are avoided in common therapeutics. In the case of MTZ and other nitro antimicrobials, this is an attractive way of targeting pathogens. Since the drug is targeting the biological pathways of the microorganism within a human, these “alarm groups” can be used to specifically alter the DNA of invading cells without risking the health of host cells. The products of MTZ reduction cause DNA damage and mutation. Reduced nitroimidazoles lead to single- and double-strand breakage as well as helix destabilization.^{19,20,25} Although useful, this mechanism of action lends itself to resistance mechanisms and poses a threat to host cells.

1.2.3 Resistance to MTZ

Resistance to MTZ is increasing in anaerobic and microaerophilic organisms. In *Helicobacter pylori*, resistance genes have been identified that produce loss-of function mutations in RdxA, the nitroreductase responsible for MTZ activation in these microaerophilic bacteria.¹⁹ In the case of *C. difficile*, resistance is increasing although not a significant problem. The mutagenic characteristics of MTZ could be inducing the

formation of resistance pathways, leading to recurrence of infection.^{26,27} The emergence of MTZ resistance is alarming and indicative of the fact that no pathway is safe from the survival strategies of microorganisms.

Nitazoxanide (NTZ) is a nitrothiazole antibiotic that is similar in structure to MTZ and is active against anaerobic bacteria and *H. pylori* like MTZ (Figure 1.3). These characteristics all suggest that NTZ shares the same mechanism of action of MTZ, however NTZ has shown activity against MTZ-resistant strains of *H. pylori*. NTZ has been shown to be reduced by NADPH nitroreductases and PFOR however NTZ is not mutagenic like MTZ.¹⁹ This data indicates that NTZ may have an alternative mechanism of action than MTZ that allows for a similar therapeutic spectrum to be reached, however further research is required to adequately investigate this possibility.

1.3 Conclusion

The rapid rate of bacterial resistance has brought about a global health crisis. Traditional antibiotics and their targets are no longer reliable, and the more that humans administer these drugs, the more bacteria become less susceptible to their mechanisms of action. There are a variety of ways that microorganisms have been able to avoid the effects of antibiotics, leaving drug developers at a medicinal crossroads. Scaffolds of classic antibiotics have been exhausted and therapeutic treatments require doctors to turn to harsh compounds as a last resort, as hospitals are teeming with infections and superbugs that cannot be treated with available antibiotics. The world is facing a fate in which everyday infections become lethal and no drug will be available to successfully kill these bugs.

Nitro-drugs are an interesting class of antibiotics that have a unique mechanism of action. Reduction of the nitro group, an alarming substituent to have on typical small molecules, can give reactive nitrogen species that are mutagenic and damage bacterial DNA. Metronidazole is an example of these compounds, showing a wide range of activity against anaerobic and microaerophilic organisms. Although MTZ is effective, resistance to the drug is quickly becoming a problem in healthcare facilities for the treatment of infections caused by *H. pylori* and *C. difficile*. Nitrothiazole (NTZ) is a nitro drug that is structurally similar to MTZ, but studies suggest that it has a different mechanism of action. Perhaps NTZ will provide an alternative means to kill those anaerobes previously eradicated by MTZ. The research presented here explores this possibility and the means to exploit a novel therapeutic mechanism in order to evade antibiotic resistance.

References

1. Shlaes, D.; SpringerLink ebooks - Biomedical and Life Sciences. *Antibiotics*; Springer: New York, 2010.
2. Hogberg, L. D.; Heddini, A.; Cars, O. The global need for effective antibiotics: challenges and recent advances. *Trends Pharmacol. Sci.* **2010**, *31*, 509-515.
3. Chan, M. World Health Organization. *Antimicrobial resistance in the European Union and the world*. Presented at Combating antimicrobial resistance: time for action, Copenhagen, Denmark, March 14, 2012; World Health Organization Web Site. (accessed November 11, 2012).
4. Davies, J.; Davies, D. Origins and evolution of antibiotic resistance. *Microbiol. Mol. Biol. Rev.* **2010**, *74*, 417-433.
5. Fischbach, M. A.; Walsh, C. T. Antibiotics for emerging pathogens. *Science* **2009**, *325*, 1089-1093.
6. Silver, L. L. Challenges of antibacterial discovery. *Clin. Microbiol. Rev.* **2011**, *24*, 71-109.
7. Fisher, J. F.; Meroueh, S. O.; Mobashery, S. Bacterial Resistance to β^2 -Lactam Antibiotics: Compelling Opportunism, Compelling Opportunity. *Chem. Rev.* **2005**, *105*, 395-424.
8. Kahne, D.; Leimkuhler, C.; Lu, W.; Walsh, C. Glycopeptide and Lipoglycopeptide Antibiotics. *Chem. Rev.* **2005**, *105*, 425-448.
9. Katz, L.; Ashley, G. W. Translation and Protein Synthesis: Macrolides. *Chem. Rev.* **2005**, *105*, 499-528.
10. Mukhtar, T. A.; Wright, G. D. Streptogramins, Oxazolidinones, and Other Inhibitors of Bacterial Protein Synthesis. *Chem. Rev.* **2005**, *105*, 529-542.
11. Mitscher, L. A. Bacterial Topoisomerase Inhibitors: Quinolone and Pyridone Antibacterial Agents. *Chem. Rev.* **2005**, *105*, 559-592.
12. Floss, H. G.; Yu, T. Rifamycin: Mode of Action, Resistance, and Biosynthesis. *Chem. Rev.* **2005**, *105*, 621-632.
13. Boucher, H. W.; Talbot, G. H.; Bradley, J. S.; Edwards, J. E., Jr.; Gilbert, D.; Rice, L. B.; Scheld, M.; Spellberg, B.; Bartlett, J. Bad Bugs, No Drugs: No ESKAPE! An Update from the Infectious Diseases Society of America. *Clin. Infect. Dis.* **2009**, *48*, 1-12.
14. Cooper, M. A.; Shlaes, D. Fix the antibiotics pipeline. *Nature* **2011**, *472*, 32.
15. Walsh; Wright Introduction: Antibiotic Resistance. *Chem. Rev.* **2005**, *105*, 391-394.
16. Andersson, D. I.; Hughes, D. Antibiotic resistance and its cost: is it possible to reverse resistance? *Nat Rev Micro* **2010**, *8*, 260-271.
17. Freeman, C. D.; Klutman, N. E.; Lamp, K. C. Metronidazole. *Drugs* **1997**, *54*, 679-708.
18. Lindmark, D. G.; Müller, M. Antitrichomonad Action, Mutagenicity, and Reduction of Metronidazole and Other Nitroimidazoles. *Antimicrob. Agents Chemother.* **1976**, *10*, 476-482.

19. Sisson, G.; Jeong, J.; Goodwin, A.; Bryden, L.; Rossler, N.; Lim-Morrison, S.; Raudonikiene, A.; Berg, D. E.; Hoffman, P. S. Metronidazole Activation Is Mutagenic and Causes DNA Fragmentation in *Helicobacter pylori* and in *Escherichia coli* Containing a Cloned *H. pylori* rdxA (Nitroreductase). *Gene. J. Bacteriol.* **2000**, *182*, 5091-5096.
20. Zahoor, A.; Lafleur, M. V. M.; Knight, R. C.; Loman, H.; Edwards, D. I. DNA damage induced by reduced nitroimidazole drugs. *Biochem. Pharmacol.* **1987**, *36*, 3299-3304.
21. Gould, C. V.; McDonald, L. C. Bench-to-bedside review: *Clostridium difficile* colitis. *Crit. Care* **2008**, *12*, 203-210.
22. Leitsch, D.; Burgess, A. G.; Dunn, L. A.; Krauer, K. G.; Tan, K.; Duchêne, M.; Upcroft, P.; Eckmann, L.; Upcroft, J. A. Pyruvate:ferredoxin oxidoreductase and thioredoxin reductase are involved in 5-nitroimidazole activation while flavin metabolism is linked to 5-nitroimidazole resistance in *Giardia lamblia*. *J. Antimicrob. Chemother.* **2011**, *66*, 1756-1765.
23. Rydzewski, R. M. *Real World Drug Discovery A Chemist's Guide to Biotech and Pharmaceutical Research*; Elsevier: Oxford, 2008; pp 460-461.
24. Kazius, J.; McGuire, R.; Bursi, R. Derivation and validation of toxicophores for mutagenicity prediction. *J. Med. Chem.* **2005**, *48*, 312-320.
25. Lockerby, D. L.; Rabin, H. R.; Laishley, E. J. Role of the phosphoroclastic reaction of *Clostridium pasteurianum* in the reduction of metronidazole. *Antimicrob. Agents Chemother.* **1985**, *27*, 863-867.
26. Huang, H.; Weintraub, A.; Fang, H.; Nord, C. E. Antimicrobial resistance in *Clostridium difficile*. *Int. J. Antimicrob. Agents* **2009**, *34*, 516-522.
27. Louie, T. J.; Miller, M. A.; Mullane, K. M.; Weiss, K.; Lentnek, A.; Golan, Y.; Gorbach, S.; Sears, P.; Shue, Y. Fidaxomicin versus vancomycin for *Clostridium difficile* infection. *N. Engl. J. Med.* **2011**, *364*, 422-431.

2

Nitazoxanide

2-((5-Nitrothiazol-2-yl)carbamoyl)phenyl acetate, or nitazoxanide (NTZ), was first described as a cestocidal drug in 1984.^{1,2} Since then, it has shown to have *in vitro* activity against a number of protozoa, bacteria and helminthes.³ NTZ is unique in its mechanism of action which gives it an advantage over common therapeutics and lowers the chance of resistance. Its broad-spectrum activity, combined with its mechanism of action, makes NTZ a promising drug in the war on antibiotics.

2.1 Nitazoxanide Uses and Relevancy

NTZ is a derivative of nitrothiazolyl-salicylamide and has a structure similar to that of metronidazole (MTZ) (Figure 2.1). NTZ acts as a prodrug, undergoing hydrolysis after absorption in the gut to form the active metabolite tizoxanide (TZ). This reaction occurs so quickly that NTZ is not detected in plasma (Figure 2.1).^{3,4,6} NTZ is poorly soluble and concentrates in the gut. As a result ~1 g/day is required for treatment.³

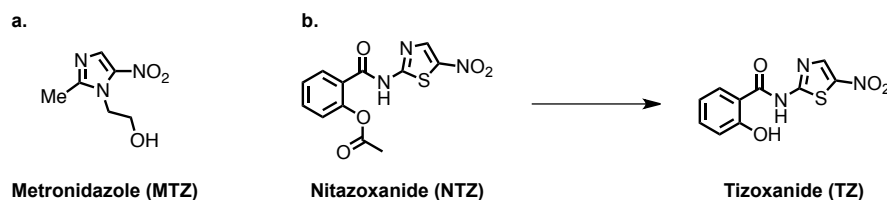


Figure 2.1. Chemical structures of MTZ (a), NTZ and its active metabolite TZ (b). The 2-acetoxy group of NTZ is hydrolyzed to the hydroxy group of TZ after absorption in the gut.

Nitazoxanide was approved by the Food and Drug Administration (FDA) in 2002 for the treatment of diarrhea caused by *Giardia lamblia* and *Cryptosporidium parvum* (Figure 2.1).²⁻⁵ It was the first FDA-approved treatment for *Giardia* infection in over 40 years and the very first treatment for *Cryptosporidium* infection.⁵ Beyond its approved indications, NTZ has been reported to be effective against a broad range of microorganisms in humans, including *Entamoeba histolytica*, *Cyclospora cayetanensis*, *Trichomonas vaginalis*, *Vitiforma corneae*, *Encephalitozoon intestinalis*, *Isospora belli*, *Blastocystis hominis*, *Balantidium coli*, *Enterocytozoon bieneusi*, *Ascaris lumbricoides*, *Trichuris trichura*, *Taenia saginata*, *Hymenolepis nana*, and *Fasciola hepatica*.⁵⁻¹² Studies have also shown that NTZ is active against both gram-negative and gram-positive bacteria like *Bacteroides*, *Clostridium* species and *Helicobacter pylori*.^{3,5,12,13} The broad-spectrum activity of NTZ gives it the potential to have a major impact on the antibiotic front.

2.2 *Clostridium difficile*

Although NTZ is approved for only two indications, its activity against other microorganisms makes it an appealing alternative to current therapeutics. NTZ is effective against *Clostridium difficile*, an anaerobic, Gram-positive bacillus that can be found in normal human intestinal flora. Toxigenic strains of *C. difficile* can lead to *C.*

difficile infection (CDI), which results in an array of potentially fatal symptoms: intestinal inflammation, severe diarrhea, dehydration, kidney failure, bowel perforation and toxic megacolon. CDI affects patients who have been treated with broad-spectrum antibiotics. These individuals lack normal intestinal microflora, allowing for the colonization of *C. difficile* (Figure 2.2).¹⁴

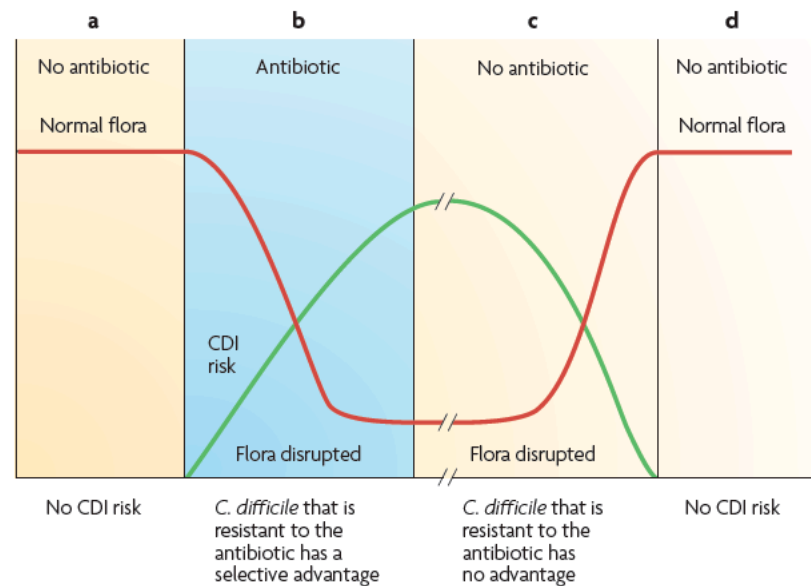


Figure 2.2. The risk of CDI after treatment with antibiotics. a) Before antibiotic treatment, gut flora levels are high, preventing toxigenic strains of *C. difficile* from colonizing. b) Initiation of antibiotic treatment disrupts the levels of normal flora in the gut, significantly increasing the patient's risk of CDI. c) Once antibiotic treatment ceases, the patient's risk remains until normal flora is regenerated (d). Reused from reference 14 with permission of the publisher.

Patients who have been treated with broad-spectrum antimicrobials such as cephalosporins, fluoroquinolones and clindamycin are vulnerable to toxigenic strains of *C. difficile* (Figure 2.2).¹⁵ Once treatment begins, protective flora in the gut is destroyed, increasing the risk of CDI (Figure 2.2b). This risk is even greater if the strain of *C. difficile* is resistant to the particular antibiotic that is administered to the patient. The risk of CDI remains even after treatment ends and does not subside until flora levels are back to normal (Figure 2.2c, d). Recurrence of infection is becoming a greater problem due to resistant strains of *C. difficile* and the detrimental effect that broad-spectrum antibiotics

can have on recovery. If the therapeutics that are being used to treat CDI are also active against microorganisms that make up the microbiota of the gut, regeneration takes longer and CDI persists. If, however, the treatment is selective for *C. difficile*, antibiotics can be used to combat, not prolong, the infection.¹⁴

2.2.1 Pathogenesis of CDI

C. difficile can only accumulate in the gut after the normal gut microflora have been disturbed. Spores of infectious *C. difficile* spores travel mainly through contact with health care workers who have touched a contaminated surface. Patients whose microflora are disrupted by antibiotics are susceptible to toxigenic strains of *C. difficile*.^{14,16,17} Toxigenic spores are able to pass through the acidic environment of the gut and reach the intestine (colon). Here, the spores release two cytotoxins A and B (TcdA and TcdB) which bind to epithelial cells in the colon and are endocytosed, causing hemorrhaging and opening tight junctions between cells.²² The release of tumor necrosis factor-alpha induces an immune response and the formation of a pseudomembrane and inflammation (Figure 2.3).^{14,22-25}

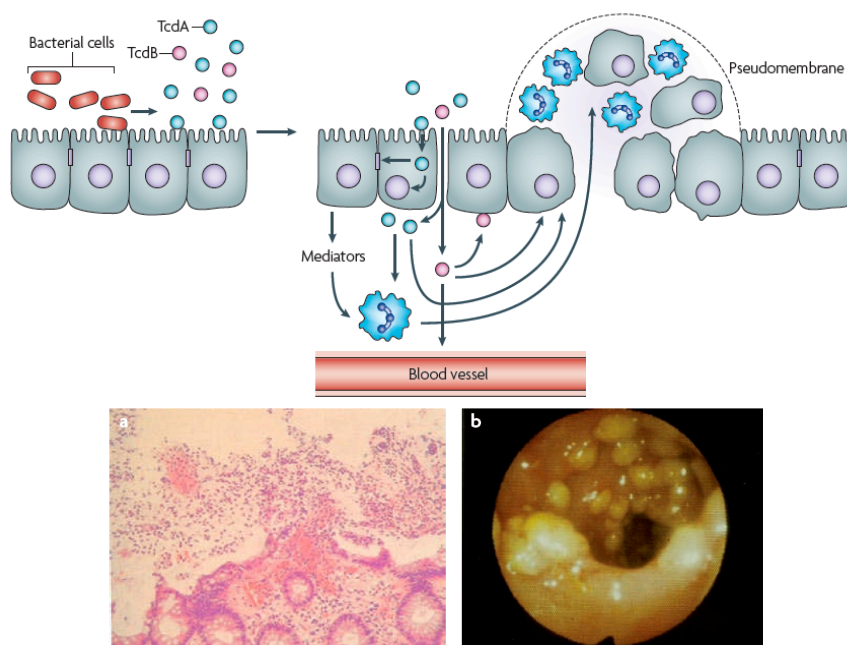


Figure 2.3. Pathogenesis of *C. difficile* (top) and clinical outcome of CDI (bottom). Colonization after treatment with antibiotics allows for cytotoxins A and B (TcdA, TcdB, top) to be released and infiltrate the epithelial cells, eliciting an immune response that forms pseudomembrane from the destroyed cells (a and b, bottom). Reused from reference 14 with permission of the publisher.

2.2.2 Change in Epidemiology

The landscape of hospital-acquired infections (HAI) has changed over the past decade. Since 2000, the diagnosis rates and severity of CDI have increased dramatically worldwide. A study done by Miller et al. showed that CDI is now the most commonly diagnosed HAI in the U.S., surpassing methicillin-resistant *Staphylococcus aureus* (MRSA).¹⁸ The prevalence of CDI can be attributed to two factors: major overhauls in hospital protocol combating MRSA and the emergence of hypervirulent strains of *C. difficile*.^{14,18} The most notorious strain is the North American pulsed-field type 1 (NAP1, or NAP1/BI/027), also known as ribotype 027.^{14,16} From 1984 to 1993, ribotype 027 accounted for less than 0.02% of U.S. strains of CDI, a number that swelled to 51% from 2000 to 2003.^{16,19,20} This ascendancy is due largely in part to the strain's resistance to first-line therapeutics like fluoroquinolones and a lack of proper practices in hospitals and

long-term care facilities.^{16,21} New antibiotics with a narrow therapeutic spectrum are required in order to fight hypervirulent strains and prevent recurrence of CDI.

2.3 Nitazoxanide and *C. difficile* Infection

The primary therapeutic protocol for CDI is to terminate administration of the antimicrobial that precipitated the infection. Additional treatment is required if infection persists after antibiotics have been discontinued (Figure 2.2). The two primary antibiotics prescribed for first-line treatment of CDI are MTZ and oral vancomycin (Figure 2.4).¹⁵ These are no longer sufficient for treating the infection. MTZ is greatly absorbed by the host, meaning that larger amounts of drug are required to reach the site of infection in the colon. MTZ resistance is increasing and thought to be due to nitroimidazole genes, reduced uptake or reduced nitroductase activity.²⁶ This resistance causes higher recurrence rates when the infection is treated with MTZ versus vancomycin.²⁷ In severe cases of CDI, the vancomycin cure rate (97%) is much greater than MTZ.^{15,28,29} Despite this data, vancomycin treatment inhibits regrowth of microflora in the gut, allowing *C. difficile* colonization to persist.^{27,30}

Recurrence and reinfection of CDI is a major concern in healthcare facilities. After treatment with MTZ or vancomycin, 20 – 30% of patients relapse within 60 days and about one-third of these patients who have been retreated with first-line therapeutics have an additional recurrence.^{27,29} Fidaxomicin is a new, narrow-spectrum antimicrobial that is effective at treating severe cases of CDI, stops recurrence better than vancomycin but does not completely prevent reinfection.²⁷ The selectivity of fidaxomicin gives it an

advantage over common therapeutics however the threat of recurrence and thus the need for a better antibiotic to treat CDI remains.

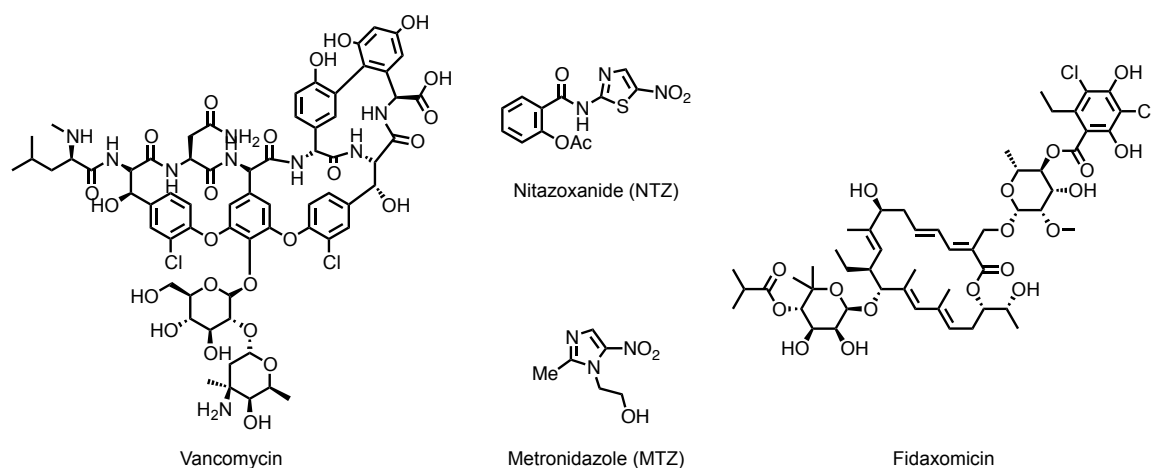


Figure 2.4. Therapeutics for the treatment of CDI. Metronidazole (MTZ) and vancomycin are the most common antibiotics. Fidaxomicin surpasses vancomycin in reducing recurrence of CDI. Nitazoxanide (NTZ) is as effective initially as fidaxomicin but is better at preventing recurrence and reinfection.^{1,3,31-33}

Nitazoxanide is effective against CDI, though it is not a common treatment.³¹ In a randomized, double-blind study of patients with CDI, NTZ was as effective as MTZ at treating infection.^{15,34} NTZ is also active against bacteria strains that are resistant to MTZ, indicating that an alternative mechanism of action may be at play.^{1,3} NTZ also exhibits a broad activity against anaerobic intestinal pathogens and shows activity against biofilms, influenza, hepatitis, rotavirus, and *Mycobacterium tuberculosis*.³⁵⁻⁴¹ Although NTZ is active against *C. difficile*, its high dosage and wide therapeutic spectrum make it susceptible to undesired outcomes. High levels of NTZ can lead to unpredictable side effects. Furthermore, the ability of NTZ to kill a variety of bacteria can mean that it works through a variety of mechanistic pathways, which is not beneficial in the case of CDI.

2.4 Nitroreduction in Nitazoxanide

NTZ is comparable in structure to MTZ and active against similar microorganisms, however its efficacy against MTZ-resistant bacteria suggests that it is mechanistically different from redox-active prodrugs like MTZ. Generally, nitrofurans, nitrothiazoles and nitroimidazoles are believed to be activated as a result from a 4-electron reduction of the 5-nitro group to biologically active redox active intermediates.⁴² The reduction of MTZ results in toxic mutagenic compounds.^{42,43} A spectrophotometric assay was developed based on nitroreduction of NTZ at 412 nm to determine that PFOR is responsible for the antimicrobial activity of NTZ against *H. pylori*.⁴² An analysis of NTZ products from the PFOR reaction by mass spectrometry discovered that nitroreduction had not occurred, and *E. coli* RdxA, a nitroreductive enzyme, did not produce mutagenic products of NTZ.^{42,44} These results indicate that nitroreduction is not part of the mechanism of action of NTZ, but the PFOR enzyme is key in the drug's bactericidal effects.

2.5 Pyruvate:ferredoxin Oxidoreductase

The oxidative decarboxylation of pyruvate is a crucial step in energy metabolism for aerobic and anaerobic organisms. In most aerobic bacteria and eukaryotic mitochondria, this reaction is catalyzed by the multienzyme pyruvate dehydrogenase (PDH) complex, reducing the coenzyme nicotinamide adenine dinucleotide (NAD) as the electron acceptor.⁴⁵ In anaerobic bacteria, pyruvate oxidation is catalyzed by pyruvate:ferredoxin oxidoreductase (PFOR).⁴⁶⁻⁴⁹ The distinction between these

organisms in the production of acetyl-coenzyme A provides an avenue to selectively target PFOR-utilizing microorganisms.

2.5.1 Overview of PFOR Function

The PFOR enzyme plays a variety of roles in anaerobic microorganisms including substrate phosphorylation and electron production for nitrogenase enzymes.⁴⁶ In bacteria like *Clostridium thermoaceticum*, PFOR connects glycolysis to the Wood-Ljungdahl acetyl-CoA synthesis pathway.⁴⁹ The decarboxylation of pyruvate by PFOR involves the transfer of electrons to ferredoxins (Fd) via [4Fe4S] clusters. Depending upon the species PFOR can exist as a homodimer, heterodimer or heterotetramer.^{50,51}

The crystal structure of the PFOR enzyme from *Desulfovibrio africanus* (2.3 Å) gives insight to the mechanism of acetyl-CoA synthesis by PFOR.⁴⁶ The enzyme exists as a homodimer with three [4Fe4S] clusters and a vitamin cofactor thiamine pyrophosphate (TPP) in the core (Figure 2.5). The complex is divided into seven domains, with the TPP binding site located at the interface of domains I and VI.⁴⁶ Oxidative pyruvate decarboxylation is carried out at this location.

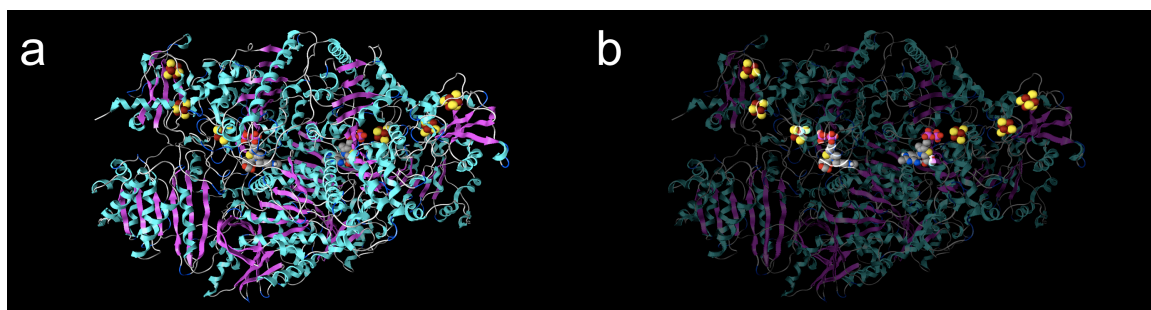


Figure 2.5. Ribbon drawing of *Desulfovibrio africanus* PFOR (2.3 Å) (a). b) The PFOR enzyme of *D. africanus* exists as a homodimer with three [4Fe4S] clusters (yellow, red) and a thiamine pyrophosphate (TPP) cofactor (gray) in the core.

PFOR differs mechanistically from PDH, making it a potential target for specific drug design. Electron acceptors such as the iron-sulfur proteins ferredoxin and flavodoxin are required in PFOR, and the enzyme carries out oxidative pyruvate decarboxylation reversibly (Figure 2.6). PDH on the other hand, uses a lipoate cofactor to perform pyruvate oxidation and the reaction cannot go in the reverse direction.⁵² The discrepancies between the two enzyme complexes allow for the selective targeting of anaerobic human pathogens without affecting metabolism in the host.

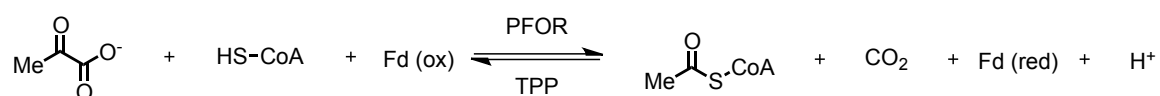
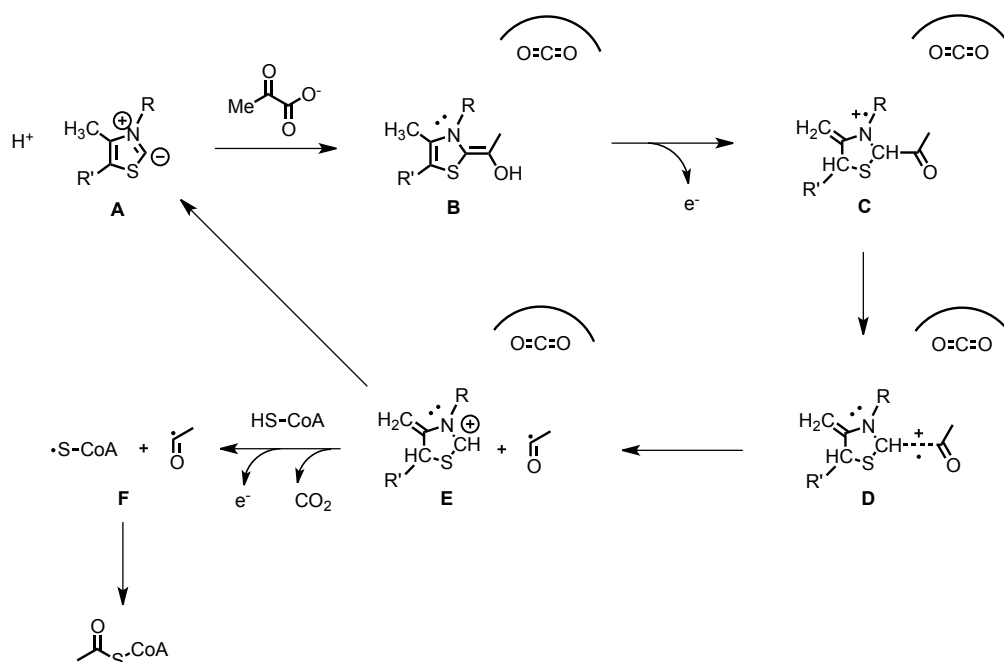


Figure 2.6. Pyruvate:ferredoxin oxidoreductase (PFOR) enzymatic reaction.

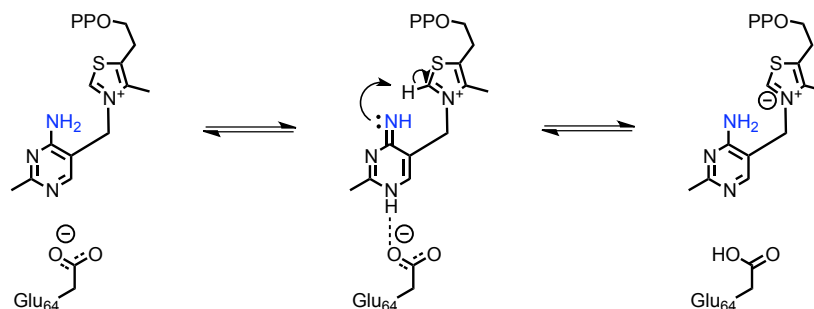
The proposed mechanism of acetyl-CoA synthesis is depicted in Scheme 2.1.^{46,53,54} The structure of the radical of PFOR shows that the thiazole ring of TPP is bent and there is an unusually long carbon-carbon bond connecting the acetyl group to TPP, suggesting a condensation mechanism with acetyl and thiyl radicals.⁵³ Pyruvate binds to the C2 carbanion of the TPP thiazole ring, releasing CO₂ that stays in the active site (Figure 2.7 A to B). A one-electron transfer occurs, giving a nitrogen radical cation and dearomatization of the thiazole ring (B to C). A one-electron rearrangement results in the observed elongated C2-C2 α bond that fragments to give an umpolung at the C2 carbon and acetyl radical. (C to E). This radical reacts with the thiyl radical to form acetyl-CoA and the aromatic thiazole ring is restored (D to F).^{46,53,54}



Scheme 2.1. Mechanism of acetyl-CoA production at PFOR by Chabrière et al.^{48,55} A) The thiazole ring of TPP is anionic at the C2 position due to the V-conformation of TPP in the PFOR pocket. B) The C2 carbanion nucleophilically attacks pyruvate, resulting in decarboxylation and enamine formation. C) Tautomerization and the first one-electron transfer from the active site to one of the [4Fe4S] clusters to give a hypothetical n-type radical cation. D) It is observed that the unpaired electron is located at either the acetyl group or C2 atom of the thiazole ring but not delocalized over the ring itself, forming a long C2-C2α bond with a σ/n radical cation. E) Proposed fragmentation to yield a C2 carbocation and the acetyl radical, after which aromaticity of the thiazole ring is restored (A) and the condensation of the thiol CoA radical with acetyl radical produces acetyl-CoA.⁵³

2.5.2 Thiamine Pyrophosphate

Thiamine pyrophosphate (TPP) is a vitamin cofactor found in many enzymes including transketolase, pyruvate oxidase and pyruvate decarboxylase (Scheme 2.2). The catalyst is activated upon deprotonation of the thiazole C2 carbon. In the active site the coenzyme has a highly constrained V-conformation which prevents the thiazole C2 atom and the pyrimidine N4' atom from being protonated at the same time.⁵³ As a result, the carbanion is able to nucleophilically attack pyruvate and initiate the formation of acetyl-CoA (Scheme 2.1).



Scheme 2.2. Activation of thiamine pyrophosphate (TPP). The coenzyme exists in a V-shaped conformation to allow for the thiazole C2 carbanion to remain deprotonated and react with pyruvate.⁵³ The ylide is formed when the N4' nitrogen of the pyrimidine ring deprotonates the C2 thiazole carbon. PP: Pyrophosphate.⁵⁵

As Scheme 2.1 shows, oxidative pyruvate decarboxylation is carried out on the thiazole ring of TPP. Without this functioning coenzyme, the formation of acetyl-CoA would not occur at PFOR. Preventing this reaction from occurring would paralyze the enzyme and kill the parent organism. Since the vitamin cofactor TPP is an essential part of energy metabolism and other biological reactions, the fitness cost that the bacteria would have to pay to avoid this antimicrobial mechanism of action is quite high. As a result, there is an evolutionary advantage to killing bacteria through this molecule. MTZ resistance results from mutations in genes that encode nitroreductases, providing a facile means for bacteria to evade redox active nitro prodrugs.^{42,43} Targeting the TPP cofactor critical to a number of enzymatic pathways provides an attractive inhibitory pathway that is not as susceptible to resistance.

2.6 Nitazoxanide Mechanism of Action

Nitazoxanide exhibits similarities in activity to MTZ and nitrofurans, however many studies suggest that NTZ is different from redox-active prodrugs.^{1,42} The broad-spectrum activity of NTZ against anaerobic parasites implies that a common target

is involved. Previous studies by our research group have proven that NTZ inhibits the PFOR enzyme, which is found in anaerobic bacteria and many other eukaryotic parasites.⁴² The 5-nitro group of NTZ is important to its bactericidal activity; replacement of the nitro group with bromine destroyed the biological activity of NTZ.^{33,43} With this in mind, our group sought to elucidate the mechanism of action of NTZ.

Multiple studies were performed to determine the mechanism by which NTZ inhibits PFOR. The first analysis looked at the occurrence of nitroreduction. A spectral shift from 418 nm to 351 nm was observed in previous studies of the PFOR reaction. This was thought to be due to nitroreduction on the thiazole ring. Negative-ion mass spectrometry was used to observe the product of the PFOR reaction at 351 nm to see if oxime (NOH) or amine (NH₂) were produced from the 5-nitro group. The study showed that the major masses of the 351 nm product were the same as those of the 418 nm-absorbing compound, indicating that nitroreduction had not occurred. This corroborates existing data that NTZ is a unique nitro drug that does not undergo reductive activation.⁴⁴

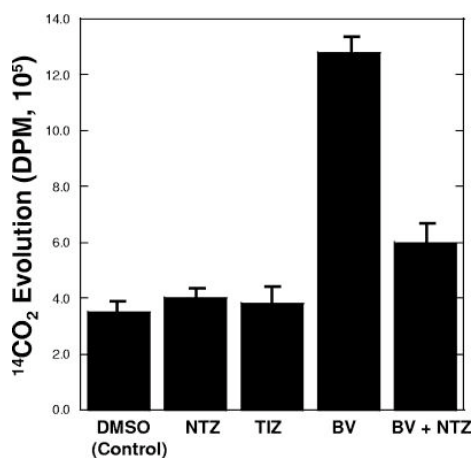


Figure 2.7. Evolution of carbon dioxide from the PFOR enzymatic reaction. ¹⁴C labeled pyruvate was added to the PFOR reaction with DMSO (negative control), NTZ, tizoxanide (TIZ), or benzyl viologen (BV) as the electron acceptor. The reactions were initiated by addition of [¹⁴C]pyruvate, and CO₂ was collected in an NaOH trap and counted by liquid scintillation. The radioactivity of the captured CO₂ is presented in dpm and the reactions were run in triplicate. Reprinted from reference 44 with permission of the publisher.

In order to determine the point in the PFOR reaction that NTZ interferes with, $^{14}\text{CO}_2$ evolution from the decarboxylation of pyruvate was collected and measured with and without NTZ. If CO_2 evolution was diminished upon adding NTZ compared to negative control and redox active BV dye, inhibition occurs before the binding of pyruvate. Alternatively, if CO_2 evolution was unaltered by NTZ compared to controls, inhibition of PFOR takes place in a later step of the PFOR reaction. Results from this study can be found in Figure 2.7. The addition of NTZ to the BV assay decreased the evolution of CO_2 , demonstrating that NTZ stops the PFOR reaction before pyruvate is able to bind to the activated TPP cofactor. To elaborate on this data, the concentration of pyruvate (substrate) was measured at intervals during the PFOR reaction. The purpose of this study was to examine the consumption of pyruvate and see if NTZ obstructs the formation of the PFOR reaction intermediate or alters the structure of pyruvate (Figure 2.8).⁴⁴

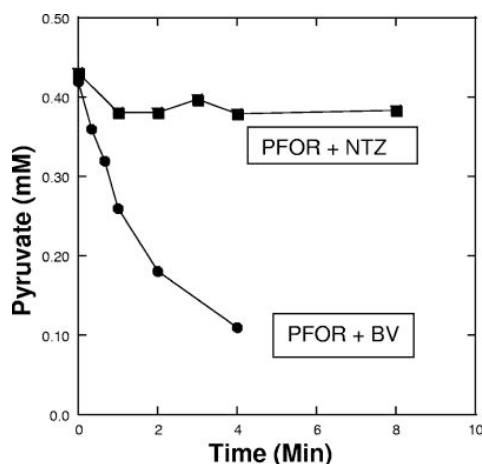


Figure 2.8. Remaining pyruvate in the PFOR reaction with NTZ. The standard PFOR reactions were run in the presence of BV and NTZ and samples were collected at designated intervals. Proteins were precipitated with perchloric acid and the neutralized supernatants were assayed for remaining pyruvate by monitoring the oxidation of NADH by lactate dehydrogenase (LDH, 4 m). The estimated remaining pyruvate was plotted for each time point of the PFOR reaction. Pyruvate was not consumed in the reaction with NTZ as the electron acceptor. Reprinted from reference 44 with permission of the publisher.

Results showed that NTZ did not affect the levels of PFOR but redox active BV did (Figure 2.8). Since NTZ did not chemically alter pyruvate, and CO₂ levels decreased with the addition of NTZ as an electron acceptor, it can be determined that NTZ interferes with the initial binding of pyruvate to TPP. The spectral shift of NTZ upon reacting with PFOR was found to be due to a pH-dependency. At pH 7.4, all PFOR reactions with NTZ showed the 480-to-351 nm spectral shift, which could be reversed by adding DMSO, an aprotic solvent, to the reaction mixture. Titration experiments showed that both compounds are in equilibrium at pH 6.18 (pK_a), so NTZ must exist in its anionic form under physiological pH conditions (Figure 2.9). The pK_a was confirmed by ¹H NMR analysis of NTZ under acidic and basic conditions. Therefore, NTZ inhibits the TPP-pyruvate reaction through deprotonation.⁴⁴

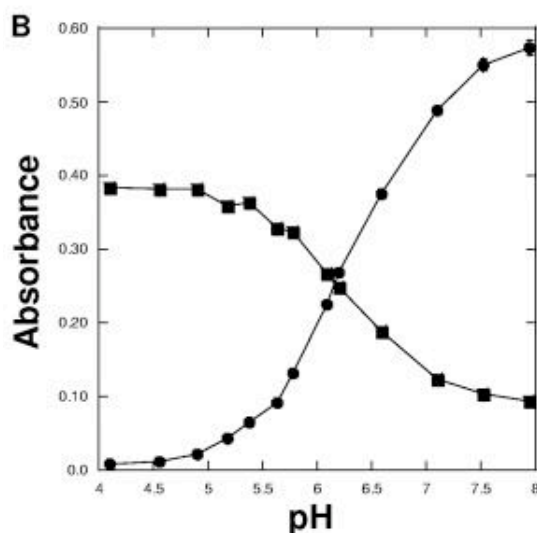


Figure 2.9. Absorbance properties during pH titration of NTZ. Titration of 0.02 mM solution of protonated (418 nm, •) and deprotonated (351 nm, ■) NTZ in 10 mM phosphate buffer at the indicated pH values (pK_a = 6.18). Assays were run in triplicate, and the means and standard deviations are shown. Reprinted from reference 44 with permission of the publisher.

The proposed mechanism of action of NTZ is shown in Figure 2.10. NTZ acts as a competitive inhibitor of PFOR with a K_i value of $\sim 5 \times 10^{-6}$ M (K_m pyruvate = $\sim 3 \times 10^{-4}$

M).⁴⁴ The 2-amino anion of the thiazole ring has a resonance structure with a formal negative charge on the 5-nitro group. This forms a salt bridge in the active site of PFOR in place of pyruvate, preventing deprotonation of the 4'-amino group of amino pyrimidine in TPP and therefore pyruvate binding (Figure 2.10).

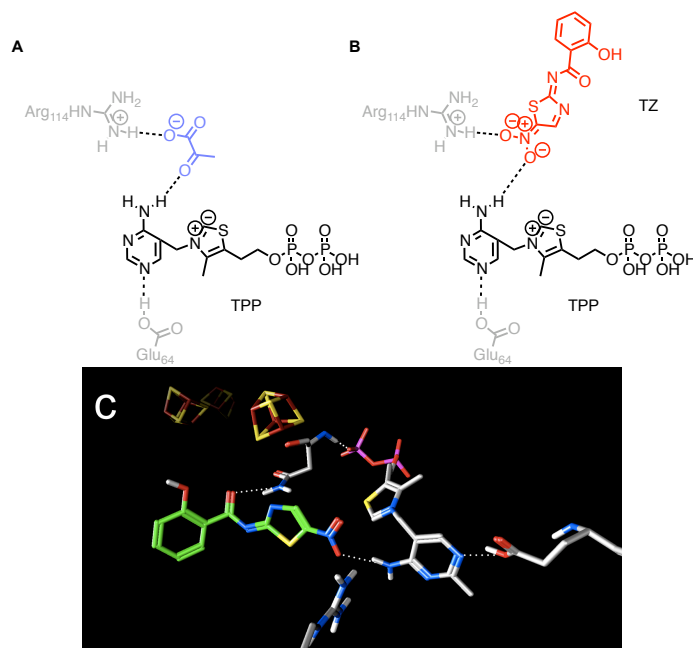


Figure 2.10. NTZ mechanism of action. A) In the PFOR enzyme, pyruvate (blue) chelates to the activated amine on the pyrimidine of TPP (black). B) TZ (red) prevents this chelation by deprotonating the amine (black) through the anionic nitro group. C) Computer modeling rendition of TZ (green) chelating to TPP (gray).⁴⁴

By targeting a cofactor of the enzymatic reaction, NTZ presents a novel therapeutic strategy that reduces the risk of antimicrobial resistance. Unlike other nitro prodrugs like MTZ, which are becoming useless as resistance mutations increase, NTZ has the potential to avoid traditional resistance pathways and succeed as a PFOR-selective antibiotic.

2.7 Conclusion

Deaths due to CDI have increased to ~ 14,000/year, making it a very prominent, yet preventable infection.⁵⁶ Nitazoxanide has the potential to successfully combat CDI without threat of recurrence or resistance. The inhibition of the PFOR enzyme at the vitamin co-factor TPP makes NTZ a unique nitro drug that is not reduced as part of its mechanism of action. This puts NTZ a step ahead of the bacteria, allowing for effective treatment without the risk of reinfection.

Despite its robust antimicrobial properties, the efficacy of NTZ is limited by its promiscuity. NTZ inhibits biofilm formation in *Staphylococcus* and *E. coli* – bacteria that do not possess the PFOR enzyme. Off-target effects could inhibit re-growth of the microflora required for patient recovery from CDI. The therapeutic spectrum of a CDI antibiotic must be specific for *C. difficile*-type organisms so that relapse and recurrence of infection does not occur.

Furthermore, it takes nearly 1g of NTZ per day to be effective against CDI. More drug is required to treat intestinal infections because NTZ is poorly soluble (<10 µg/mL). A large dosage such as this can lead to erratic side effects that are compounded by prolonged infection due to off-target effects. In order to narrow the therapeutic spectrum of NTZ and increase bioavailability, the structure must be optimized to achieve the desired pharmacodynamic and pharmacokinetic properties.

References

1. Gilles, H. M.; Hoffman, P. S. Treatment of intestinal parasitic infections: a review of nitazoxanide. *Trends Parasitol.* **2002**, *18*, 95-97.
2. Rossignol, J.; Maisonneuve, H. Nitazoxanide in the treatment of *Taenia saginata* and *Hymenolepis nana* infections. *Am. J. Trop. Med. Hyg.* **1984**, *33*, 511-512.
3. Anderson, V. R.; Curran, M. P. Nitazoxanide. *Drugs* **2007**, *67*, 1947-1967.
4. Romark Laboratories L.C. Alinia. (Nitazoxanide) tablets. (Nitazoxanide) for oral suspension. <http://www.romark.com> (accessed August, 2013).
5. Fox, L. M.; Saravolatz, L. D. Nitazoxanide: A New Thiazolide Antiparasitic Agent. *Clin. Infect. Dis.* **2005**, *40*, 1173-1180.
6. Abaza, H.; El-Zayadi, A. R.; Kabil, S. M.; Rizk, H. Nitazoxanide in the treatment of patients with intestinal protozoan and helminthic infections: a report on 546 patients in Egypt. *Current therapeutic research* **1998**, *59*, 116-121.
7. Rossignol, J.; Maisonneuve, H.; Cho, Y. Nitroimidazoles in the treatment of trichomoniasis, giardiasis, and amebiasis. *Int. J. Clin. Pharmacol. Ther. Toxicol.* **1984**, *22*, 63-72.
8. Ortiz, J. J.; Ayoub, A.; Gargala, G.; Chegne, N.; Favennec, L. Randomized clinical study of nitazoxanide compared to metronidazole in the treatment of symptomatic giardiasis in children from Northern Peru. *Aliment. Pharmacol. Ther.* **2001**, *15*, 1409-1415.
9. Rossignol, J.; Ayoub, A.; Ayers, M. S. Treatment of Diarrhea Caused by *Giardia intestinalis* and *Entamoeba histolytica* or *E. dispar*: A Randomized, Double-Blind, Placebo-Controlled Study of Nitazoxanide. *J. Infect. Dis.* **2001**, *184*, 381-384.
10. Rossignol, J. A.; Ayoub, A.; Ayers, M. S. Treatment of diarrhea caused by *Cryptosporidium parvum*: a prospective randomized, double-blind, placebo-controlled study of nitazoxanide. *J. Infect. Dis.* **2001**, *184*, 103-106.
11. Rossignol, J.; Abaza, H.; Friedman, H. Successful treatment of human fascioliasis with nitazoxanide. *Trans. R. Soc. Trop. Med. Hyg.* **1998**, *92*, 103-104.
12. Dubreuil, L.; Houcke, I.; Mouton, Y.; Rossignol, J. In vitro evaluation of activities of nitazoxanide and tizoxanide against anaerobes and aerobic organisms. *Antimicrob. Agents Chemother.* **1996**, *40*, 2266-2270.
13. Mégraud, F.; Occhialini, A.; Rossignol, J. F. Nitazoxanide, a Potential Drug for Eradication of *Helicobacter pylori* with No Cross-Resistance to Metronidazole. *Antimicrob. Agents Chemother.* **1998**, *42*, 2836-2840.
14. Rupnik, M.; Wilcox, M. H.; Gerding, D. N. *Clostridium difficile* infection: new developments in epidemiology and pathogenesis. *Nature Reviews Microbiology* **2009**, *7*, 526-536.
15. Gould, C. V.; McDonald, L. C. Bench-to-bedside review: *Clostridium difficile* colitis. *Crit. Care* **2008**, *12*, 203-210.
16. Carroll, K. C.; Bartlett, J. G. Biology of *Clostridium difficile*: implications for epidemiology and diagnosis. *Annu. Rev. Microbiol.* **2011**, *65*, 501-521.

17. Sehulster, L.; Chinn, R. Y.; Arduino, M.; Carpenter, J.; Donlan, R.; Ashford, D.; Besser, R.; Fields, B.; McNeil, M.; Whitney, C. Guidelines for environmental infection control in health-care facilities. *Morbidity and Mortality Weekly Report Recommendations and Reports RR* **2003**, 1-249.
18. Miller MD, B. A.; Chen MD, L. F.; Sexton MD, D. J.; Anderson MD, D. J. Comparison of the burdens of hospital-onset, healthcare facility-associated *Clostridium difficile* infection and of healthcare-associated infection due to methicillin-resistant *Staphylococcus aureus* in community hospitals. *Infection control and hospital epidemiology* **2011**, 32, 387-390.
19. McDonald, L. C.; Killgore, G. E.; Thompson, A.; Owens Jr, R. C.; Kazakova, S. V.; Sambol, S. P.; Johnson, S.; Gerding, D. N. An epidemic, toxin gene-variant strain of *Clostridium difficile*. *N. Engl. J. Med.* **2005**, 353, 2433-2441.
20. O'Connor, J. R.; Johnson, S.; Gerding, D. N. *Clostridium difficile* Infection Caused by the Epidemic BI/NAP1/027 Strain. *Gastroenterology* **2009**, 136, 1913-1924.
21. Redelings, M. D.; Sorvillo, F.; Mascola, L. Increase in *Clostridium difficile*-related mortality rates, United States, 1999-2004. *Emerging infectious diseases* **2007**, 13, 1417-1419.
22. Jank, T.; Giesemann, T.; Aktories, K. Rho-glucosylating *Clostridium difficile* toxins A and B: new insights into structure and function. *Glycobiology* **2007**, 17, 15R-22R.
23. Poutanen, S. M.; Simor, A. E. *Clostridium difficile*-associated diarrhea in adults. *Can. Med. Assoc. J.* **2004**, 171, 51-58.
24. Borriello, S. Pathogenesis of *Clostridium difficile* infection. *J. Antimicrob. Chemother.* **1998**, 41, 13-19.
25. Poxton, I.; McCoubrey, J.; Blair, G. The pathogenicity of *Clostridium difficile*. *Clin. Microbiol. Infect.* **2001**, 7, 421-427.
26. Huang, H.; Weintraub, A.; Fang, H.; Nord, C. E. Antimicrobial resistance in *Clostridium difficile*. *Int. J. Antimicrob. Agents* **2009**, 34, 516-522.
27. Louie, T. J.; Miller, M. A.; Mullane, K. M.; Weiss, K.; Lentnek, A.; Golan, Y.; Gorbach, S.; Sears, P.; Shue, Y. Fidaxomicin versus vancomycin for *Clostridium difficile* infection. *N. Engl. J. Med.* **2011**, 364, 422-431.
28. Zar, F. A.; Bakkanagari, S. R.; Moorthi, K.; Davis, M. B. A comparison of vancomycin and metronidazole for the treatment of *Clostridium difficile*-associated diarrhea, stratified by disease severity. *Clin. Infect. Dis.* **2007**, 45, 302-307.
29. Johnson, S.; Adelman, A.; Clabots, C. R.; Peterson, L. R.; Gerding, D. N. Recurrences of *Clostridium difficile* diarrhea not caused by the original infecting organism. *J. Infect. Dis.* **1989**, 159, 340-343.
30. Tannock, G. W.; Munro, K.; Taylor, C.; Lawley, B.; Young, W.; Byrne, B.; Emery, J.; Louie, T. A new macrocyclic antibiotic, fidaxomicin (OPT-80), causes less alteration to the bowel microbiota of *Clostridium difficile*-infected patients than does vancomycin. *Microbiology* **2010**, 156, 3354-3359.
31. McVay, C. S.; Rolfe, R. D. In vitro and in vivo activities of nitazoxanide against *Clostridium difficile*. *Antimicrob. Agents Chemother.* **2000**, 44, 2254-2258.

32. Ortiz, J. J.; Chegne, N. L.; Gargala, G.; Favennec, L. Comparative clinical studies of nitazoxanide, albendazole and praziquantel in the treatment of ascariasis, trichuriasis and hymenolepiasis in children from Peru. *Trans. R. Soc. Trop. Med. Hyg.* **2002**, *96*, 193-196.
33. Pankuch, G. A.; Appelbaum, P. C. Activities of Tizoxanide and Nitazoxanide Compared to Those of Five Other Thiazolides and Three Other Agents against Anaerobic Species. *Antimicrob. Agents Chemother.* **2006**, *50*, 1112-1117.
34. Musher, D. M.; Logan, N.; Hamill, R. J.; DuPont, H. L.; Lentnek, A.; Gupta, A.; Rossignol, J. Nitazoxanide for the treatment of *Clostridium difficile* colitis. *Clin. Infect. Dis.* **2006**, *43*, 421-427.
35. Ballard, T. E.; Wang, X.; Olekhovich, I.; Koerner, T.; Seymour, C.; Salamoun, J.; Warthan, M.; Hoffman, P. S.; Macdonald, T. L. Synthesis and Antimicrobial Evaluation of Nitazoxanide-Based Analogues: Identification of Selective and Broad Spectrum Activity. *ChemMedChem* **2011**, *6*, 362-377.
36. de Carvalho, L. P. S.; Lin, G.; Jiang, X.; Nathan, C. Nitazoxanide kills replicating and nonreplicating *Mycobacterium tuberculosis* and evades resistance. *J. Med. Chem.* **2009**, *52*, 5789-5792.
37. Rossignol, J.; Abu-Zekry, M.; Hussein, A.; Santoro, M. G. Effect of nitazoxanide for treatment of severe rotavirus diarrhoea: randomised double-blind placebo-controlled trial. *Lancet* **2006**, *368*, 124-129.
38. Rossignol, J.; Elfert, A.; El-Gohary, Y.; Keefe, E. B. Improved virologic response in chronic hepatitis C genotype 4 treated with nitazoxanide, peginterferon, and ribavirin. *Gastroenterology* **2009**, *136*, 856-862.
39. Rossignol, J. F.; La Frazia, S.; Chiappa, L.; Ciucci, A.; Santoro, M. G. Thiazolides, a new class of anti-influenza molecules targeting viral hemagglutinin at the post-translational level. *J. Biol. Chem.* **2009**, *284*, 29798-29808.
40. Shamir, E. R.; Warthan, M.; Brown, S. P.; Nataro, J. P.; Guerrant, R. L.; Hoffman, P. S. Nitazoxanide inhibits biofilm production and hemagglutination by enteroaggregative *Escherichia coli* strains by blocking assembly of AafA fimbriae. *Antimicrob. Agents Chemother.* **2010**, *54*, 1526-1533.
41. Tchouaffi-Nana, F.; Ballard, T. E.; Cary, C. H.; Macdonald, T. L.; Sifri, C. D.; Hoffman, P. S. Nitazoxanide Inhibits Biofilm Formation by *Staphylococcus epidermidis* by Blocking Accumulation on Surfaces. *Antimicrob. Agents Chemother.* **2010**, *54*, 2767-2774.
42. Sisson, G.; Goodwin, A.; Raudonikiene, A.; Hughes, N. J.; Mukhopadhyay, A. K.; Berg, D. E.; Hoffman, P. S. Enzymes Associated with Reductive Activation and Action of Nitazoxanide, Nitrofurans, and Metronidazole in *Helicobacter pylori*. *Antimicrob. Agents Chemother.* **2002**, *46*, 2116-2123.
43. Sisson, G.; Jeong, J.; Goodwin, A.; Bryden, L.; Rossler, N.; Lim-Morrison, S.; Raudonikiene, A.; Berg, D. E.; Hoffman, P. S. Metronidazole Activation Is Mutagenic and Causes DNA Fragmentation in *Helicobacter pylori* and in *Escherichia coli* Containing a Cloned *H. pylori* rdxA (Nitroreductase) Gene. *J. Bacteriol.* **2000**, *182*, 5091-5096.

44. Hoffman, P. S.; Sisson, G.; Croxen, M. A.; Welch, K.; Harman, W. D.; Cremades, N.; Morash, M. G. Antiparasitic Drug Nitazoxanide Inhibits the Pyruvate Oxidoreductases of *Helicobacter pylori*, Selected Anaerobic Bacteria and Parasites, and *Campylobacter jejuni*. *Antimicrob. Agents Chemother.* **2007**, *51*, 868-876.
45. Patel, M. S.; Roche, T. E. Molecular biology and biochemistry of pyruvate dehydrogenase complexes. *The FASEB Journal* **1990**, *4*, 3224-3233.
46. Chabrière, E.; Charon, M.; Volbeda, A.; Pieulle, L.; Hatchikian, E. C.; Fontecilla-Camps, J. Crystal structures of the key anaerobic enzyme pyruvate: ferredoxin oxidoreductase, free and in complex with pyruvate. *Nature Structural & Molecular Biology* **1999**, *6*, 182-190.
47. Uyeda, K.; Rabinowitz, J. C. Pyruvate-ferredoxin oxidoreductase III. Purification and properties of the enzyme. *J. Biol. Chem.* **1971**, *246*, 3111-3119.
48. Brostedt, E.; Nordlund, S. Purification and partial characterization of a pyruvate oxidoreductase from the photosynthetic bacterium *Rhodospirillum rubrum* grown under nitrogen-fixing conditions. *Biochem. J.* **1991**, *279*, 155-158.
49. Menon, S.; Ragsdale, S. W. Unleashing hydrogenase activity in carbon monoxide dehydrogenase/acetyl-CoA synthase and pyruvate: ferredoxin oxidoreductase. *Biochemistry (N. Y.)* **1996**, *35*, 15814-15821.
50. Kletzin, A.; Adams, M. Molecular and phylogenetic characterization of pyruvate and 2-ketoisovalerate ferredoxin oxidoreductases from *Pyrococcus furiosus* and pyruvate ferredoxin oxidoreductase from *Thermotoga maritima*. *J. Bacteriol.* **1996**, *178*, 248-257.
51. Zhang, Q.; Iwasaki, T.; Wakagi, T.; Oshima, T. 2-Oxoacid: ferredoxin oxidoreductase from the thermoacidophilic archaeon, *Sulfolobus* sp. strain 7. *J. Biochem.* **1996**, *120*, 587-599.
52. Ciszak, E. M.; Korotchkina, L. G.; Dominiak, P. M.; Sidhu, S.; Patel, M. S. Structural basis for flip-flop action of thiamin pyrophosphate-dependent enzymes revealed by human pyruvate dehydrogenase. *J. Biol. Chem.* **2003**, *278*, 21240-21246.
53. Chabrière, E.; Vernède, X.; Guigliarelli, B.; Charon, M.; Hatchikian, E. C.; Fontecilla-Camps, J. C. Crystal structure of the free radical intermediate of pyruvate: ferredoxin oxidoreductase. *Science* **2001**, *294*, 2559-2563.
54. Charon, M.; Volbeda, A.; Chabriere, E.; Pieulle, L.; Fontecilla-Camps, J. C. Structure and electron transfer mechanism of pyruvate: ferredoxin oxidoreductase. *Curr. Opin. Struct. Biol.* **1999**, *9*, 663-669.
55. Ragsdale, S. W. Pyruvate ferredoxin oxidoreductase and its radical intermediate. *Chem. Rev.* **2003**, *103*, 2333-2346.
56. Lucado, J.; Gould, C.; Elixhauser, A. *Clostridium difficile* infections (CDI) in hospital stays, 2009. *Agency for Healthcare Research and Quality* **2012**.

3

Nitazoxanide Derivative Design and Discovery

The unique inhibitory effect by the anionic metabolite of nitazoxanide (NTZ) at pyruvate:ferredoxin oxidoreductase (PFOR) led researchers in the Macdonald laboratory at the University of Virginia to examine other small molecules that utilize the key components of NTZ for selective antimicrobial properties. In this study, a large library of compounds was created using readily available starting materials and facile synthetic routes to examine the structure—activity relationships (SAR) of molecules in the PFOR pocket. Systematic modifications were made to the NTZ scaffold to observe electronic and steric relationships between inhibitors and the target enzyme.

3.1 Nitazoxanide-Based Inhibitor Discovery

In order to elucidate the structural characteristics of the PFOR target and rationally design first-generation antimicrobial analogues of NTZ, it was necessary to obtain SAR data of active NTZ derivatives. Our group sought to create a library of compounds with systematic changes to the structure of NTZ to pinpoint structural properties that relate to increased binding between the PFOR pocket and inhibitors. Those modifications that correspond to increased activity allows the medicinal chemist to

better understand the structure of the target and design logical derivatives of the lead compound.

Previous studies of NTZ derivatives did not include modifications to the overall structure beyond replacing the nitro group of NTZ with halides.¹⁻³ With the mechanism of action of NTZ and target determined, a compound library was designed using the basic structure of NTZ as a probe to explore SAR and guide optimization efforts. To perform a systematic analysis of each portion of the molecule, NTZ was divided into two main regions separated by an amide linker: the benzene region, or tail group, and the 5-nitrothiazole region, or head group (Figure 3.1).⁵

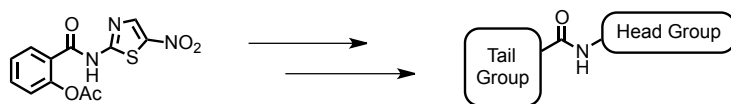


Figure 3.1. Inhibitor design from NTZ. Proposed analogues contain modifications of the benzene (tail group) and 5-nitrothiazole (head group) moieties of NTZ to observe (SAR).

The first-generation compound library was created with the goal of optimizing the head group to increase binding interactions with thiamine pyrophosphate (TPP) followed by tail group modifications to explore chemical space within the PFOR pocket. Analysis of the head group of NTZ will provide significant information regarding the necessary components for binding at TPP. The strength of the polar interactions between the negatively charged head group and the cofactor of PFOR is key for inhibition, and any modifications to this portion of the molecule should have a significant effect on activity. Secondly, the tail region of NTZ can be modified or replaced to examine hydrophobic interactions and spatial requirements in the PFOR pocket.

3.2 Head Region Analysis

Antimicrobial properties could be achieved by altering the relatively simple structure of NTZ at the thiazole (head group) moiety. Previous studies of thiazolides indicate that the 5-nitrothiazole head group of NTZ is crucial for *in vitro* activity and removal of this moiety diminishes drug activity.²⁻⁴ Our research sought to modify this region by adding to the existing nitrothiazole group or replacing the head group with derivatives that offered similar steric and electronic characteristics. Five aliphatic and aromatic tail regions were chosen from a library of ~100 NTZ derivatives to analyze a series of head group analogues (Figure 3.2).⁵

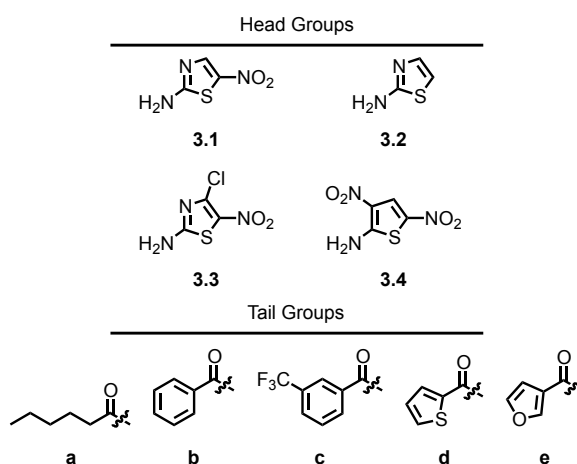


Figure 3.2. Composition of library head groups (top) and tail groups (bottom).⁵

The interaction between NTZ and the cofactor TPP is crucial for biological activity at PFOR.⁶ Deprotonation of the NTZ amide allows for resonance of the negative charge to the nitro *N2'* and *N3'* nitrogens of the nitrothiazole head group, mimicking pyruvate in the PFOR pocket and competitively inhibiting the enzyme's activity (Figure 3.3).⁵ It was proposed that the addition of electron withdrawing groups to head-group heterocycles could enhance amide acidity and therefore increase PFOR inhibition. The

tail regions encompassed aliphatic and aromatic moieties lacking the 2-acetoxy group of NTZ (Figure 3.2).⁵

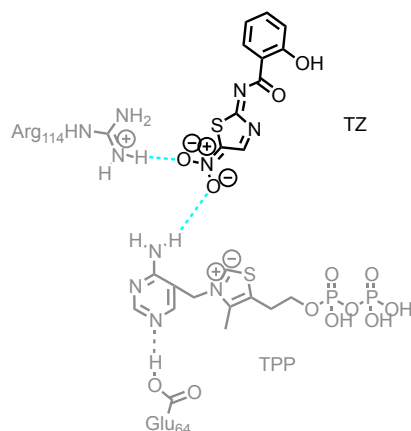
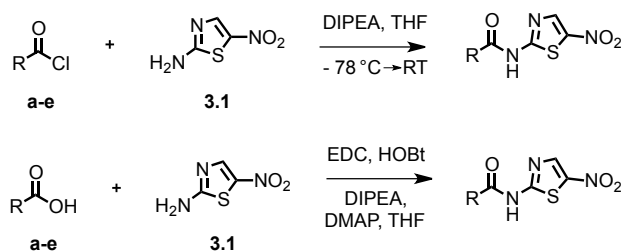


Figure 3.3. Interaction between TPP and TZ anion. The negative charges on the nitro *N2'* and *N3'* nitrogens of the 5-nitrothiazole head group of tizoxanide (TZ, black) chelate to TPP in the PFOR pocket (gray). This interaction (blue) is crucial for activity and PFOR inhibition.⁶

The synthesis of compounds **3.1a-e** – **3.4a-e** was carried out by coupling the commercially available acid chloride/carboxylic acid of tail regions **a** – **e** with the respective amino head group **3.1** – **3.4** to form the amide bond (Scheme 3.1). All head group moieties were purchased except for **3.3**.⁵

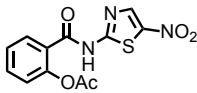
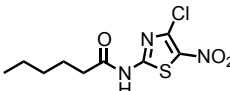
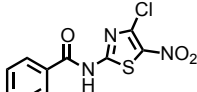
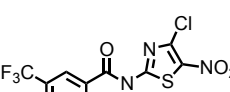
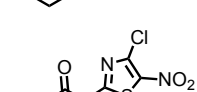
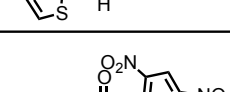
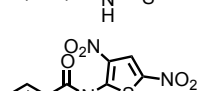
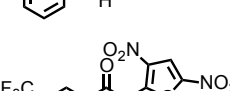
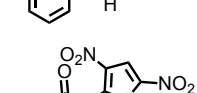
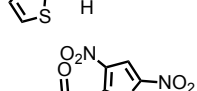


Scheme 3.1. Representative syntheses of compound library with varied head groups. Amide coupling reactions were performed using heterocyclic head-groups **3.1** – **3.4** and either the commercially available acid chloride (top) or carboxylic acid (bottom) forms of tail groups **a** – **e**.⁵

Once synthesized, the compounds were screened for minimum inhibitory concentration (MIC), or the concentration of drug required to inhibit *in vitro* cell growth by 99%. To ensure selectivity and rule out activity at pyruvate dehydrogenase-utilizing

bacteria, the compound library was screened against Gram-negative and Gram-positive bacterium as well as *Escherichia coli* before direct PFOR enzyme inhibition was measured.

The derivatives were first subjected to *in vitro* MIC testing against the Gram-negative bacterium *Helicobacter pylori* and *Campylobacter jejuni* as well as *E. coli* to rule out activity against organisms that utilize the PDH enzyme complex. Analogues of head groups **3.1** – **3.4** were the most active against PFOR and target organisms out of 38 compounds. These were subjected to further testing against *C. difficile* and for direct PFOR inhibition.⁵ Biological evaluation gave results similar to those of previous studies.^{1,2,4} Overall, most of the head group analogues proved inactive against the target bacteria with double to triple-digit micromolar MIC values. Of the four tested, two head groups **3.3** and **3.4** were comparable to NTZ. Control compounds **3.2a** – **d** were completely inactive, confirming the significance of the 5-nitro substituent (data not shown).⁵ Activities listed in Table 3.1 show that all tail region variations of analogues **3.3** and **3.4** were active against target organisms. Additionally, these compounds were inactive against *E. coli*, proving that the compounds are selective for non-PDH utilizing organisms (data not shown).

| Analogue | Structure | MIC (μM) | | | PFOR Inhibition [Drug] = 40 μM (%) |
|----------|---|-----------------------|------------------|---------------------|--|
| | | <i>H. pylori</i> | <i>C. jejuni</i> | <i>C. difficile</i> | |
| NTZ |  | 13.0 | 39.1 | 0.8 | 54 \pm 7 |
| 3.3a |  | 0.9 | 3.6 | 28.8 | 63 |
| 3.3b |  | 8.8 | 7.0 | >28.2 | 59 |
| 3.3c |  | 5.7 | 34.1 | >22.7 | 27 \pm 2 |
| 3.3d |  | 6.9 | 13.8 | >13.8 | 51 |
| 3.4a |  | 2.6 | 0.9 | 27.8 | 80 \pm 8 ^a |
| 3.4b |  | 1.3 | 0.9 | 27.3 | 55 |
| 3.4c |  | 0.5 | 2.1 | 4.2 | 47 |
| 3.4d |  | 2.5 | 1.0 | 20.0 | 77 |
| 3.4e |  | 2.6 | 0.4 | 3.5 | 66 \pm 13 ^a |

^a Complex pattern of inhibition with two different rates.

Table 3.1. MIC and percent PFOR inhibition values for head region analogues **3.3** and **3.4** compared to NTZ.⁵

Derivatives **3.3a – d** utilize the head group of NTZ with an additional 4-chloro substituent, adding steric and electronic effects to the thiazole ring. Although these compounds were more active than NTZ, their activities were slightly lower than the non-chloro analogues **3.1a – e**, suggesting that the electronic effects of the chloro group are

not effective enough to counter the steric interaction with the 5-nitro group. The significant resonance stabilization of the anionic amide by the nitro group of TZ displayed in Figure 3.3 is disrupted by the chloro substituent. It is likely that the steric bulk of the chlorine pushes the nitro group out-of-plane with the ring, lowering the resonance stability and therefore activity.

Dinitrothiophene head group **3.4** was more active than **3.3** against *H. pylori* and *C. jejuni*, with comparable activity against *C. difficile*. Direct PFOR inhibition assays concluded that dinitrothiophene analogues were the same if not better than NTZ however compounds **3.4a** and **3.4e** showed different rates of inhibition. This could be due to multiple mechanisms of inhibition at play including nitroreduction.

To determine if this was the case, compounds **3.4a – e** were subjected to an NfsB nitroreductase assay. The aliphatic derivative **3.4a** was more vulnerable to nitroreduction than analogues **3.4b – e** compared to NTZ (data not shown).⁵ It can therefore be concluded that these derivatives (**3.4b – e**) are selective for PFOR containing organisms through direct PFOR inhibition like NTZ and not operating through nitroreductive pathways.

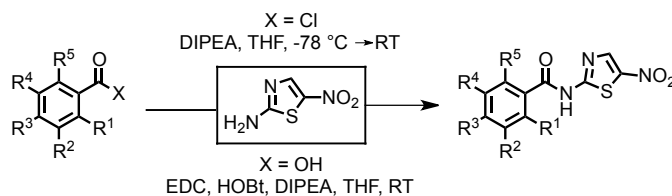
3.3 Tail Region Analysis

Previous studies of NTZ included only minor modifications to the tail region, leaving the area facing away from the binding interaction virtually unexplored.⁵ Systematic alterations to the tail region were made to improve the biological activity of nitrothiazole derivatives and further explore the PFOR target. Using the optimized nitrothiazole moiety as the head group, substitution patterns on the benzene ring were

modified and the 2-acetoxy group was removed. Additionally, the phenyl ring was replaced with unsubstituted and substituted heterocyclic groups.

3.3.1 Benzene Ring Substitution

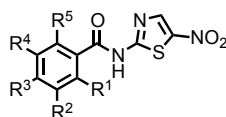
Electron donating and withdrawing groups were added to positions R¹ – R⁵ of the benzene ring (Scheme 3.2).⁷ These substituents impose steric and electronic effects on the molecule by adding bulk around and altering the electron density of the benzene ring thus affecting amide acidity. Both mono- and di-substituted derivatives were achieved through coupling of 2-amino-5-nitrothiazole (2AT) to the corresponding benzoic acid or benzoyl chloride, with the exception of **3.21**, which was achieved through methylation of *p*-trifluoromethyl salicylic acid followed by saponification of the methyl ester and subsequent EDC coupling of the carboxylic acid (Scheme 3.2).⁷



Scheme 3.2. Synthetic routes towards modified tail regions. The benzoyl chloride (top) or benzoic acid (bottom) of the desired tail groups were coupled to the 2-amino-5-nitrothiazole head group.⁷

Mono and di-substituted compounds were assessed for biological activity against *H. pylori* and *C. jejuni* (Table 3.3). Overall, halogenated derivatives **3.5**, **3.6**, **3.9**, **3.10**, **3.14** and **3.15** were more potent than NTZ. Increased substitution (**3.19**) yielded decreased activity compared to **3.5**, **3.9** and **3.14**. Other substitutions including trifluoromethyl (CF₃), methoxy (OCH₃) and cyano (CN) had better activities than NTZ but were not as active as the halogenated compounds described above. Of all the

substitution patterns, *para*-substitution (R^3) proved most active compared to *ortho*- (R^1 and R^5) and *meta*- (R^2 and R^4), with the exception of *para*-cyano compound **3.18**. Disubstituted analogues gave comparable activities to NTZ. Compounds with an electron-donating methoxy group (**3.8**, **3.13** and **3.17**) showed similar activities to an electron-withdrawing trifluoromethyl substituent (**3.7**, **3.11** and **3.16**), indicating that the electronic characteristics of the benzene ring may not play a large role in the activity of NTZ derivatives. Furthermore, deletion of the 2-acetoxy group in analogues **3.5** – **3.18** did not have an adverse effect on drug activity, indicating that this substituent is not crucial for PFOR inhibition.



| Compound ^a | R ¹ | R ² | R ³ | R ⁴ | R ⁵ | MIC (μM) | |
|-----------------------|------------------|------------------|------------------|-----------------|----------------|------------------|------------------|
| | | | | | | <i>H. pylori</i> | <i>C. jejuni</i> |
| NTZ | | | | | | 13.0 | 39.1 |
| 3.5 | F | | | | | 0.5 | 5.6 |
| 3.6 | Cl | | | | | 0.3 | 7.8 |
| 3.7 | CF ₃ | | | | | 1.6 | 18.9 |
| 3.8 | OCH ₃ | | | | | 1.8 | 17.9 |
| 3.9 | | F | | | | 0.9 | 11.2 |
| 3.10 | | Cl | | | | 1.0 | 6.5 |
| 3.11 | | CF ₃ | | | | 3.5 | 4.7 |
| 3.12 | | OCH ₃ | | | | 1.3 | 7.2 |
| 3.13 | | CN | | | | 4.1 | 36.5 |
| 3.14 | | | F | | | 0.9 | 2.8 |
| 3.15 | | | Cl | | | 0.7 | 6.5 |
| 3.16 | | | CF ₃ | | | 1.6 | 4.7 |
| 3.17 | | | OCH ₃ | | | 1.8 | 4.5 |
| 3.18 | | | CN | | | 9.1 | 43.8 |
| 3.19 | F | | F | | | 0.4 | 7.0 |
| 3.20 | CF ₃ | | F | | | 3.4 | 23.9 |
| 3.21 | OCH ₃ | | CF ₃ | | | 0.9 | 92.1 |
| 3.22 | OCH ₃ | | NO ₂ | | | 0.6 | 9.3 |
| 3.23 | NO ₂ | | CF ₃ | | | 8.3 | 88.3 |
| 3.24 | Cl | | | CF ₃ | | 1.1 | 17.1 |
| 3.25 | F | | | | F | 0.7 | 14.0 |
| 3.26 | | | | | | 1.3 | 39.1 |

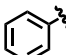
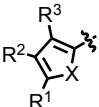
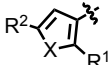
^a R = H unless otherwise noted.

Table 3.2. Biological evaluation of mono- and di-substituted benzene ring analogues. Activities against *H. pylori* and *C. jejuni* were measured and compared to NTZ.⁷

The analogues that displayed the largest improvement in activity at PFOR-utilizing organisms compared to NTZ were *para*-substituted compounds **3.14** – **3.17**. It is not clear if the success of these compounds is due to electronic modulation on the benzene ring or steric preference in the PFOR pocket. With this substitution pattern in mind, heteroaromatic tail regions were proposed to determine the significance of the benzene ring of NTZ.

3.3.2 Heteroaromatic Tail Groups

To further investigate the SAR of nitazoxanide analogues, heteroaromatic derivatives including furans and thiophenes were synthesized following the routes previously described and subjected to biological activity assays against *H. pylori* and *C. jejuni*.⁷ Furan and thiophene analogues displayed activity similar to the substituted aromatic compounds and several were more active than NTZ (Table 3.3). The addition of halogens to the thiophene ring increased activity whereas furan compounds lost activity when halogenated.

| | | | | MIC (μ M) ^b | | |
|--|---|-------------|---|-----------------------------|------------------|------------------|
| | | | | Analogue ^a | <i>H. pylori</i> | <i>C. jejuni</i> |
|  3.26 |  | |  | NTZ | 13.0 | 39.1 |
| | X = O, R ¹⁻³ = H; 3.27 | | | 3.26 | 1.3 | 3.0 |
| | X = O, R ¹ = Br; 3.28 | | | 3.27 | 1.0 | 8.4 |
| | X = O, R ^{1,2} = Br; 3.29 | | | 3.28 | 1.6 | 12.6 |
| | X = O, R ¹ = NO ₂ ; 3.30 | | | 3.29 | 2.8 | 20.2 |
| | X = S, R ¹⁻³ = H; 3.31 | | | 3.30 | 21.1 | 7.0 |
| | X = S, R ¹ = Cl; 3.32 | | | 3.31 | 2.9 | 2.9 |
| | X = S, R ³ = Cl; 3.33 | | | 3.32 | 5.2 | 6.9 |
| | X = S, R ¹ = Br; 3.34 | | | 3.33 | 5.2 | 20.7 |
| | | | | 3.34 | 3.0 | 9.9 |
| | | | | 3.35 | 0.8 | 12.5 |
| | | 3.36 | 0.7 | 5.9 | | |
| | | 3.37 | 1.5 | 2.3 | | |

^a R = H unless otherwise noted. ^b The MIC values represent the mean of 3-6 experiments performed in triplicate and the errors were within acceptable limits.

Table 3.3. Furan and thiophene analogues of NTZ and evaluation against *H. pylori* and *C. jejuni*. Compounds were synthesized using previously described coupling methods and examined for activity against PFOR-utilizing organisms.⁷

3.3.3 Full Biological Evaluation of Select Tail Region Analogues

Preliminary biological analysis of the library of tail region modifications identified compounds that outperform NTZ against *H. pylori* and *C. jejuni*. To evaluate

derivative selectivity for PFOR-containing bacteria, compounds were examined against *C. difficile*, a gram-positive PFOR-utilizing bacterium, and *E. coli*, *S. epidermidis* and *S. aureus*, which do not use PFOR for energy catabolism. It was hypothesized that the analogues of NTZ would have little to no activity against non-PFOR organisms (>50 μM), indicating that the compounds do not exhibit off-target effects at PDH. This data would also suggest low human toxicity since humans also utilize PDH. Human foreskin cell toxicity assays were performed to further support this and eliminate the risk of toxicity (Table 3.4).

$R^{1-4} = \text{H};$ **3.26**
 $R^3 = \text{Cl};$ **3.15**
 $R^3 = \text{F};$ **3.14**
 $R^2 = \text{CF}_3;$ **3.11**

$X = \text{O}, R^{1-3} = \text{H};$ **3.27**
 $X = \text{O}, R^1 = \text{NO}_2;$ **3.30**
 $X = \text{S}, R^{1-3} = \text{H};$ **3.31**

$X = \text{O};$ **3.35**
 $X = \text{S};$ **3.36**

| Analogue ^a | CC ₅₀ (μM) ^b foreskin ^c | PFOR Inhibition [Drug] = 40 μM (%) | MIC (μM) ^b | | | | |
|-----------------------|---|--|------------------------------------|------------------|---------------------|------------------|-----------------------|
| | | | <i>H. pylori</i> | <i>C. jejuni</i> | <i>C. difficile</i> | <i>S. aureus</i> | <i>S. epidermidis</i> |
| NTZ | >52.1 | 54 \pm 7 | 13.0 | 39.1 | 1.2 | 39.1 | 52.1 |
| 3.11 | >50.4 | 41.5 \pm 5.5 | 3.5 | 4.7 | 0.5 | 3.2 | 12.6 |
| 3.14 | 29.9 | 85 ^d | 0.9 | 2.8 | 3.3 | 8.4 | 15.0 |
| 3.15 | 56.4 | 55 | 0.7 | 6.5 | 0.8 | 2.0 | 26.1 |
| 3.26 | 46.3 | 68 \pm 5 ^d | 1.3 | 3.0 | 6.0 | 12.0 | 32.1 |
| 3.27 | 66.9 | 42 ^d | 1.0 | 8.4 | 2.4 | 50.2 | 66.9 |
| 3.30 | >56.3 | n.d. | 21.1 | 7.0 | n.d. | 112.6 | 28.1 |
| 3.31 | >62.7 | 56 \pm 6 ^d | 2.9 | 2.9 | 1.5 | 15.7 | 31.3 |
| 3.35 | >66.9 | 58 \pm 2 ^d | 0.8 | 12.5 | 1.7 | 50.2 | 33.4 |
| 3.36 | >62.7 | 58.5 \pm 3.5 ^d | 0.7 | 5.9 | 2.9 | 23.5 | 15.7 |

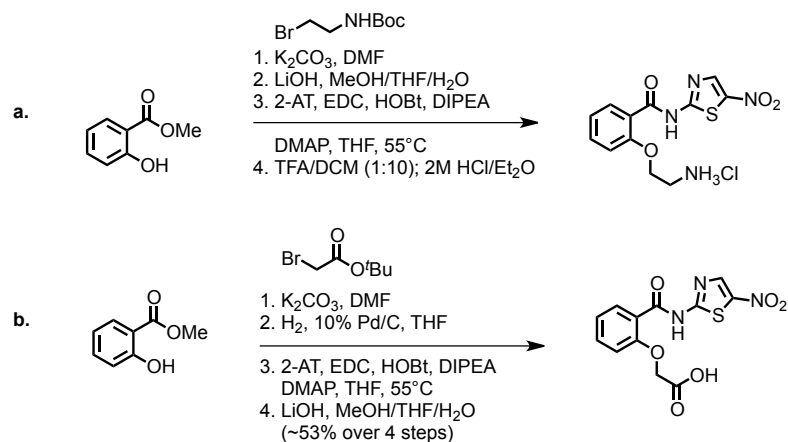
^a R = H unless otherwise noted. ^b The CC₅₀ values represent the mean of 2-3 experiments performed in triplicate, and the errors were within acceptable limits; the MIC values represent the mean of 3-6 experiments performed in triplicate, and the errors were within acceptable limits; n.d. = not determined. ^c 48 h time point. ^d Complex pattern of inhibition with two different rates.

Table 3.4. Evaluation of selected analogues against human foreskin cells and a summary of biological data.⁷

NTZ has no antibacterial activity against *E. coli* which does not possess the PFOR enzyme. Ideally, the furan and thiophene analogues would show similar inactivity to *E. coli*, confirming the role of PFOR in the mechanism of action. Only compounds **3.11** and **3.30** displayed <50 μM activity (37.8 μM and 14.1 μM respectively) at *E. coli*, indicating that the library has minimal off-target activity related to PDH inhibition (data not shown). Overall, the selected compounds were rather inactive against *S. epidermidis* and *S. aureus*. These results, combined with high CC_{50} foreskin values, suggest that the library is not active at PDH and achieves the desired selectivity at PFOR. Inhibition of PFOR was comparable to NTZ for all analogues which does not correspond with the observed increased potency at PFOR utilizing bacteria. Many compounds also exhibited a pattern of differing inhibition rates that suggest a secondary mechanism of action, perhaps due to nitroreduction.⁷

3.3.4 Solubilizing Moieties

In addition to activity issues, NTZ exhibits poor solubility and bioavailability.⁸ We sought to improve upon these characteristics by removing the 2-acetoxy group and adding solubilizing moieties like aliphatic amine tails and ether linkages. Compounds **3.38** – **3.43** were prepared using syntheses similar to those described in Scheme 3.3 and subjected to preliminary biological evaluation against *H. pylori*, *C. jejuni* and *S. aureus*, followed by secondary screening for *C. difficile* activity and direct PFOR inhibition.^{5,7,9}



Scheme 3.3. Representative syntheses towards NTZ derivatives with solubilizing groups. Synthesis of amine ether (**a**) and carboxylic acid ether (**b**).^{5,7,9}

Compounds were designed to incorporate moieties that would improve the solubility of nitrothiazole antibiotics (<10 µg/mL) and assess the electrostatics of the PFOR pocket by incorporating the carboxylic acid moiety of **3.39** and the amine tails of compounds **3.38** and **3.40** – **3.43**.⁹ The significance of the hydrogen-bond accepting *ortho*- oxygen was examined by comparing compounds **3.38** and **3.43**. Activity was assessed at *H. pylori* and *C. jejuni* before PFOR inhibition and selectivity were tested.

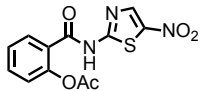
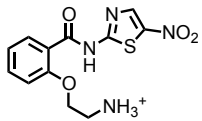
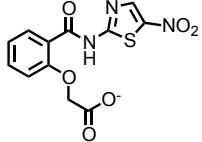
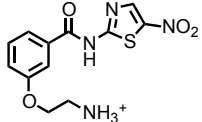
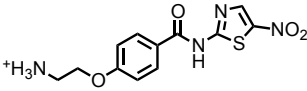
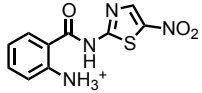
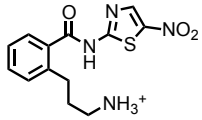
| Analogue | Structure | PFOR Inhibition [Drug] = 40 μ M (%) | MIC (μ g/mL) | | | |
|----------|---|--|-------------------|------------------|---------------------|------------------|
| | | | <i>H. pylori</i> | <i>C. jejuni</i> | <i>C. difficile</i> | <i>S. aureus</i> |
| NTZ |  | 54 \pm 7 | 4.0 | 12 | 0.125-0.25 | 16 |
| 3.38 |  | 61 | 0.5 | 4.0 | 0.5-1.0 | >32 |
| 3.39 |  | n.d. | 16 | 32 | n.d. | >32 |
| 3.40 |  | n.d. | 2 | 16 | n.d. | 32 |
| 3.41 |  | n.d. | 1 | 2 | n.d. | 16 |
| 3.42 |  | n.d. | 1 | 4 | n.d. | 32 |
| 3.43 |  | 75 \pm 0.5 | 1.0 | 6.0 | 0.25-1.0 | >32 |

Table 3.5. Biological evaluation of NTZ derivatives with solubilizing ether and aliphatic amine moieties in place of the 2-acetoxy group of NTZ.⁹

The addition of an ether linkage in place of the 2-acetoxy group of NTZ (**3.38**) showed improved activity at PFOR and decreased MIC values against *H. pylori* and *C. jejuni* compared to NTZ. Similar additions to the *meta*- and *para*- positions of the benzene ring (**3.40** and **3.41**) did not have the same success as **3.38** (Table 3.5). Compound **3.39** was prepared in order to examine the electrostatic properties of the PFOR pocket at the *ortho*- position. MIC values for **3.39** show that this substitution did not promote inhibition of bacteria growth in PFOR-utilizing organisms. Amine substituents at the *ortho*- position were also examined for electrostatic purposes.

Compound **3.42** did not show promising activity at *H. pylori* or *C. jejuni*, so no further analysis was pursued. The formal positive charge presented by the amine of **3.38** performed better than the formal negative charge of **3.42**, giving some information about the electronic properties of amino acid residues in the PFOR pocket.

The increase in PFOR inhibition and activity of compound **3.38** inspired the synthesis of **3.43**, as the propylamine substituent provided a means by which the length of the *ortho*- moiety of **3.38** could be shortened and the necessity of the ether linkage could be examined. Compound **3.43**, or amixicile (AMX), showed a drastic improvement in PFOR inhibition and comparable activities at PFOR-utilizing organisms. This provided a promising lead compound for further biological evaluation.

3.4 Amixicile

Amixicile (AMX) was discovered as a more soluble and potent alternative to NTZ, increasing solubility 1000-fold (10 mg/mL) and inhibitory activity at PFOR *in vitro* ~1.5-fold.⁹ MIC studies showed that AMX is more selective for PFOR-containing organisms than NTZ (Table 3.6). Additionally, AMX does not inhibit pili formation in *E. coli* (EAEC) or biofilm formation by *S. epidermidis* (data not shown).⁹ NTZ inhibits these processes which are necessary for regeneration of gut microflora and recovery from *C. difficile* infection.^{10,11} These properties make AMX a suitable candidate for *in vivo* evaluation.

| Analogue | MIC ($\mu\text{g/mL}$) ^a | | | | | CC ₅₀ for HFSK ^b | PFOR Inhibition (%) ^c |
|----------|---------------------------------------|------------------|------------------|----------------|------------------|--|----------------------------------|
| | <i>C. difficile</i> | <i>H. pylori</i> | <i>C. jejuni</i> | <i>E. coli</i> | <i>S. aureus</i> | | |
| NTZ | 0.125-0.25 | 4.0 | 12 | >32 | 16 | 16 | 52 \pm 4 |
| AMX | 0.25-1.0 | 1.0 | 6.0 | >32 | >32 | >32 | 75 \pm 0.5 |

^a MICs for *C. difficile* were determined by agar dilution, and those for the other bacteria were determined by microdilution. The MIC range depicted for *C. difficile* is from at least three independent determinations for each analogue. ^b Human foreskin (HFSK) cells were used for cytotoxicity testing and the drug concentration achieving 50% inhibition (CC₅₀) is reported in $\mu\text{g/mL}$. The 48h time point is depicted. The > symbol indicates that there was no toxicity over controls at the highest concentration tested. ^c The inhibitory activity of the analogues against PFOR is reported as percent inhibition at a fixed concentration of 40 μM and relative to 40 μM NTZ, which achieves 50% inhibition.

Table 3.6. Summary of *in vitro* data for NTZ versus AMX.⁹

3.4.1 *In vivo* Evaluation

In order to translate the PFOR inhibition and MIC studies to human-like conditions, AMX was given to mice in a CDI disease model. AMX was tested for mouse toxicity by gavage at concentrations of 20 and 200 mg/kg/day. At the maximum dose, AMX had a clinical score of 0.5 (data not shown) and produced a clinical score of <1 when administered via intraperitoneal injection. To compare the competitive efficacy of AMX to vancomycin and fidaxomicin, an optimized mouth lethal challenge model was used in which infected mice die of *C. difficile* infection by day 4 postinfection (Figure 3.4).⁹

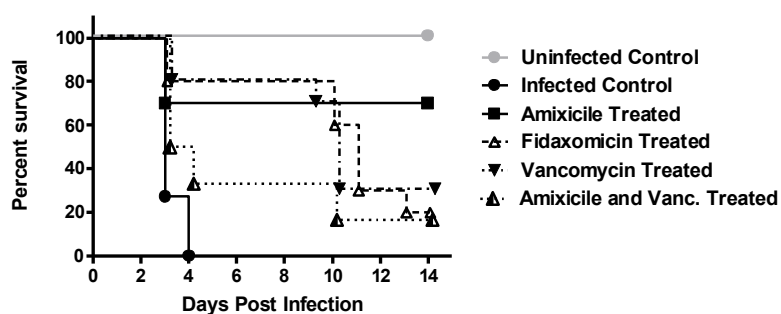


Figure 3.4. *C. difficile* infected mouse survival curves. An optimized mouse lethal challenge model was used and treatment started on day 2. The denominator for the study is 10 except for the uninfected-control and AMX and vancomycin groups, each with $n=6$.⁹

As displayed in Figure 3.4, all uninfected mice survived the study period while the infected control mice had succumbed to CDI by day 4. Initial infection survival was similar for all treatments until day 4. Animals treated with fidaxomicin and vancomycin suffered from relapse of CDI by day 10. In contrast, AMX-treated mice maintained 70% survival rate throughout the study until 14 days post infection.⁹ The lethal challenge model, which is thought to be predictive of human outcomes, shows that AMX outperforms vancomycin and fidaxomicin in treating CDI and reduces recurrence of infection similar to NTZ (Figure 3.4).

3.4.2 *In silico* Evaluation

Docking simulations (MOE; molecular operating environment 20010.0 release by Chemical Computing Group) with the 2.3 Å crystal structure of PFOR from *Desulfovibrio africanus* were performed to rationalize the proposed mechanism of action of NTZ and AMX.⁹ Simulations of NTZ binding at the lowest energy state of the PFOR active site indicated that the 5-nitro group of 2AT is anionic upon binding. This is the most probable resonance form taken by deprotonated TZ in the binding site (Figure 3.5).^{5,7,9}

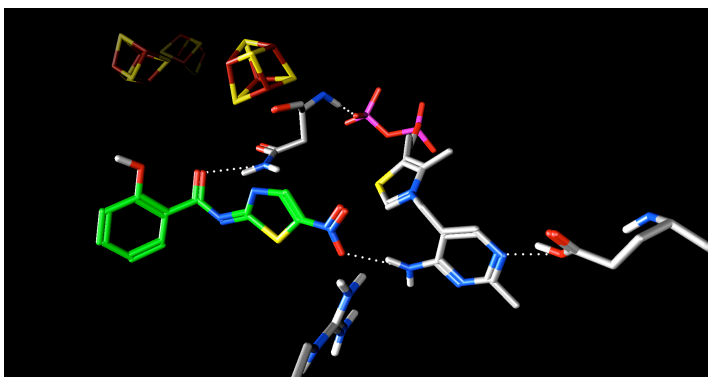


Figure 3.5. NTZ docked in PFOR crystal structure. Docking studies using the 2.3 Å PFOR crystal structure from *Desulfovibrio africanus* indicate that the anionic 5-nitro group is the most prominent resonance form in the PFOR active site. Image generated with MOE software.

Substitution of the acetoxy group (NTZ) to propylamine (AMX) greatly improves solubility. The *in silico* studies suggest that improved binding of AMX might result from electrostatic interactions of the amine tail with the acidic side chain of Asp456 that mediates acetylation of coenzyme A in the pocket, taking advantage of unexplored chemical space and leading to better selectivity (Figure 3.6). This knowledge, combined with the previous studies of benzene ring substitution, allow for further derivatives of AMX to be explored.

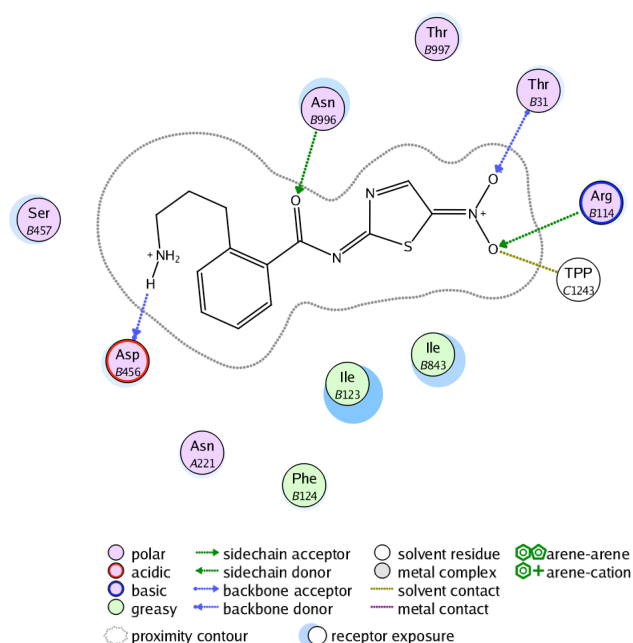


Figure 3.6. AMX presentation in the PFOR pocket. *In silico* docking studies suggest that the propylamine tail of AMX forms an electrostatic interaction with aspartic acid residue in the PFOR pocket, leading to increased percent PFOR inhibition *in vitro* and enhanced selectivity. Image generated with MOE software.

3.5 Conclusion

Initial SAR studies of NTZ derivatives proved largely inconclusive. Compounds synthesized were prepared using mostly purchasable materials which led to a vast and somewhat chaotic compound library that did not provide a logical direction for lead

development. This “flat” SAR study left a few hits with comparable biological activity to NTZ.

The strategy for developing NTZ analogues was based on previous studies where 2AT was identified as the crucial moiety for biological activity.¹⁻⁵ Head group analysis reaffirmed that the nitrothiazole group of NTZ is the most favorable of the proposed analogues when coupled with a variety of tail groups.⁵ With this knowledge, tail region derivatives were prepared using the optimized head group. Overall conclusions that can be drawn from first-generation NTZ analogues include the significance of *para*-substitution on the benzene tail region. Replacement of the benzene ring with furan and thiophene moieties did not significantly improve activity at PFOR utilizing organisms, and most showed <50 μ M activity at *S. aureus* and *S. epidermidis* which could be due to unfavorable secondary inhibition pathways. Furthermore, most compounds created were too hydrophobic to allow for in-depth biological evaluation. From the library of ~250 compounds, benzene ring substitutions and carboxylic acid couplings to 2AT preserved activity at PFOR and selectivity against PFOR-containing bacteria.⁵⁻⁷

Computer modeling of the binding interaction between PFOR and NTZ alluded to the significance of the anionic 5-nitro group and the positioning of NTZ tail region facing away from the binding site with room for motion that could be enhanced with steric bulk. The addition of solubilizing aliphatic amines to the *ortho*- position of the benzene ring in place of the 2-acetoxy group or ether linkages greatly improved PFOR inhibition and solubility. Amixicile (AMX) was discovered as a more potent, soluble and non-toxic antibiotic compared to NTZ, and outperformed current therapies in a mouse lethal challenge model of CDI. By selectively inhibiting PFOR-containing organisms and

allowing for biofilm formation without recurrence of infection, patients may recover from CDI faster with AMX.

Although AMX is more active at PFOR than NTZ, it is not as potent against PFOR-utilizing bacteria. MIC studies showed that NTZ inhibits the growth of *C. difficile* at 0.125-0.25 µg/mL while the MIC value of AMX is 0.25-1.0 µg/mL. This discrepancy could be due to differences in drug uptake that need to be resolved.⁹

References

1. Gargala, G.; Le Goff, L.; Ballet, J.; Favennec, L.; Stachulski, A. V.; Rossignol, J. Evaluation of New Thiazolide/Thiadiazolide Derivatives Reveals Nitro Group-Independent Efficacy against In Vitro Development of *Cryptosporidium parvum*. *Antimicrob. Agents Chemother.* **2010**, *54*, 1315-1318.
2. Stadelmann, B.; Scholl, S.; Müller, J.; Hemphill, A. Application of an in vitro drug screening assay based on the release of phosphoglucose isomerase to determine the structure-activity relationship of thiazolides against *Echinococcus multilocularis* metacestodes. *J. Antimicrob. Chemother.* **2010**, *65*, 512-519.
3. Pankuch, G. A.; Appelbaum, P. C. Activities of Tizoxanide and Nitazoxanide Compared to Those of Five Other Thiazolides and Three Other Agents against Anaerobic Species. *Antimicrob. Agents Chemother.* **2006**, *50*, 1112-1117.
4. Rossignol, J. F. US20080097106, 2008.
5. Ballard, T. E.; Wang, X.; Olekhovich, I.; Koerner, T.; Seymour, C.; Hoffman, P. S.; Macdonald, T. L. Biological activity of modified and exchanged 2-amino-5-nitrothiazole amide analogues of nitazoxanide. *Bioorg. Med. Chem. Lett.* **2010**, *20*, 3537-3539.
6. Hoffman, P. S.; Sisson, G.; Croxen, M. A.; Welch, K.; Harman, W. D.; Cremades, N.; Morash, M. G. Antiparasitic Drug Nitazoxanide Inhibits the Pyruvate Oxidoreductases of *Helicobacter pylori*, Selected Anaerobic Bacteria and Parasites, and *Campylobacter jejuni*. *Antimicrob. Agents Chemother.* **2007**, *51*, 868-876.
7. Ballard, T. E.; Wang, X.; Olekhovich, I.; Koerner, T.; Seymour, C.; Salamoun, J.; Warthan, M.; Hoffman, P. S.; Macdonald, T. L. Synthesis and Antimicrobial Evaluation of Nitazoxanide-Based Analogues: Identification of Selective and Broad Spectrum Activity. *ChemMedChem* **2011**, *6*, 362-377.
8. Stockis, A.; Deroubaix, X.; Lins, R.; Jeanbaptiste, B.; Calderon, P.; Rossignol, J. Pharmacokinetics of nitazoxanide after single oral dose administration in 6 healthy volunteers. *Int. J. Clin. Pharmacol. Ther.* **1996**, *34*, 349-351.
9. Warren, C. A.; van Opstal, E.; Ballard, T. E.; Kennedy, A.; Wang, X.; Riggins, M.; Olekhovich, I.; Warthan, M.; Kolling, G. L.; Guerrant, R. L.; Macdonald, T. L.; Hoffman, P. S. Amixicile, a Novel Inhibitor of Pyruvate:Ferredoxin Oxidoreductase, Shows Efficacy against *Clostridium difficile* in a Mouse Infection Model. *Antimicrob. Agents Chemother.* **2012**, *56*, 4103-4111.
10. Shamir, E. R.; Warthan, M.; Brown, S. P.; Nataro, J. P.; Guerrant, R. L.; Hoffman, P. S. Nitazoxanide Inhibits Biofilm Production and Hemagglutination by Enteroaggregative *Escherichia coli* Strains by Blocking Assembly of AafA Fimbriae. *Antimicrob. Agents Chemother.* **2010**, *54*, 1526-1533.
11. Tchouaffi-Nana, F.; Ballard, T. E.; Cary, C. H.; Macdonald, T. L.; Sifri, C. D.; Hoffman, P. S. Nitazoxanide Inhibits Biofilm Formation by *Staphylococcus epidermidis* by Blocking Accumulation on Surfaces. *Antimicrob. Agents Chemother.* **2010**, *54*, 2767-2774.

4

Pyruvate:ferredoxin Oxidoreductase Homology Models and Rational Design of Amixicile Analogues

Amixicile (AMX) was discovered as a more soluble, potent and non-toxic alternative to nitazoxanide (NTZ), reducing *C. difficile* infection (CDI) recurrence over first-line therapeutics in a mouse crisis model. The solubility of AMX was achieved through the replacement of the 2-acetoxy group of NTZ with an aliphatic propylamine tail. While this modification greatly increased solubility and direct enzyme inhibition at pyruvate:ferredoxin oxidoreductase (PFOR), the minimum concentration of drug required to prevent the growth of *C. difficile* in whole cells was higher than that of NTZ.¹ Therefore, further investigation of the properties and structure-activity relationship at PFOR of AMX and other aminonitrothiazoles is needed to better understand the utility of this class of compounds.

4.1 Pyruvate:ferredoxin Oxidoreductase Homology Model

The homology model previously used to elucidate NTZ's mechanism of action was utilized to better understand AMX's increased inhibition of PFOR. The amino substituent of AMX appears to have a stabilizing electrostatic interaction with Asp456 in the peripheral space of the PFOR pocket, producing the drug's observed increased

binding affinity, selectivity and enzyme inhibition. By understanding the orientation of the compound in the PFOR pocket, a series of AMX derivatives were incorporated into docking studies using the 2.3 Å PFOR crystal structure from *Desulfovibrio africanus* and the preferred resonance structure of the deprotonated aminonitrothiazole.

Previous studies done by our group indicated that NTZ interferes with the PFOR enzymatic reaction prior to CO₂ production.² As a result, the PFOR crystal structure in which pyruvate is bound (but not reacting) was chosen for the development of the homology model. Since the carboxylate moiety of pyruvate chelates to the thiamine pyrophosphate (TPP) cofactor of PFOR, the anionic nitro group of NTZ was placed in the active site in a similar conformation. The head group, amide linker and benzene ring of NTZ were then built into the PFOR pocket and a library of conformers was assembled and screened. Those conformations that scored the lowest in a rigid enzyme model were minimized and re-scored, this time allowing both the ligand and the protein to move. The best scoring orientation became the template for second-generation NTZ analogues. With this as a guide, various tail groups and benzene linker substitution patterns were built, screened and scored to predict their efficacy *in vitro*.

4.2 Tail Length Analysis

A conclusive SAR was required to set rational structural limits and propose compounds that would optimize binding interactions at PFOR. Previous studies by the Macdonald group and other researchers have focused on the thiazolidine moiety and benzene ring.^{1,3-6,8} The addition of a propylamine tail to the NTZ scaffold introduced a new region for optimization that could lead to more potent inhibitors in whole cells. To design such

inhibitors, the AMX scaffold was broken down into three parts for structural analysis (Figure 4.1).

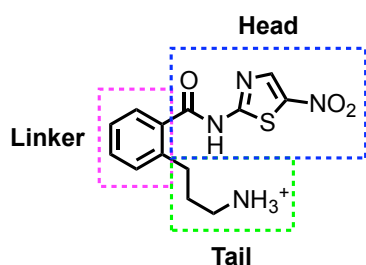
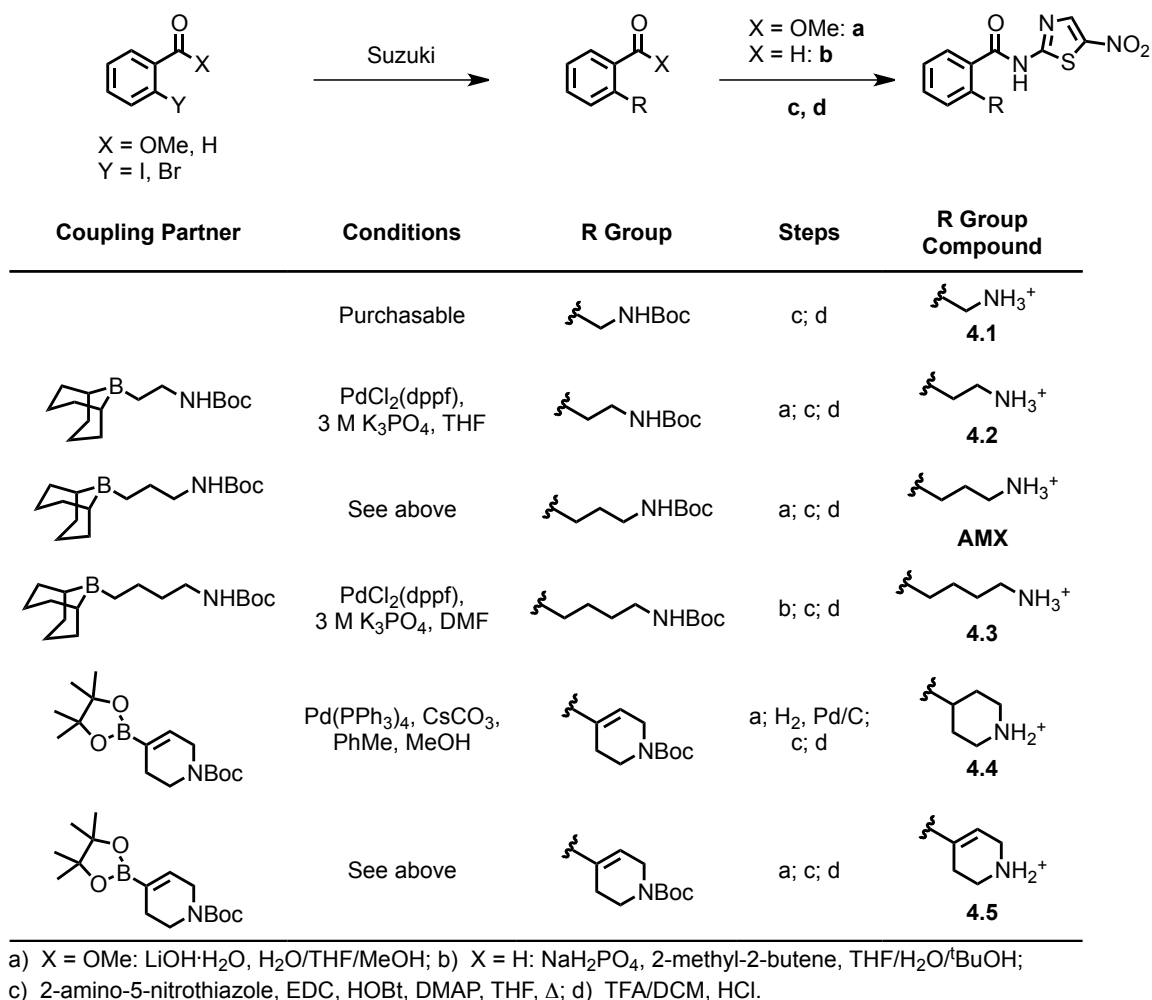


Figure 4.1. Inhibitor design from AMX. The scaffold of AMX was divided into three sections for second-generation SAR studies: the head group region (blue), linker region (pink) and tail region (green).

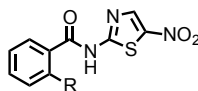
To begin optimizing the structure of AMX, the length of the tail region was analyzed. The tail in the *ortho*- position was systematically shortened, lengthened and rigidified to determine the optimal length and presentation allowed in the PFOR pocket. Compounds were prepared by first coupling the commercially available methyl benzoate or aldehyde to the desired tail region coupling partner under Suzuki conditions (Scheme 4.1).⁷ Once the tail group was added, the resulting ester or aldehyde was oxidized to the respective carboxylic acid via saponification or Pinnick oxidation.⁸ Finally, the 2-amino-5-nitrothiazole (2AT) head group was appended using EDC coupling methods previously described and the amine was deprotected to form the hydrochloric acid salt (Scheme 4.1).¹



Scheme 4.1. Synthetic routes towards proposed AMX tail analogues. Suzuki coupling was performed to append the desired amine tail to the methyl benzoate or benzaldehyde linker region, after which a Pinnick oxidation or saponification was performed to convert the carbonyl to the carboxylic acid.^{7,8} An EDC amide coupling was performed to attach the 2AT head group followed by deprotection of the amine group.^{1,6,8}

All of the compounds proposed in Scheme 4.1 were successfully synthesized.

This provided a logical series of derivatives to assess the spatial tolerance of the PFOR pocket. Previous computer modeling studies show an electrostatic interaction between the amine tail and Asp456 that could be amplified by adjusting the length and structural fluidity of the tail group. The small library was subjected to direct PFOR inhibition assays to assess preliminary activity at the enzyme (Table 4.1).¹



| Compound | R Group | PFOR Inhibition [40 μ M], % ^a |
|-------------|---------|---|
| 3.42 | | n.d. |
| 4.1 | | 51 |
| 4.2 | | n.d. |
| AMX | | 75 |
| 4.3 | | 91 |
| 4.4 | | 88 |
| 4.5 | | 95 |

^a Inhibitory activity of the analogues against PFOR is reported as percent inhibition at a fixed concentration of 40 μ M and relative to 40 μ M NTZ, which achieves 50% inhibition.

Table 4.1. Percent direct enzyme inhibition of PFOR by tail region analogues.¹

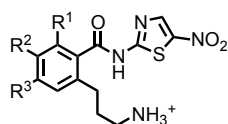
Modifying the amine tail from zero to four carbons allowed for the area of the PFOR pocket facing away from the active site to be analyzed. Preliminary PFOR inhibition assays revealed that activity drops significantly below three carbons (AMX) and the four-carbon tail of **4.3**, while more effective at the enzyme than AMX, is less active than the best three-carbon compound **4.5**. Due to the high cost of the coupling partner required for **4.3** and **4.4**, further optimization studies were performed using the propylamine tail of AMX for preliminary analysis (Scheme 4.1).

4.3 Linker Region Analysis

The Macdonald group produced a vast compound library of NTZ derivatives with relatively flat SAR in previous studies. As a result, very few conclusions could be made regarding the electronic and steric preferences of the PFOR pocket for the benzene

region.¹¹ Amixicile provided a new scaffold to build upon the linker region with some guidance from the previous studies (Figure 4.1).

A new series of AMX derivatives were proposed using the propylamine tail in the *ortho*-position (Figure 4.2). Previous SAR studies, while largely inconclusive, provided clues to substituents that could further increase activity at the PFOR enzyme and in whole cells.¹¹ Electron-donating and withdrawing groups (EDG and EWG, respectively) were added to the benzene ring linker region of AMX to establish a correlation between the spatial and electronic properties of the ring in the pocket and activity.



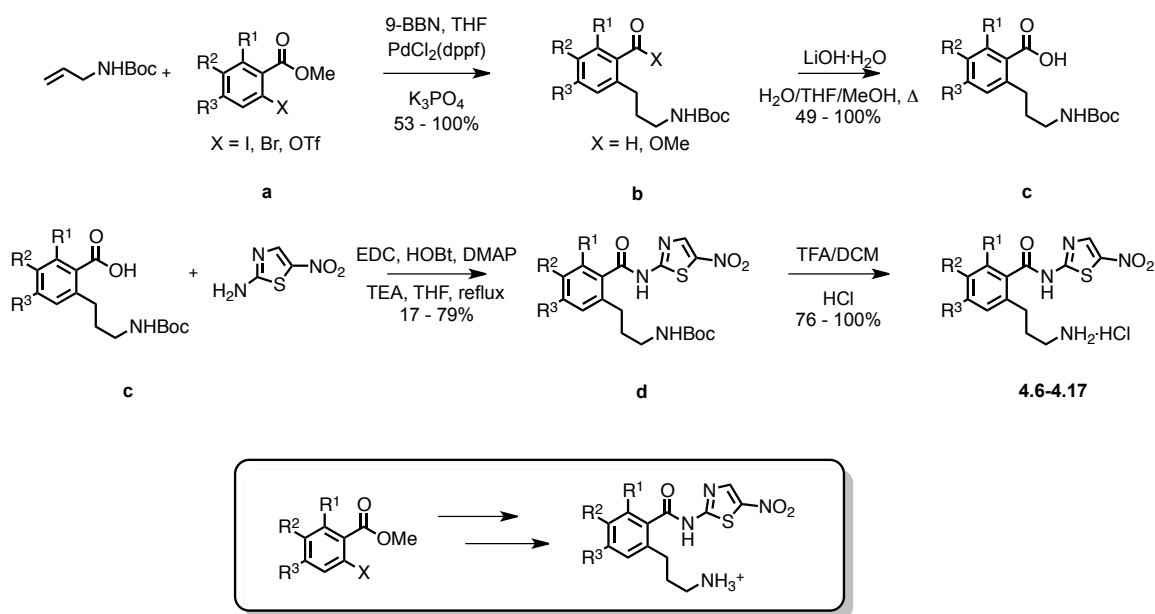
| Compound | R ¹ | R ² | R ³ | Compound | R ¹ | R ² | R ³ |
|-------------|----------------|-----------------|----------------|-------------|----------------|----------------|------------------|
| 4.6 | F | | | 4.12 | | | CH ₃ |
| 4.7 | | CH ₃ | | 4.13 | | | OCH ₃ |
| 4.8 | | F | | 4.14 | | | CN |
| 4.9 | | F | F | 4.15 | | | CF ₃ |
| 4.10 | | Cl | | 4.16 | | | Cl |
| 4.11 | | CF ₃ | | 4.17 | | | F |

^a R = H unless otherwise noted.

Figure 4.2. Proposed AMX analogues with benzene ring substitution.

The reasoning behind the benzene ring substitution was two-fold. Previous studies of NTZ revealed that *para*-substituted analogues were more active at PFOR-containing organisms than NTZ.⁸ Secondly, we sought to alter the electron density of the aromatic ring to attenuate the acidity of the amide proton ($pK_a = 6.18$ in NTZ²), shifting the equilibrium to the anionic state and leading to tighter binding. In order to manipulate the acidity of the amide proton, EDG and EWG were added to the AMX scaffold (**4.6** – **4.17**, Figure 4.2).

The optimized synthesis of AMX was used to afford a facile, 4 – 5 step synthetic route towards the proposed analogues (Scheme 4.2). Compounds **4.6** – **4.17** were prepared first by forming the appropriate methyl benzoate derivative **a** for each derivative (50 – 96% yield).⁹⁻¹¹ A Suzuki coupling to append the Boc-protected propylamine tail to the respective iodo-, bromo- and triflyl- benzoates using $\text{PdCl}_2(\text{dppf})$ at room temperature to yield compounds **b** in 53 – 100% yield.⁷ The esters were saponified to give their respective carboxylic acids **c** in 49 – 100% yield.⁸ The acids were then coupled to 2-amino-5-nitrothiazole (2AT) using EDC, HOBt and DMAP in THF and TEA to give amides **d** in 17 – 79% yield.⁸ Following the coupling reaction, the amine tail was deprotected with TFA in DCM and the hydrochloric acid salts **4.6** – **4.17** were prepared using HCl in excess ether in 76 – 100% yield (Scheme 4.2).¹



Scheme 4.2. General synthetic plan towards AMX derivatives.

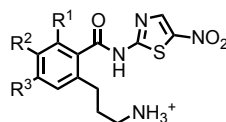
The EDC reaction to couple carboxylic acids **c** with 2AT gave the lowest yields in the synthesis of AMX derivatives **4.6** – **4.17**. These results can be attributed to the electron withdrawing effects of the 5-nitro group on the thiazole ring. Electron density is

able to resonate from the amine nitrogen to the nitro group, drastically reducing the nucleophilicity of the amine. As synthetic work progressed, refluxing with longer reaction times increased the yields of this step.

Once synthesized and assessed for purity, the compounds were submitted for biological evaluation. A direct PFOR enzyme assay was performed to observe *in vitro* effects of the analogues.^{2,6} Compounds were tested at 40 μ M, the amount of NTZ that inhibits PFOR activity by 50%. Whole cell analysis was performed in *H. pylori*, *C. difficile* and *E. coli* to assess compound selectivity for PFOR-utilizing compounds (Table 4.2).

All of the compounds that have been fully analyzed for PFOR inhibition are more active at PFOR than NTZ and AMX (Table 4.2). Moreover, these compounds proved to be ineffective towards non-PFOR-containing bacteria (>32 μ g/mL), displaying a narrow therapeutic spectrum. By selectively targeting *C. difficile* and not bacteria without the PFOR enzyme, the drug allows beneficial gut flora to regenerate, which is crucial for patient recovery from CDI. In accordance with previous trends, *para*-substituted compounds **4.12** – **4.17** were comparable to AMX at *C. difficile* with *para*-CH₃ **4.12** showing the greatest improvement in activity (0.06 μ M versus AMX 0.125 μ M). Despite this enhanced activity, the compounds are still not as active as NTZ at *C. difficile* (Table 4.2). Interestingly, *meta*-substituted compounds **4.10** and **4.11**, had the second lowest MIC value of 0.0625 μ M at *C. difficile* and much greater percent inhibition of PFOR inhibition of 97% and 93% respectively. These data show a marked improvement compared to previous studies of compounds without the propylamine tail.⁸ Of all the

substitution patterns, electron withdrawing groups in the R² (*meta*-) position have shown the greatest increase in activity and potency.



| | | | | |
|--------------------------|--|------------------|---|-----------------------|
| | R ¹ = F; 4.6 R ² = CH ₃ 4.7 R ² = F 4.8 R ^{2,3} = F 4.9 R ² = Cl 4.10 R ² = CF ₃ 4.11 | | R ³ = CH ₃ 4.12 R ³ = OCH ₃ 4.13 R ³ = CN 4.14 R ³ = CF ₃ 4.15 R ³ = Cl 4.16 R ³ = F 4.17 | |
| MIC (μg/mL) ^b | | | | |
| Analogue ^a | PFOR Inhibition [Drug] = 40 μM (%) | <i>H. pylori</i> | <i>C. difficile</i> | <i>S. epidermidis</i> |
| NTZ | 50 | 1 | 0.025 | >32 |
| AMX | 75 | 1 | 0.125 | >32 |
| 4.6 | 95 | 0.5 | 0.25 | >32 |
| 4.7 | n.d. | n.d. | n.d. | n.d. |
| 4.8 | 93 | 0.125 | 0.125 | >32 |
| 4.9 | 90 | 0.5-1 | 0.125 | >32 |
| 4.10 | 97 | 1 | 0.0625 | >32 |
| 4.11 | 93 | 0.5-1 | 0.0625 | >32 |
| 4.12 | n.d. | 1 | 0.06 | n.d. |
| 4.13 | n.d. | 0.5 | 0.125 | n.d. |
| 4.14 | n.d. | 4 | n.d. | n.d. |
| 4.15 | n.d. | 1 | 0.125 | n.d. |
| 4.16 | 94 | 0.5 | 0.164 | >32 |
| 4.17 | 86 | 1 | 0.125 | >32 |

^a R = H unless otherwise noted. ^b The MIC values represent the mean of 3-6 experiments performed in triplicate. n.d. = not determined.

Table 4.2. Biological evaluation of AMX analogues with EDG and EWG additions to the benzene linker region.

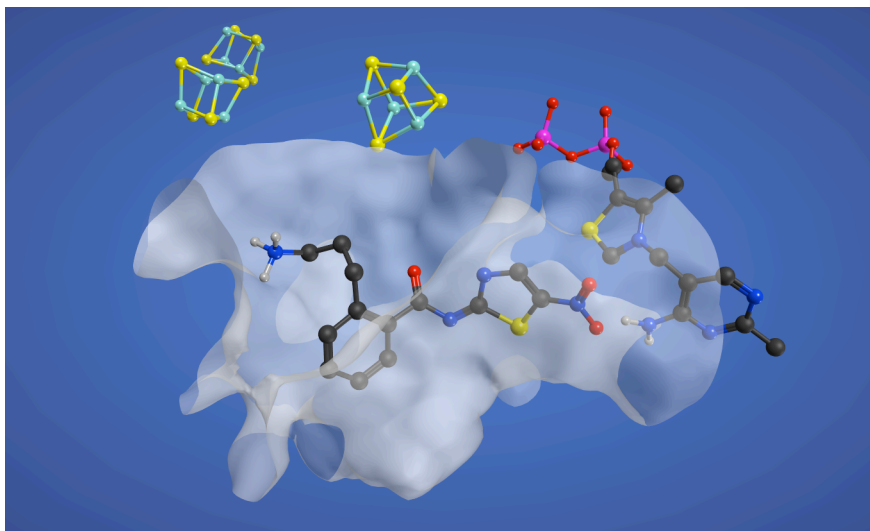


Figure 4.3. *In silico* docking image of AMX in the PFOR pocket. A crevice in the R² position explains increased *in vitro* activity at PFOR and *C. difficile*. Protein surface: white.

The *meta*-substitution pattern of **4.8**, **4.10** and **4.11** corresponds well with *in silico* docking studies of AMX, which shows a cavity that can accommodate substituents in the R² position. Fluorine, chlorine and trifluoromethyl (CF₃) are suitable substituents to fit in this cavity, with chlorine and CF₃ having larger covalent radii than fluorine. Evaluation of the *meta*-CH₃ compound **4.7** will be useful to determine if electronics also play a role in the observed increase in activity, as the methyl group is similar in size to chlorine and CF₃. Qualitative evaluation of the physical environment of the PFOR pocket supports the improved activity of compounds with R² substitution.

Despite the enhanced potency, there continue to be inconsistencies between *in vitro* enzyme and *in vivo* whole cell data. The percent PFOR inhibition has nearly doubled from NTZ, yet the MIC values for our compounds remain over twice those of NTZ (Table 4.2). This may not be detrimental to the overall goal, however, as AMX still outperforms NTZ in a CDI mouse model even with this discrepancy.¹

4.4 Hybrid Molecules

The success of the modifications to the benzene linker region can be exploited with the optimized tail region. As indicated by Table 4.1, the highest inhibition of PFOR was achieved through rigidifying the propylamine tail of AMX to the cyclized 1,2,3,6-tetrahydropyridine in compound **4.5** (Figure 4.4). This slight modification achieved 95% PFOR inhibition compared to 75% with AMX. With this in mind, hybrid molecules were proposed combining the optimized tail region of **4.5** with the *meta*-substituted linker regions of **4.10** and **4.11** (Figure 4.4).

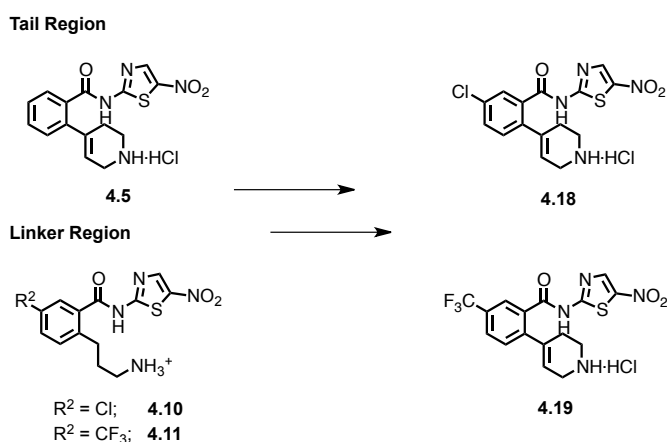
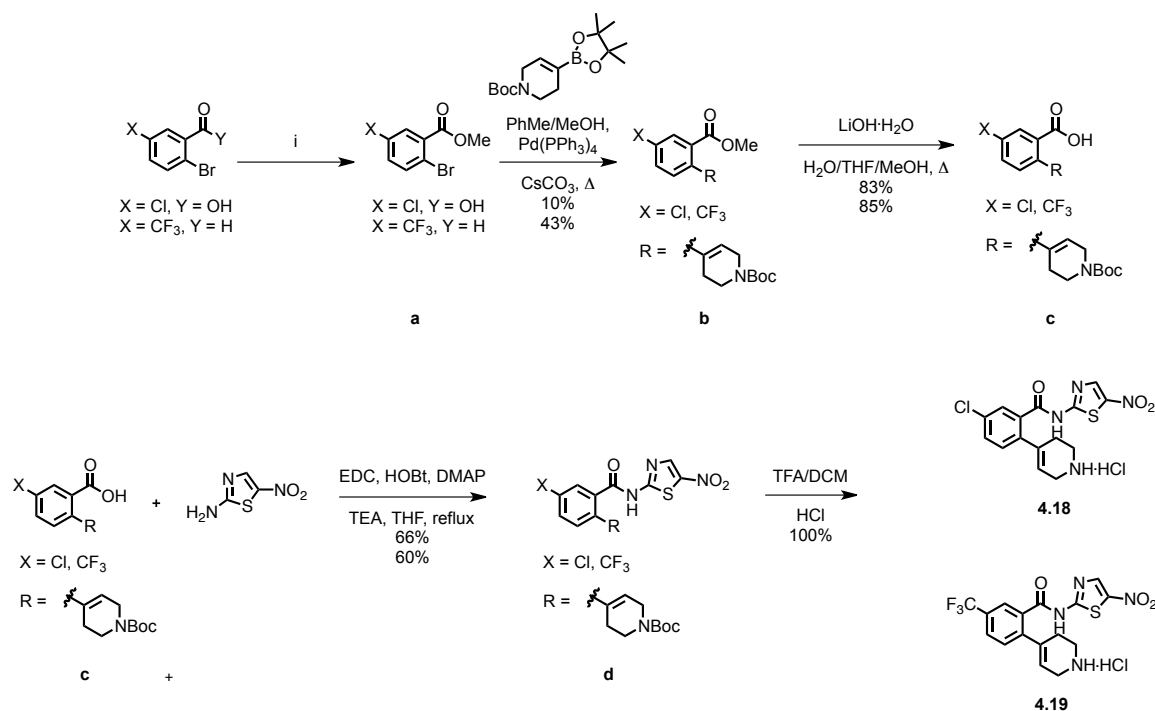


Figure 4.4. Hybrid AMX analogues. Derivatives **4.18** and **4.19** combine the optimized tail region of **4.5** with linker regions of **4.10** and **4.11** respectively.

The hybrid molecules were prepared by first converting the carboxylic acid (**4.18**) or aldehyde (**4.19**) to the respective methyl benzoate (100% and 69% yield respectively) and coupling this to *N*-Boc-1,2,3,6-tetrahydropyridine-4-boronic acid pinacol ester (10% and 43% yield respectively). The resulting methyl ester was then saponified to yield the carboxylic acid which was then coupled to 2AT, deprotected and converted to the HCl salt using previously described procedures (Scheme 4.3).¹



Scheme 4.3. Synthesis towards AMX hybrid molecules **4.18** and **4.19**. i.) When X = Cl, Y = OH: acetyl chloride, MeOH, 65°C. 100%; When X = CF₃, Y = H: 1. NaH₂PO₄, 2-methyl-2-butene, THF/H₂O/^tBuOH 2. KHCO₃, DMF, CH₃I. 69%.

The compounds are currently being subjected to biological evaluation at PFOR and bacteria cells. It is hypothesized that combining the most successful tail and linker regions to the previously optimized nitrothiazole head group will afford a more potent compound that is similar in solubility to AMX but active at *C. difficile* like NTZ.

4.5 Conclusion

The optimization of NTZ has proven successful with the synthesis of AMX, providing a more selective antibiotic that treats and prevents recurrence of CDI. Despite its improved inhibitory effect and solubility, AMX was not as potent at *C. difficile* as its predecessor.¹ In order to accrue SAR data and propose rational designs of second-

generation NTZ derivatives, computer modeling indicated a series of tail and linker region analogues to be synthesized that were effective in primary quantitative analysis.

A series of tail region derivatives was prepared to assess the spatial capacity for the amine tail in the PFOR pocket. Carbon chains that varied from 0 – 4 in length and rigidity were prepared and the three-carbon tail of AMX and its rigid analogues **4.4** and **4.5** were most effective at PFOR (Table 4.1). Further optimization on the AMX scaffold was performed in the linker (benzene) region, using *in silico* data and previous studies to design AMX analogues with varied substitution in R¹ – R³ positions (Figure 4.2). All of the derivatives proved more effective at PFOR than AMX and NTZ, however MIC values for the compounds do not reflect this improvement. Compounds with substitution at the R² or *meta*- position proved most active *in vitro* and *in vivo*, a trend that could be rationalized by looking at the binding of AMX in the PFOR pocket. Further biological evaluation on electron releasing and donating functionalities is required to complete this study, including percent PFOR inhibition and MIC values. It is our hope that a complete data set will allow us to determine sufficient SAR to rationalize the derivatives and their activities at PFOR and in whole cells.

Preliminary biological evaluation pinpointed favorable modifications to the tail and linker regions of AMX. The most effective tail group of compound **4.5** was combined with the linker regions of **4.10** and **4.11** to give **4.18** and **4.19**. It is our hope that these compounds will increase inhibition at PFOR and perhaps resolve the issue of cell transport and give lower MIC values at *C. difficile*. These compounds are currently undergoing biological evaluation .

Pending the results of the linker region library and **4.10** and **4.11**, a series of compounds will be prepared to address the discrepancy between predicted and experimental MIC values of AMX. This inconsistency is thought to be due to poor uptake of drug or efflux of compound from the bacterial cell, preventing the drug from performing to its maximum potential *in vivo*. While the aliphatic amine tail of AMX drastically improves the solubility of these compounds compared to NTZ, the cationic nature of the amine is susceptible to removal from the inside of the cell by bacterial multidrug transporters. To avoid this efflux, the basicity of the amine group can be attenuated with the addition of electronegative fluorine to the aliphatic chain and/or alkylation of the amine (Figure 4.5). We hope to find a tail that maintains adequate solubility (albeit lower than the free amine tail of AMX) and enhanced activity against PFOR-containing bacteria. Once synthesized, these compounds will be evaluated *in vitro* and *in vivo*, and hybrid molecules will be produced that combine the best amine tail with the most effective linker regions (after complete biological evaluation). *In silico* modeling and analysis of PFOR inhibitors will continue using Molecular Operating Environment (MOE) software to rationalize the success or ineffectiveness of the analogues.

References

1. Warren, C. A.; van Opstal, E.; Ballard, T. E.; Kennedy, A.; Wang, X.; Riggins, M.; Olekhnovich, I.; Warthan, M.; Kolling, G. L.; Guerrant, R. L.; Macdonald, T. L.; Hoffman, P. S. Amixicile, a Novel Inhibitor of Pyruvate:Ferredoxin Oxidoreductase, Shows Efficacy against *Clostridium difficile* in a Mouse Infection Model. *Antimicrob. Agents Chemother.* **2012**, *56*, 4103-4111.
2. Hoffman, P. S.; Sisson, G.; Croxen, M. A.; Welch, K.; Harman, W. D.; Cremades, N.; Morash, M. G. Antiparasitic Drug Nitazoxanide Inhibits the Pyruvate Oxidoreductases of *Helicobacter pylori*, Selected Anaerobic Bacteria and Parasites, and *Campylobacter jejuni*. *Antimicrob. Agents Chemother.* **2007**, *51*, 868-876.
3. Stadelmann, B.; Scholl, S.; Müller, J.; Hemphill, A. Application of an in vitro drug screening assay based on the release of phosphoglucose isomerase to determine the structure–activity relationship of thiazolides against *Echinococcus multilocularis* metacestodes. *J. Antimicrob. Chemother.* **2010**, *65*, 512-519.
4. Pankuch, G. A.; Appelbaum, P. C. Activities of Tizoxanide and Nitazoxanide Compared to Those of Five Other Thiazolides and Three Other Agents against Anaerobic Species. *Antimicrob. Agents Chemother.* **2006**, *50*, 1112-1117.
5. Rossignol, J. H. US20080097106, **2008**.
6. Ballard, T. E.; Wang, X.; Olekhnovich, I.; Koerner, T.; Seymour, C.; Hoffman, P. S.; Macdonald, T. L. Biological activity of modified and exchanged 2-amino-5-nitrothiazole amide analogues of nitazoxanide. *Bioorg. Med. Chem. Lett.* **2010**, *20*, 3537-3539.
7. Kamatani, A.; Overman, L. E. A Suzuki Coupling Method for Directly Introducing a Protected β -Aminoethyl Group into Arenes and Alkenes. Convenient Synthesis of Phenethyl and Homoallylic Amines. *J. Org. Chem.* **1999**, *64*, 8743-8744.
8. Ballard, T. E.; Wang, X.; Olekhnovich, I.; Koerner, T.; Seymour, C.; Salamoun, J.; Warthan, M.; Hoffman, P. S.; Macdonald, T. L. Synthesis and Antimicrobial Evaluation of Nitazoxanide-Based Analogues: Identification of Selective and Broad Spectrum Activity. *ChemMedChem* **2011**, *6*, 362-377.
9. Guo, W.; Li, J.; Fan, N.; Wu, W.; Zhou, P.; Xia, C. A simple and effective method for chemoselective esterification of phenolic acids. *Synth. Commun.* **2005**, *35*, 145-152.
10. Anderson, M. O.; Sherrill, J.; Madrid, P. B.; Liou, A. P.; Weisman, J. L.; DeRisi, J. L.; Guy, R. K. Parallel synthesis of 9-aminoacridines and their evaluation against chloroquine-resistant *Plasmodium falciparum*. *Bioorg. Med. Chem.* **2006**, *14*, 334-343.
11. Li, Y.; Combs, A.; Yue, E.; Li, H. *Substituted Fused Aryl and Heteroaryl Derivatives as PI3K Inhibitors*. US 12,972,155, **2011**.

5

Experimental Procedures

5.1 Biological Methods

Bacterial strains and MIC testing for *H. pylori*, *C. jejuni*, *E. coli* and *Staphylococci*.

H. pylori strain 26695 and *C. jejuni* strain H840 was done by broth dilution in 96-well microplates as previously described.^{1,2} MIC testing for staphylococcal strains and *E. coli* was performed as described previously.¹ Analogues were serially diluted beginning at 32 µg/mL and the MIC value was determined by plate reader (Molecular Dynamics) and visually at 27 h. The MIC value is the concentration of drug that completely inhibited bacterial growth. All MIC testing was performed in triplicate and individually repeated at least one time.

Bacterial strain and MIC testing for *C. difficile*.

C. difficile VPI strain 10463 was used in experiments as previously described.^{1,2} The strain was grown overnight anaerobically in chopped meat medium from stock and was subsequently subcultured to a new chopped meat medium for 5 h at 37°C. The culture was standardized to an optical density of 0.1 at OD₆₀₀. Derivatives were diluted into the agar media at concentrations ranging from

0.125-0.8 $\mu\text{g/mL}$. 10 μL aliquots of the standardized inoculum were delivered to the plates. The number of viable bacteria contained in each inoculum was $\sim 7 \times 10^4$ and 3.5×10^4 organisms. Plates were incubated in an anaerobic chamber for 18 h and read visually for growth or no growth. Anaerobic plates without compounds were used as controls. All experiments were performed in triplicate and repeated in 3 independent experiments. Acceptable limits of the assays were within one serial dilution.¹

Direct PFOR inhibition assays. *H. pylori* PFOR enzyme complex was overexpressed and purified from *E. coli* as previously described.¹⁻³ Enzyme assays were carried out at 25°C in 1 mL cuvettes in a modified Cary-14 spectrophotometer equipped with an OLIS data acquisition and Olis Spectral Works software system (On Line Instrument Co., Bogart, GA). PFOR was assayed under anaerobic conditions with 100 mM potassium phosphate (pH 7.4), 10 mM sodium pyruvate, 5 mM benzyl viologen (BV; $\epsilon = 9.2 \text{ mM}^{-1} \text{ cm}^{-1}$ at 546 nm), 0.18 mM coenzyme A (CoA), and 1 mM MgCl_2 . Analogues and NTZ were added at 40 μM and the reduction of redox-active BV dye was monitored at 546 nm. Inhibition was determined in triplicate and expressed as percentage of the uninhibited control.¹

5.2 Chemical Synthesis

General Materials and Methods: Unless otherwise noted, all nonaqueous reactions were performed under nitrogen in oven or flame-dried glassware. The nitrogen was dried by passing through a tube of Drierite. Anhydrous diethyl ether (Et_2O), chloroform

(CHCl₃), dimethyl sulfoxide (DMSO), toluene (PhMe), dichloromethane (CH₂Cl₂), methanol (MeOH), ethanol (EtOH), tetrahydrofuran (THF) and *N,N*-dimethylformamide (DMF) were purchased from Aldrich and used as received. THF, CHCl₂, and DMF were dried over activated molecular sieves (4 Å) prior to use. All reagents were purchased from commercial suppliers and used without further purification. Reactions were monitored by thin layer chromatography (TLC) on 0.25 mm Whatman precoated silica gel plates. Flash chromatography was performed with the indicated solvents and 60 Å standard grade silica gel (Sorbtech). ¹H and ¹³C NMR spectra were recorded on a Varian 300MHz or 500 MHz spectrometers at 300K unless otherwise noted. Chemical shifts (δ) are reported in ppm values relative to the residual solvent peak: ¹H CDCl₃: δ = 7.24; ¹³C CDCl₃: δ = 77.0; ¹H DMSO: δ = 2.50; ¹³C DMSO δ = 39.5. All high-resolution mass spectrometry was carried out by the Mass Spectrometry Laboratory in the School of Chemical Sciences at the University of Illinois Urbana-Champaign (Urbana, IL).

TLC Stains: KMnO₄; 3 g KMnO₄ and 20 g in K₂CO₃ in 300 mL water and 5 mL 5% NaOH. Seebach's Dip; To a stirred solution of 25 g phosphomolybdic acid and 7.5 g cerium (IV) sulfate in 479 mL water was added 25 mL conc. sulfuric acid dropwise. Ninhydrin; 1.5 g ninhydrin in 5 mL AcOH and 500 mL 95% EtOH. DNP; 12 g 2,4-dinitrophenylhydrazine in 80 mL water and 200 mL 95% EtOH was carefully diluted with 60 mL conc. sulfuric acid. All stains except DNP required TLC development on a hot plate set to 80 °C.

Other abbreviations: 1,1'-bis(diphenylphosphino)ferrocene (dppf), *N,N*-diisopropylethylamine (DIPEA), 1,1'-bis(diphenylphosphino)ferrocene (dppf), 4-dimethylaminopyridine (DMAP), 9-borabicyclo[3.3.1]nonane (9-BBN), *tert*-butoxycarbonyl (Boc), ethyl acetate (EtOAc), *N,N*-dimethylformamide (DMF), dimethylsulfoxide (DMSO), 1-ethyl-3-(3-dimethylaminopropyl)carbodiimide (EDC), *N*-hydroxybenzotriazole (HOBt), tetrahydrofuran (THF), triethylamine (TEA), methanol (MeOH), trifluoroacetic acid (TFA), minute (min), hour (h), room temperature (r.t.), singlet (s), broad singlet (bs), doublet (d), broad doublet (bd), triplet (t), quintet (quin.), doublet of doublets (dd), multiplet (m).

Liquid Chromatography and Mass Spectrometry for Evaluation of Chemical Purity. All compounds submitted for biological evaluation were determined to be > 95% pure by liquid chromatography – mass spectrometry (LCMS) evaluation carried out by the Mass Spectrometry Laboratory in the School of Chemical Sciences at the University of Illinois Urbana-Champaign (Urbana, IL). High performance LCMS was performed using Agilent 2.1x50 mm C-18 column and a Micromass Q-tof Ultima mass spectrometer. Mobile phase A consisted of HPLC grade H₂O and 0.01% TFA; mobile phase B consisted of MeCN and 0.01% TFA. LCMS identification and purity utilized a binary gradient starting with 90% A and 10% B and linearly increasing to 100% B over the course of 6 min, followed by an isocratic flow of 100%B for an additional 3 min. A flow rate of 0.5 mL / min was maintained throughout the HPLC method. The purity of all products was determined by integration of the total ion count (TIC) spectra. Retention times are abbreviated as t_R ; mass to charge ratios are abbreviated as m/z .

General Procedure A: Suzuki Coupling of Propylamine Tail.⁴ A 0.5 M solution of 9-BBN in THF (2.6 eq.) was added to *tert*-butyl *N*-allyl carbamate (1.3 eq.) at r.t. and stirred until consumption of alkene was indicated by TLC analysis (4 h unless otherwise noted). The reaction was then treated with 3 M K₃PO₄ (2.6 eq.) and diluted with THF (0.2M relative to aryl bromide, iodide, or triflate). The aryl bromide, iodide, or triflate (1.0 eq.) and PdCl₂(dppf) (3-10%) were then sequentially added and the reaction was let stir for 16-24 h. The reaction was diluted with EtOAc and washed with 1 N HCl. The organic layer was then dried over Na₂SO₄, filtered, evaporated to a dark red/brown oil, and purified by flash chromatography (15% EtOAc/hexanes) to obtain the product.

General Procedure B: Suzuki Coupling of 1,2,3,6-tetrahydropyridine Tail. *N*-Boc-1, 2, 3, 6-tetrahydropyridine boronic acid pinacol ester (1.0 eq.) was dissolved in a mixture of PhMe/MeOH (3:1) (0.14 M) and CsCO₃ (1.5 eq.) and Pd(PPh₃)₄ (5-10%) were then sequentially added. An aryl bromide or iodide (1.0 eq.) was added and the reaction was heated to reflux and stirred until consumption of aryl iodide or bromide was indicated by TLC analysis (1 h unless otherwise noted). The reaction was quenched with 1 N HCl (100x the volume of reaction), extracted with EtOAc (100x the volume of reaction), and washed with 1 N HCl (100x the volume of reaction). The organic layer was then dried over Na₂SO₄, filtered, evaporated to an oil, and purified by flash chromatography to obtain the product.

General Procedure C: Methyl Ester Saponification.¹ A methyl ester (1.0 eq.) was dissolved in a mixture of MeOH/THF/H₂O (1:1:1) (0.15 M), then LiOH•H₂O (3.0 eq.) was added. The solution was stirred at 50 °C until completion by TLC analysis (4 – 16 h). The reaction was cooled to r.t. and quenched with 1 M HCl (100x the volume of the reaction), then extracted into EtOAc (100x the volume of the reaction). The organic layer was dried over Na₂SO₄, filtered and evaporated to dryness to obtain the product.

General Procedure D: Carboxylic acid Esterification with Acetyl Chloride.¹ MeOH and acetyl chloride (5 : 1) were combined and benzoic acid (6% in MeOH) was added. The reaction was refluxed at 65 °C until complete by TLC analysis (4 – 16 h). The reaction was neutralized with NaHCO₃ and extracted with an equal volume of EtOAc. The organic layer was dried over Na₂SO₄, filtered, and evaporated to obtain the product.

General Procedure E: Carboxylic acid Esterification with Iodomethane.⁵ Carboxylic acid (1.0 eq.) was dissolved in DMF (0.67 M) and KHCO₃ (1.2 eq.) was added. The reaction was stirred ~10 m at r.t. and iodomethane (1.5 eq.) was added. The reaction was stirred at 40 °C until completion by TLC analysis (3 – 24 h). The reaction was cooled to r.t. and quenched with H₂O (3x the volume of reaction), then extracted with EtOAc (100x the volume of reaction), washed with 5 % NaHCO₃ (100x the volume of reaction), then 5 % NaCl (100x the volume of reaction). The organic layer was dried over Na₂SO₄, filtered, and evaporated to an oil unless otherwise noted.

General Procedure F: Carboxylic acid EDC Coupling.¹ Carboxylic acid (1.0 eq.), HOBT (1.1 eq.), 2-amino-5-nitrothiazole (1.5 eq.), DMAP (0.1 eq.), and EDC (1.1 eq.) were dissolved in THF (0.1 M), and TEA (4.0 eq.) was added. The solution was heated to reflux at 55 °C. Once judged complete by TLC analysis (16 – 24 h), the reaction was diluted with EtOAc (100x the volume of reaction) and washed twice with 1M HCl (100x the volume of reaction), once with saturated NaHCO₃ (100x the volume of reaction), dried over Na₂SO₄, then filtered and evaporated to dryness. The resulting residue was purified by flash chromatography (40% EtOAc/hexanes unless otherwise noted) to obtain the product.

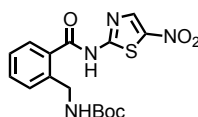
General Procedure G: N-Boc deprotection and HCl Salt Formation.^{1,2} Boc protected amine (1.0 eq.) was dissolved in CH₂Cl₂ (0.08M) and TFA (3 : 2) was added at r.t. and let stir 1 h. The solution was diluted in CHCl₃ and evaporated to dryness twice, then 6 N HCl (2.0 eq.) was added followed immediately by excess dry Et₂O to induce crystallization of the amine•HCl salt. The Et₂O was evaporated and the resulting solid was dissolved in neat H₂O, frozen at -78 °C, and lyophilized to yield the deprotected product.

General Procedure H: Conversion of Phenol to Aryl Triflate. A hydroxybenzoate (1.0 eq.) was dissolved in CH₂Cl₂ (0.41 M) and TEA (2.0 eq.) was added. The reaction mixture was cooled to 0 °C and let stir 10 m, then trifluoromethane sulfonic anhydride (1.1 eq.) was added and the reaction was let stir at r.t. until complete by TLC analysis (16 h). The reaction was quenched with NH₄Cl (100x the volume of reaction) and extracted with CH₂Cl₂ (100x the volume of reaction). The organic layer was washed with saturated

NaHCO₃ (100x the volume of reaction), dried over Na₂SO₄, filtered and evaporated to dryness to obtain the crude product.

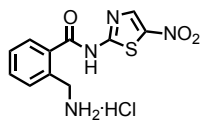
General Procedure I: Pinnick Oxidation. To a solution of an aldehyde (1.0 eq.), NaH₂PO₄ (8.0 eq.), and 2-methyl-2-butene (10 eq.) in THF, water, and tBuOH (4:4:1) (0.04 M) at rt was added sodium chlorite (4.0 eq.) and let stir for 1 h. The reaction was diluted with EtOAc (10x the volume of the reaction's mixture of solvents), and washed 3x with 1 N HCl (5x the volume of the reaction's mixture of solvents). The organic layer was then dried with Na₂SO₄, and evaporated to a white solid. No further purification was undertaken.

***tert*-Butyl 2-((5-nitrothiazol-2-yl)carbamoyl)benzylcarbamate (4.1d)**

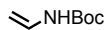


4.1d

General procedure **F** was used to couple 2-(Bocaminomethyl) benzoic acid (250 mg, 0.99 mmol) to 2-amino-5-nitrothiazole (216 mg, 1.49 mmol) with 1.0 eq. DMAP and 2.0 eq. TEA. Purified by flash chromatography (35 – 40% EtOAc/hexanes) to yield 150 mg of the title compound. 40%. Tan powder. R_f = 0.69 (50% EtOAc in hexanes). ¹H NMR (300 MHz, Chloroform-d) δ 7.77 (s, 1H), 7.66 (d, J = 7.6 Hz, 1H), 7.58 (d, J = 7.4 Hz, 2H), 7.40 (td, J = 7.3, 1.8 Hz, 1H), 7.26 (s, 1H), 5.65 (s, 1H), 4.40 (d, J = 6.3 Hz, 2H), 1.35 (s, 9H). ¹³C NMR (75 MHz, Chloroform-d) δ 168.12, 162.71, 140.48, 133.02, 130.95, 128.75, 127.99, 80.41, 42.86, 28.50.

2-(Aminomethyl)-N-(5-nitrothiazol-2-yl)benzamide hydrochloride (4.1)**4.1**

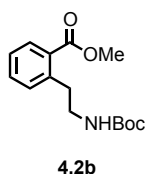
General procedure **G** was performed to deprotect **4.1d** (135 mg, 0.36 mmol) to yield 113 mg of the title compound. 99%. Pink powder. ^1H NMR (500 MHz, DMSO- d_6) δ 13.78 (s, 1H), 8.73 (d, J = 1.8 Hz, 1H), 8.57 – 8.32 (m, 3H), 7.90 (d, J = 7.7 Hz, 1H), 7.73 – 7.65 (m, 2H), 7.57 (m, J = 8.2, 5.3, 3.2 Hz, 1H), 4.22 (q, J = 5.9 Hz, 2H). ^{13}C NMR (126 MHz, DMSO- d_6) δ 168.21, 162.69, 147.95, 142.95, 142.49, 134.39, 132.93, 131.70, 129.99, 129.16.

***tert*-Butyl vinylcarbamate (4.2e)⁶****4.2e**

To a solution of sodium azide (9.58 g, 147 mmol) in a mixture of $\text{H}_2\text{O}/\text{PhMe}$ (5:3) (1.5 M) at 0°C was added acryloyl chloride (10.0 mL, 123 mmol). The reaction mixture was stirred for 5 h at 0°C and the aqueous layer was removed. The organic layer was washed 2x with 10% Na_2CO_3 , dried over Na_2SO_4 and added to a solution of hydroquinone (0.05 eq.), pyridine (0.06 eq.) and $t\text{BuOH}$ (1.2 eq.). The mixture was heated to reflux at 90°C and let stir until complete by TLC analysis (30 m). The reaction mixture was cooled to r.t. and evaporated to dryness. Purified by flash chromatography (10% EtOAc/hexanes) to yield 5.02 g of the title compound. 28%. White solid. R_f = 0.49 (10% EtOAc in hexanes; Ninhydrin/ Δ). ^1H NMR (300 MHz, Chloroform- d) δ 7.15 (d, J = 11.0 Hz, 1H),

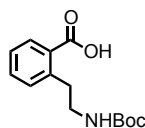
6.55 (dt, $J = 15.6, 9.8$ Hz, 1H), 4.36 (d, $J = 15.8$ Hz, 1H), 4.05 (d, $J = 8.8$ Hz, 1H), 1.33 (s, 9H). ^{13}C NMR (75 MHz, Chloroform- d) δ 153.27, 130.38, 92.24, 80.26, 28.33.

Methyl 2-(2-((*tert*-butoxycarbonyl)amino)ethyl)benzoate (4.2b)



A 0.5 M solution of 9-BBN in THF (3.0 eq.) was added to a solution of **4.2e** (1.28 g, 8.94 mmol) in THF (0.25 M) at 0°C. The reaction mixture was warmed to r.t. and stirred until consumption of alkene was indicated by TLC analysis (9 h). The reaction was then cooled to 0°C and treated with 3 M K_3PO_4 (3.0 eq.) and 2-iodomethylbenzoate (875 μL , 5.96 mmol) and $\text{PdCl}_2(\text{dppf})$ (5%) were then sequentially added and the reaction was let stir for 16 h. Boc_2O was added (1.3 g, 5.96 mmol) and the reaction was let stir 30 m. The reaction was diluted with EtOAc and washed with neat H_2O . The organic layer was then dried over Na_2SO_4 , filtered, evaporated to an oil, and purified by flash chromatography (20% EtOAc/hexanes) to yield 371 mg of the title compound which was taken on to the next step. 22%. Clear gel. $R_f = 0.46$ (20% EtOAc in hexanes; Ninhydrin/ Δ). ^1H NMR (300 MHz, Chloroform- d) δ 8.58 (s, 0H), 7.81 (d, $J = 8.0$ Hz, 1H), 7.41 – 7.31 (m, 1H), 7.28 – 7.15 (m, 2H), 3.80 (s, 3H), 3.31 (q, $J = 6.6$ Hz, 2H), 3.06 (t, $J = 7.0$ Hz, 2H), 1.33 (s, 9H). ^{13}C NMR (75 MHz, Chloroform- d) δ 168.07, 156.18, 141.27, 132.28, 131.82, 130.93, 129.74, 126.55, 78.97, 52.12, 28.52.

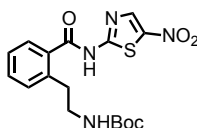
2-(2-((*tert*-Butoxycarbonyl)amino)ethyl)benzoic acid (4.2c)



4.2c

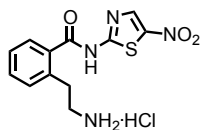
General procedure **C** was used to saponify **4.2b** (186 mg, 0.67 mmol). Extraction of the reaction mixture yielded 20 mg of the title compound. Product was taken on to next reaction without further purification and analysis. 11%.

***tert*-Butyl 2-((5-nitrothiazol-2-yl)carbamoyl)phenethylcarbamate (4.2d)**

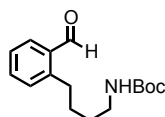


4.2d

General procedure **F** was used to couple **4.2c** (20 mg, 0.075 mmol) to 2-amino-5-nitrothiazole (16 mg, 0.11 mmol). Purified by flash chromatography (40% EtOAc/hexanes) to yield 10 mg of the title compound. 34%. Off-white solid. R_f = 0.69 (50% EtOAc in hexanes; Ninhydrin/ Δ). ^1H NMR (300 MHz, Chloroform- d) δ 11.79 (s, 1H), 7.86 (s, 1H), 7.56 (t, J = 7.4 Hz, 2H), 7.38 (dd, J = 8.4, 6.6 Hz, 2H), 4.90 (s, 1H), 3.44 (q, J = 6.7 Hz, 2H), 3.01 (t, J = 6.8 Hz, 2H), 1.32 (s, 9H).

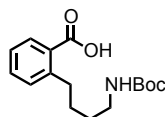
2-(2-Aminoethyl)-N-(5-nitrothiazol-2-yl)benzamide hydrochloride (4.2)**4.2**

General procedure **G** was performed to deprotect **4.2d** (10 mg, 0.025 mmol) to yield 8.2 mg of the title compound. Quant. ^1H NMR (500 MHz, DMSO- d_6) δ 13.62 (s, 1H), 8.71 (d, $J = 0.9$ Hz, 1H), 7.85 (s, 3H), 7.72 (d, $J = 7.7$ Hz, 1H), 7.58 (t, $J = 7.8$ Hz, 1H), 7.44 (t, $J = 7.4$ Hz, 2H), 3.14 – 2.95 (m, 4H). LCMS: $m/z = 293.1$. HRMS m/z calc. for $\text{C}_{12}\text{H}_{13}\text{N}_4\text{O}_3\text{S}$ (M+H), 293.0708; found, 293.0709.

***tert*-Butyl (4-(2-formylphenyl)butyl)carbamate (4.3b)****4.3b**

General procedure **A** was used to couple *tert*-butyl but-3-en-1-yl carbamate (1.54 g, 8.97 mmol) to 2-bromobenzaldehyde (805 μL , 6.90 mmol) in DMF (0.3 M). Purified by flash chromatography (15% EtOAc/hexanes) to yield 1.709 g of the title compound. 89%. Clear, colorless oil. $R_f = 0.5$ (20% EtOAc in hexanes; KMnO_4/Δ). ^1H NMR (300 MHz, Chloroform- d) δ 10.09 (s, 1H), 7.66 (dt, $J = 7.6, 1.4$ Hz, 1H), 7.43 – 7.30 (m, 1H), 7.29 – 7.18 (m, 1H), 7.13 (d, $J = 7.6$ Hz, 1H), 5.06 – 4.82 (m, 1H), 4.33 – 4.13 (m, 1H), 3.03 (q, $J = 14.7, 10.6$ Hz, 2H), 2.90 (t, $J = 7.3$ Hz, 2H), 1.54 – 1.40 (s, 9H). ^{13}C NMR (75 MHz, Chloroform- d) δ 192.51, 156.22, 145.18, 133.85, 133.75, 132.43, 131.17, 126.63, 78.85, 40.14, 32.27, 29.98, 29.29, 28.52, 26.54.

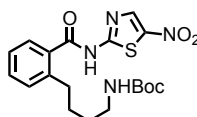
2-(4-((*tert*-Butoxycarbonyl)amino)butyl)benzoic acid (4.3c**)**



4.3c

General procedure **I** was performed to oxidize aldehyde **4.3b** (1.71 g, 6.16 mmol). Purified by flash chromatography (20% EtOAc/hexanes) to yield 900 mg of the title compound. 50%. Clear, colorless oil. R_f = 0.12 (20% EtOAc in hexanes; KMnO_4/Δ). ^1H NMR (500 MHz, Chloroform- d) δ 13.46 – 9.45 (s, 1H), 7.99 (d, J = 8.0 Hz, 1H), 7.40 (t, J = 7.6 Hz, 1H), 7.22 (t, J = 7.4 Hz, 2H), 6.45 (s, 1H), 5.06 – 4.61 (m, 1H), 3.34 – 2.76 (m, 4H), 1.73 – 1.57 (m, 2H), 1.43 (d, J = 25.0 Hz, 9H). ^{13}C NMR (126 MHz, Chloroform- d) δ 172.02, 156.20, 144.98, 132.48, 131.50, 131.09, 128.63, 125.89, 79.10, 40.22, 34.01, 29.83, 28.79, 28.39.

***tert*-Butyl (4-(2-((5-nitrothiazol-2-yl)carbamoyl)phenyl)butyl)carbamate (**4.3d**)**

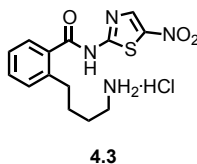


4.3d

General procedure **F** was used to couple **4.3c** (900 mg, 3.07 mmol) to 2-amino-5-nitrothiazole (668 mg, 4.61 mmol). Purified by flash chromatography (30-45% EtOAc/hexanes) to yield 85 mg of the title compound. 7%. Tan solid. R_f = 0.61 (50% EtOAc in hexanes; Ninhydrin/ Δ). ^1H NMR (300 MHz, DMSO- d_6) δ 13.53 (s, 1H), 8.68 (s, 1H), 7.59 (dd, J = 7.7, 1.3 Hz, 1H), 7.49 (td, J = 7.5, 1.4 Hz, 1H), 7.41 – 7.28 (m, 2H), 6.75 (t, J = 5.8 Hz, 1H), 2.86 (q, J = 6.6 Hz, 2H), 2.72 (t, J = 7.6 Hz, 2H), 1.59 – 1.41 (m,

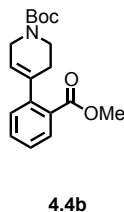
2H), 1.32 (s, 9H). ^{13}C NMR (75 MHz, Chloroform- d) δ 174.22, 167.42, 160.96, 148.23, 147.46, 147.00, 137.62, 136.87, 135.69, 133.93, 131.29, 82.73, 37.64, 34.82, 33.89, 33.66.

2-(4-Aminobutyl)-*N*-(5-nitrothiazol-2-yl)benzamide hydrochloride (4.3)



General procedure **G** was used to deprotect **4.3d** (60 mg, 0.14 mmol). Sublimation yielded 49.0 mg of the title compound. 99%. Off-white solid. ^1H NMR (300 MHz, DMSO- d_6) δ 13.58 (s, 1H), 8.68 (s, 1H), 8.05 (s, 3H), 7.61 (d, J = 7.5 Hz, 1H), 7.55 – 7.46 (m, 1H), 7.44 – 7.29 (m, 2H), 2.74 (t, J = 6.6 Hz, 4H), 1.67 – 1.47 (m, 4H). ^{13}C NMR (75 MHz, DMSO- d_6) δ 169.37, 162.64, 143.34, 142.71, 141.84, 132.73, 132.23, 130.96, 129.31, 126.68, 39.12, 32.70, 28.60, 27.44. LCMS: t_R = 2.58; m/z = 321.1. HRMS m/z calc. for $\text{C}_{14}\text{H}_{17}\text{N}_4\text{O}_3\text{S}$ ($\text{M}+\text{H}$), 321.1021; found, 321.1012.

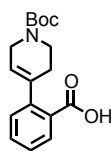
***tert*-Butyl 4-(2-(methoxycarbonyl)phenyl)-5,6-dihydropyridine-1(2*H*)-carboxylate (4.4b)**



General procedure **B** was performed to couple 2-iodomethylbenzoate (238 μL , 1.62 mmol) to *N*-Boc-1, 2, 3, 6-tetrahydropyridine-4-boronic acid pinacol ester (500 mg, 1.62

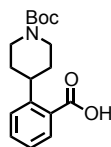
mmol). Purified by flash chromatography (10-15% EtOAc/hexanes) to yield 514 mg of the title compound. 99%. Clear, colorless oil. $R_f = 0.82$ (20% EtOAc in hexanes; Ninhydrin/ Δ). ^1H NMR (500 MHz, Chloroform- d) δ 7.79 (dd, $J = 7.8, 1.3$ Hz, 1H), 7.41 (td, $J = 7.5, 1.4$ Hz, 1H), 7.28 (td, $J = 7.7, 1.3$ Hz, 1H), 7.15 (dd, $J = 7.6, 1.2$ Hz, 1H), 5.47 (s, 1H), 3.99 (s, 2H), 3.80 (s, 3H), 3.69 – 3.55 (m, 2H), 2.32 (d, $J = 26.3$ Hz, 2H), 1.46 (s, 9H). ^{13}C NMR (126 MHz, Chloroform- d) δ 168.00, 144.02, 131.77, 130.08, 129.61, 129.18, 127.08, 120.84, 79.49, 52.04, 43.76, 39.96, 30.23, 28.47.

2-(1-(*tert*-Butoxycarbonyl)-1,2,3,6-tetrahydropyridin-4-yl)benzoic acid (4.4c)

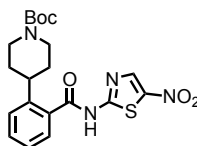


4.4c

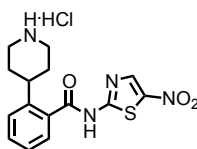
General procedure **C** was used to saponify **4.4b** (514 mg, 1.62 mmol). Extraction of the reaction mixture yielded 486 mg of the title compound. 99%. ^1H NMR (300 MHz, Chloroform- d) δ 11.28 (s, 1H), 7.96 (d, $J = 7.9$ Hz, 1H), 7.47 (t, $J = 7.6$ Hz, 1H), 7.33 (t, $J = 7.6$ Hz, 1H), 7.19 (d, $J = 7.6$ Hz, 1H), 5.50 (s, 1H), 4.03 (s, 2H), 3.73 – 3.47 (m, 2H), 2.35 (s, 2H), 1.48 (s, 9H). ^{13}C NMR (75 MHz, Chloroform- d) δ 172.10, 155.46, 145.08, 138.77, 132.78, 131.18, 130.21, 128.52, 127.45, 120.76, 80.11, 44.00, 40.38, 30.58, 28.72.

2-(1-(*tert*-Butoxycarbonyl)piperidin-4-yl)benzoic acid (4.4e)**4.4e**

Alkene **4.4c** (479 mg, 1.58 mmol) was solvated in EtOAc (0.23 M) and transferred to a flask containing 20% Pd(OH)₂/C (200 mg, 8% wt.). The reaction flask was evacuated and flushed with H₂ for 2 h. The H₂ was released and the reaction mixture was diluted with EtOAc, filtered through Celite and evaporated to dryness to yield 482 mg of the title compound. 99%. Clear, colorless oil. R_f = 0.62 (5% MeOH in CH₂Cl₂; KMnO₄/Δ). ¹H NMR (300 MHz, Chloroform-d) δ 11.55 (s, 1H), 7.89 (dd, J = 7.8, 1.4 Hz, 1H), 7.43 (td, J = 7.6, 1.4 Hz, 1H), 7.35 – 7.27 (m, 1H), 7.22 (td, J = 7.6, 1.3 Hz, 1H), 4.45 – 4.12 (m, 2H), 3.66 (tt, J = 12.1, 3.2 Hz, 1H), 2.80 (t, J = 13.1 Hz, 2H), 1.90 – 1.72 (m, 2H), 1.60 (dp, J = 11.6, 8.3, 6.6 Hz, 2H), 1.46 (d, J = 1.4 Hz, 9H). ¹³C NMR (75 MHz, Chloroform-d) δ 172.42, 155.33, 147.38, 132.66, 131.19, 129.54, 127.04, 126.21, 79.97, 44.85, 38.44, 33.29, 28.69.

tert*-Butyl 4-(2-((5-nitrothiazol-2-yl)carbamoyl)phenyl)piperidine-1-carboxylate*(4.4d)****4.4d**

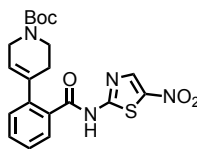
General procedure **F** was used to couple **4.4e** (482 mg, 1.58 mmol) to 2-amino-5-nitrothiazole (344 mg, 2.37 mmol). Purified by flash chromatography (30-45% EtOAc/hexanes) to yield 465 mg of the title compound. 68%. Off-white solid. R_f = 0.58 (50% EtOAc in hexanes; Ninhydrin/ Δ). ^1H NMR (500 MHz, DMSO- d_6) δ 13.57 (s, 1H), 8.68 (s, 1H), 7.54 (ddd, J = 16.9, 7.5, 1.4 Hz, 2H), 7.48 (dd, J = 8.0, 1.3 Hz, 1H), 7.36 (td, J = 7.5, 1.3 Hz, 1H), 4.04 (d, J = 12.8 Hz, 2H), 3.33 (s, 1H), 2.99 (tt, J = 12.0, 3.4 Hz, 1H), 2.72 (s, 2H), 2.49 (h, J = 2.0 Hz, 2H), 1.81 – 1.66 (m, 2H), 1.54 (qt, J = 10.0, 4.3 Hz, 2H), 1.40 (s, 9H). ^{13}C NMR (126 MHz, DMSO- d_6) δ 169.33, 162.31, 154.27, 144.88, 143.05, 142.57, 132.87, 132.01, 128.69, 127.44, 126.51, 79.02, 38.78, 33.14, 28.57.

***N*-(5-nitrothiazol-2-yl)-2-(piperidin-4-yl)benzamide hydrochloride (4.4)****4.4**

General procedure **G** was used to deprotect **4.4d** (451 mg, 1.04 mmol). Sublimation yielded 381 mg of the title compound. 99%. Tan solid. ^1H NMR (500 MHz, DMSO- d_6)

δ 13.61 (s, 1H), 9.30 – 9.10 (m, 1H), 9.03 (d, J = 11.1 Hz, 1H), 8.69 (s, 1H), 7.60 (td, J = 7.4, 1.2 Hz, 2H), 7.48 – 7.34 (m, 2H), 3.43 – 3.23 (m, 3H), 3.14 (tt, J = 12.0, 3.4 Hz, 1H), 3.03 – 2.83 (m, 2H), 2.01 (qd, J = 12.6, 3.6 Hz, 2H), 1.95 – 1.80 (m, 2H). ^{13}C NMR (126 MHz, DMSO- d_6) δ 169.16, 162.39, 143.96, 143.04, 142.54, 132.97, 132.20, 128.88, 126.98, 126.90, 43.83, 36.23, 29.75. LCMS: m/z = 333.1. HRMS m/z calc. for $\text{C}_{15}\text{H}_{17}\text{N}_4\text{O}_3\text{S}$ (M+H), 333.1021; found, 333.1015.

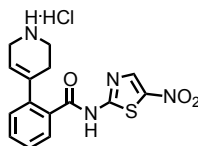
***tert*-Butyl 4-(2-((5-nitrothiazol-2-yl)carbamoyl)phenyl)-5,6-dihydropyridine-1(2H)-carboxylate (4.5d)**



4.5d

General procedure **F** was used to couple **4.4c** (228 mg, 0.75 mmol) to 2-amino-5-nitrothiazole (164 mg, 1.13 mmol). Purified by flash chromatography (30-45% EtOAc/hexanes) to yield 274 mg of the title compound. 85%. Tan solid. R_f = 0.51 (50% EtOAc in hexanes; Ninhydrin/ Δ). ^1H NMR (300 MHz, DMSO- d_6) δ 13.47 (s, 1H), 8.65 (s, 1H), 8.30 (s, 1H), 7.67 – 7.49 (m, 2H), 7.49 – 7.31 (m, 2H), 5.58 (s, 1H), 3.81 (q, J = 2.8 Hz, 2H), 3.43 (t, J = 5.4 Hz, 2H), 2.40 – 2.23 (m, 2H), 1.36 (s, 9H). ^{13}C NMR (75 MHz, DMSO- d_6) δ 169.72, 162.53, 154.48, 143.38, 142.66, 142.13, 136.16, 132.62, 131.93, 129.05, 128.93, 127.79, 124.36, 79.85, 44.16, 43.69, 41.41, 29.56, 28.71.

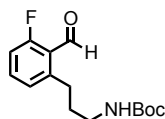
***N*-(5-nitrothiazol-2-yl)-2-(1,2,3,6-tetrahydropyridin-4-yl)benzamide hydrochloride (4.5)**



4.5

General procedure **G** was used to deprotect **4.5d** (270 mg, 0.63 mmol). Sublimation yielded 228 mg of the title compound. 99%. Tan solid. ^1H NMR (300 MHz, DMSO- d_6) δ 13.59 (s, 1H), 9.28 (s, 2H), 8.69 (s, 1H), 7.65 (d, $J = 1.0$ Hz, 1H), 7.59 (s, 1H), 7.47 (d, $J = 1.1$ Hz, 1H), 7.37 (s, 1H), 5.60 (s, 1H), 3.59 (s, 2H), 3.16 (s, 2H), 2.52 (s, 2H). ^{13}C NMR (75 MHz, DMSO- d_6) δ 169.28, 162.57, 143.38, 142.75, 141.26, 136.30, 132.32, 132.21, 129.29, 129.14, 128.31, 120.35, 41.74, 26.24. LCMS: $t_R = 2.58$; $m/z = 331.1$. HRMS m/z calc. for $\text{C}_{15}\text{H}_{15}\text{N}_4\text{O}_3\text{S}$ ($\text{M}+\text{H}$), 331.0865; found, 331.0854.

***tert*-Butyl (3-(3-fluoro-2-formylphenyl)propyl)carbamate (4.6b)**

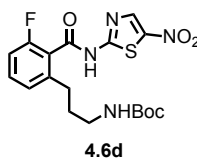


4.6b

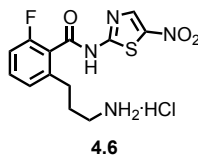
General procedure **A** was used to couple 2-bromo-6-fluorobenzaldehyde (500 mg, 2.46 mmol) and *tert*-butyl *N*-allyl carbamate (503 mg, 3.20 mmol). Purified by flash chromatography (20% EtOAc/hexanes) to yield 542 mg of the title compound. 78%. Clear and colorless oil. $R_f = 0.43$ (20 % EtOAc in hexanes; Ninhydrin/ Δ). ^1H NMR (300 MHz, CDCl_3) δ 10.44 (s, 1H), 7.40 (dd, $J = 7.6, 6.5$ Hz, 1H), 7.11 – 6.89 (m, 1H), 6.83 (t, $J = 7.5$ Hz, 1H), 4.96 (s, 1H), 3.12 (dt, $J = 6.2, 6.1$ Hz, 2H), 2.93 (t, $J = 7.7$ Hz, 2H), 1.61

– 1.50 (m, 2H), 1.39 (s, 9H). ^{13}C NMR (75 MHz, CDCl_3) δ 189.21 (d, $J = 11.4$ Hz), 166.79 (d, $J = 257.9$ Hz), 156.33 (s), 146.34 (s), 135.56 (d, $J = 10.4$ Hz), 127.14 (s), 114.29 (d, $J = 21.8$ Hz), 79.14 (s), 40.37 (s), 31.39 (s), 31.00 (s), 28.59 (s).

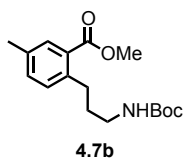
***tert*-Butyl (3-(3-fluoro-2-((5-nitrothiazol-2-yl)carbamoyl)phenyl)propyl)carbamate (4.6d)**



General procedure **I** was performed to oxidize aldehyde **4.6b** (432 mg, 1.54 mmol) to 2-(3-((*tert*-butoxycarbonyl)amino)propyl)-6-fluorobenzoic acid **4.6c** and immediately submitted to the conditions described in general procedure **F**. Purified by flash chromatography (40% EtOAc/hexanes) to yield 222 mg of the title compound. 34% over 2 steps. Yellow gel. $R_f = 0.64$ (50 % EtOAc in hexanes; KMnO_4). ^1H NMR (300 MHz, CDCl_3) δ 12.94 (s, 1H), 7.53 – 7.38 (m, 2H), 7.16 (d, $J = 7.7$ Hz, 1H), 7.03 (t, $J = 8.9$ Hz, 1H), 4.90 (s, $J = 8.8$ Hz, 1H), 3.07 (dt, $J = 6.3, 6.2$ Hz, 2H), 2.68 (t, $J = 7.5$ Hz, 2H), 1.84 – 1.71 (m, 2H), 1.31 (s, 9H). ^{13}C NMR (75 MHz, CDCl_3) δ 164.38 (s), 162.21 (s), 159.54 (d, $J = 249.6$ Hz), 156.34 (s), 143.61 (s), 139.67 (s), 133.04 (d, $J = 8.6$ Hz), 126.15 (s), 121.68 (d, $J = 15.7$ Hz), 113.89 (d, $J = 21.3$ Hz), 79.38 (s), 40.02 (s), 31.64 (s), 30.56 (s), 28.49 (s).

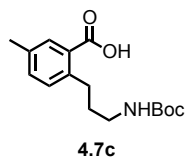
2-(3-Aminopropyl)-6-fluoro-N-(5-nitrothiazol-2-yl)benzamide hydrochloride (4.6)

General procedure **G** was performed to deprotect **4.6d** (222 mg, 0.17 mmol) to yield 188 mg of the title product. Quant. Off-white solid. ^1H NMR (500 MHz, DMSO- d_6) δ 13.86 (s, 1H), 8.70 (s, 1H), 8.04 (s, 3H), 7.56 (dd, $J = 14.4, 6.8$ Hz, 1H), 7.31 – 7.20 (m, 2H), 2.76 (dt, $J = 6.9, 6.1$ Hz, 3H), 2.69 (t, $J = 7.6$ Hz, 2H), 1.90 – 1.78 (m, 2H). ^{13}C NMR (126 MHz, DMSO- d_6) δ 165.02 (s), 161.47 (s), 159.10 (d, $J = 247.0$ Hz), 143.00 (d, $J = 13.4$ Hz), 142.80 (s), 141.90 (s), 132.98 (s), 125.89 (s), 122.46 (d, $J = 17.0$ Hz), 114.10 (s), 38.70 (s), 29.64 (s), 28.84 (s). LCMS: $t_R = 2.94$; $m/z = 325.1$. HRMS m/z calc. for $\text{C}_{13}\text{H}_{14}\text{N}_4\text{O}_3\text{F}_1\text{S}$ (M+H), 325.0771; found, 325.0778.

Methyl 2-(3-((*tert*-butoxycarbonyl)amino)propyl)-5-methylbenzoate (4.7b)

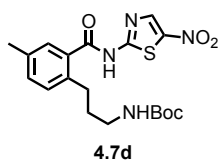
General procedure **A** was used to couple methyl 2-iodo-5-methylbenzoate (298 μL , 1.81 mmol) and *tert*-butyl *N*-allyl carbamate (369.4 mg, 2.35 mmol). Purified by flash chromatography (15 % EtOAc/hexanes) to yield 476 mg of the title compound. 86%. Light yellow oil. $R_f = 39$ (20 % EtOAc in hexanes; Ninhydrin/ Δ). ^{13}C NMR (75 MHz, CDCl_3) δ 167.94, 155.99, 140.53, 135.41, 132.77, 131.10, 130.86, 128.87, 78.66, 51.76, 40.14, 31.73, 31.04, 28.33, 20.66.

2-(3-((*tert*-Butoxycarbonyl)amino)propyl)-5-methylbenzoic acid (4.7c)



General procedure **C** was used to saponify **4.7b** (476 mg, 1.55 mmol). Extraction of the reaction mixture yielded 454 mg of the title compound. Quant. Beige solid. ^1H NMR (300 MHz, Chloroform- d) δ 12.17 (s, 1H), 7.84 (d, J = 1.8 Hz, 1H), 7.25 (dd, J = 7.6, 2.2 Hz, 1H), 7.14 (d, J = 7.8 Hz, 1H), 4.86 (s, 1H), 3.29 – 3.07 (m, 2H), 2.99 (dd, J = 9.1, 6.4 Hz, 2H), 2.33 (s, 3H), 1.80 (p, J = 7.0 Hz, 2H), 1.45 (s, 9H). ^{13}C NMR (75 MHz, CDCl_3) δ 172.49, 156.29, 141.54, 135.75, 133.61, 132.22, 131.22, 128.32, 79.37, 40.47, 31.90, 31.42, 28.50, 20.84.

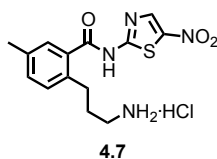
***tert*-Butyl (3-(4-methyl-2-((5-nitrothiazol-2-yl)carbamoyl)phenyl)propyl)carbamate (4.7d)**



General procedure **F** was used to couple **4.7c** (454 mg, 1.55 mmol) to 2-amino-5-nitrothiazole (338 mg, 2.33 mmol). Purified by flash chromatography (35 % EtOAc/hexanes) to yield 105 mg of the title compound. 16%. Light yellow solid. R_f = 0.54 (40 % EtOAc in hexanes; Ninhydrin/ Δ). ^1H NMR (800 MHz, $\text{DMSO}-d_6$) δ 13.48 (s, 1H), 8.70 (s, 1H), 7.44 (s, 1H), 7.33 (dd, J = 7.7, 1.8 Hz, 1H), 7.27 (d, J = 7.8 Hz, 1H), 6.79 (t, J = 5.8 Hz, 1H), 2.89 (q, J = 6.6 Hz, 2H), 2.69 (dd, J = 8.8, 6.8 Hz, 2H), 2.34 (s, 3H), 1.61 (p, J = 7.2 Hz, 2H), 1.34 (s, 9H). ^{13}C NMR (201 MHz, DMSO) δ 191.91,

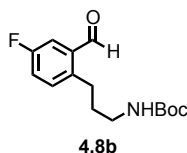
161.99, 155.52, 142.67, 142.01, 138.18, 135.08, 132.07, 131.97, 130.16, 128.94, 77.33, 47.11, 31.50, 29.58, 28.21, 20.38.

2-(3-Aminopropyl)-5-methyl-N-(5-nitrothiazol-2-yl)benzamide hydrochloride (4.7)



General Procedure **G** was used to deprotect **4.7d** (94 mg, 0.22 mmol). Sublimation yielded 80.8 mg of the title compound. Quant. Light orange solid. ^1H NMR (600 MHz, DMSO- d_6) δ 13.49 (s, 1H), 8.66 (s, 1H), 7.93 (s, 3H), 7.46 (d, J = 1.7 Hz, 1H), 7.34 – 7.31 (m, 1H), 7.27 (d, J = 7.8 Hz, 1H), 2.72 (dt, J = 14.2, 7.4 Hz, 4H), 2.30 (s, 3H), 1.84 – 1.74 (m, 2H). ^{13}C NMR (151 MHz, DMSO) δ 168.63, 162.04, 142.65, 142.00, 137.35, 135.48, 132.29, 131.83, 130.17, 129.24, 38.44, 29.13, 28.91, 20.39. LCMS: t_R = 3.15; m/z = 321.1. HRMS m/z calc. for $\text{C}_{14}\text{H}_{17}\text{N}_4\text{O}_3\text{S}$ ($\text{M}+\text{H}$), 321.1021; found, 321.1012.

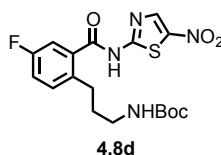
***tert*-Butyl (3-(4-fluoro-2-formylphenyl)propyl)carbamate (4.8b)**



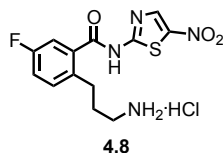
General procedure **A** was used to couple 2-bromo-5-fluorobenzaldehyde (500 mg, 2.46 mmol) and *tert*-butyl *N*-allyl carbamate (503 mg, 3.20 mmol). Purified by flash chromatography (20% EtOAc/hexanes) to yield 523 mg of the title compound. 76%.

Clear and colorless oil. $R_f = 0.33$ (20 % EtOAc in heanes; KMnO_4). ^1H NMR (300 MHz, CDCl_3) δ 10.12 (d, $J = 1.5$ Hz, 1H), 7.43 (dd, $J = 8.8, 2.7$ Hz, 1H), 7.27 – 7.09 (m, 2H), 4.95 (s, $J = 4.3$ Hz, 1H), 3.12 (dt, $J = 6.3, 6.3$ Hz, 2H), 2.94 (t, $J = 7.9$ Hz, 2H), 1.74 (tt, $J = 7.4, 7.1$ Hz, 2H), 1.37 (s, 9H). ^{13}C NMR (75 MHz, CDCl_3) δ 191.07 (s), 161.53 (d, $J = 247.1$ Hz), 156.30 (s), 140.40 (s), 135.14 (s), 133.01 (d, $J = 6.8$ Hz), 121.11 (d, $J = 21.2$ Hz), 117.93 (d, $J = 21.6$ Hz), 79.28 (s), 40.22 (s), 32.62 (s), 32.23 (s), 28.56 (s).

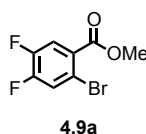
***tert*-Butyl (3-(4-fluoro-2-((5-nitrothiazol-2-yl)carbamoyl)phenyl)propyl)carbamate**
(**4.8d**)



General procedure **I** was performed to oxidize aldehyde **4.8b** (237 mg, 0.842 mmol) to 2-(3-((*tert*-butoxycarbonyl)amino)propyl)-5-fluorobenzoic acid **4.8c** and immediately submitted to the conditions described in general procedure **F**. Purified by flash chromatography (40% EtOAc/hexanes) to yield 156 mg of the title compound. 44% over 2 steps. Yellow gel. $R_f = 0.79$ (50 % EtOAc in hexanes; KMnO_4). ^1H NMR (300 MHz, CDCl_3) δ 12.76 (s, 1H), 7.78 (s, $J = 19.8$ Hz, 1H), 7.41 – 4.89 (m, 3H), 4.93 (s, $J = 5.2$ Hz, 1H), 3.10 (dt, $J = 6.1, 6.1$ Hz, 2H), 2.88 – 2.59 (m, 2H), 1.89 – 1.68 (m, 2H), 1.34 (s, 9H). ^{13}C NMR (75 MHz, CDCl_3) δ 167.18 (s), 162.66 (s), 160.68 (d, $J = 247.8$ Hz), 156.41 (s), 143.50 (s), 139.99 (s), 138.01 (s), 133.24 (d, $J = 6.2$ Hz), 132.88 (d, $J = 6.9$ Hz), 119.33 (d, $J = 20.7$ Hz), 115.20 (d, $J = 22.8$ Hz), 79.38 (s), 40.12 (s), 31.94 (s), 30.11 (s), 28.51 (s).

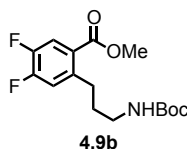
2-(3-Aminopropyl)-5-fluoro-N-(5-nitrothiazol-2-yl)benzamide hydrochloride (4.8)

General procedure **G** was performed to deprotect **4.8d** (156 mg, 0.368 mmol) to yield 133 mg of the title product. Quant. Off-white solid. ^1H NMR (500 MHz, DMSO- d_6) δ 13.64 (s, 1H), 8.70 (s, 1H), 8.04 (s, 3H), 7.55 (dd, J = 9.2, 2.7 Hz, 1H), 7.46 (dd, J = 8.6, 2.8 Hz, 1H), 7.40 (td, J = 8.5, 2.8 Hz, 1H), 2.74 (m, 4H), 1.83 (dt, J = 7.7, 7.5 Hz, 2H). ^{13}C NMR (126 MHz, DMSO- d_6) δ 167.78 (s), 162.26 (s), 160.27 (d, J = 244.0 Hz), 142.98 (s), 142.62 (s), 136.87 (s), 134.17 (s), 132.63 (s), 118.87 (d, J = 20.6 Hz), 116.17 (d, J = 23.9 Hz), 38.77 (s), 29.26 (s). LCMS: t_R = 3.01; m/z = 325.1. HRMS m/z calc. for $\text{C}_{13}\text{H}_{14}\text{N}_4\text{O}_3\text{F}_1\text{S}$ (M+H), 325.0771; found, 325.0763.

Methyl 2-bromo-4,5-difluorobenzoate (4.9a)

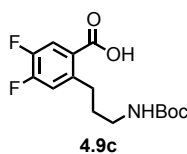
General procedure **D** was used to esterify 2-bromo-4,5-difluorobenzoic acid (700 mg, 2.97 mmol) with acetyl chloride (9.9 mL) in MeOH (49.5 mL). Extraction of the reaction mixture yielded 690 mg of the title compound. 93%. Clear oil. ^1H NMR (300 MHz, CDCl_3) δ 7.58 (dd, J = 10.6, 8.3 Hz, 1H), 7.36 (dd, J = 9.6, 7.2 Hz, 1H), 3.80 (s, 3H). ^{13}C NMR (75 MHz, CDCl_3) δ 152.15 (dd, J = 216.7, 12.7 Hz), 148.77 (dd, J = 207.9, 12.6 Hz), 128.22 (d, J = 4.1 Hz), 123.56 (d, J = 20.2 Hz), 120.61 (d, J = 20.1 Hz), 116.75 (d, J = 4.1 Hz), 52.68 (s).

Methyl 2-(3-((*tert*-butoxycarbonyl)amino)propyl)-4,5-difluorobenzoate (4.9b)



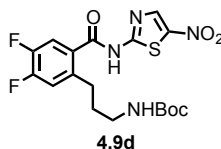
General procedure **A** was used to couple **4.9a** (690 mg, 2.75 mmol) and *tert*-butyl *N*-allyl carbamate (560 mg, 3.57 mmol). Purified by flash chromatography (20 % EtOAc/hexanes) to yield 715 mg of the title compound. 81%. Clear oil. R_f = 0.58 (20 % EtOAc in hexanes; Ninhydrin/ Δ). ^1H NMR (300 MHz, CDCl_3) δ 7.64 (dd, J = 11.1, 8.3 Hz, 1H), 6.97 (dd, J = 11.1, 7.7 Hz, 1H), 4.97 (s, 1H), 3.78 (s, 3H), 3.12 – 2.99 (m, 2H), 2.91 – 2.80 (m, 2H), 1.84 – 1.60 (m, 2H), 1.34 (s, 9H). ^{13}C NMR (75 MHz, CDCl_3) δ 165.88 (s), 156.25 (s), 152.41 (dd, J = 255.9, 12.5 Hz), 148.08 (dd, J = 247.8, 13.1 Hz), 142.36 (d, J = 3.4 Hz), 125.45 (s), 120.27 (d, J = 18.4 Hz), 119.68 (d, J = 17.1 Hz), 79.09 (s), 52.31 (s), 40.24 (s), 32.18 (s), 31.14 (s), 28.49 (s).

2-(3-((*tert*-Butoxycarbonyl)amino)propyl)-4,5-difluorobenzoic acid (4.9c)



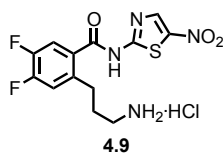
General procedure **C** was used to saponify **4.9b** (715 mg, 2.17 mmol). Extraction of the reaction mixture yielded 334 mg of the title compound. 49%. Oil. ^1H NMR (300 MHz, CDCl_3) δ 7.90 – 7.80 (m, 1H), 7.11 – 6.99 (m, 1H), 4.84 (s, 1H), 3.21 – 3.09 (m, 2H), 3.03 – 2.92 (m, 2H), 1.90 – 1.71 (m, 2H), 1.43 (s, 9H).

***tert*-Butyl (3-(4,5-difluoro-2-((5-nitrothiazol-2-yl)carbamoyl)phenyl)propyl)carbamate (4.9d)**



General procedure **F** was used to couple **4.9c** (334 mg, 0.761 mmol) to 2-amino-5-nitrothiazole (165 mg, 1.14 mmol). Purified by flash chromatography (40 % EtOAc/hexanes) to yield 276 mg of the title compound. 59%. Light yellow solid. ^1H NMR (800 MHz, DMSO- d_6) δ 13.60 (s, 1H), 8.75 (s, 1H), 7.86 (dd, J = 10.6, 8.2 Hz, 1H), 7.57 (dd, J = 11.6, 7.8 Hz, 1H), 2.98 (p, J = 6.4, 5.9 Hz, 2H), 2.84 – 2.73 (m, 2H), 1.71 (dt, J = 15.4, 7.5 Hz, 2H), 1.41 (s, 3H). ^{13}C NMR (201 MHz, DMSO- d_6) δ 167.14 (s), 162.37 (s), 156.04 (s), 151.20 (d, J = 251.0 Hz), 147.39 (d, J = 245.5 Hz), 142.79 (d, J = 57.8 Hz), 140.30 (s), 129.60 (s), 119.58 (d, J = 17.4 Hz), 118.72 (d, J = 19.0 Hz), 79.64 (s), 40.57 (s), 32.37 (s), 29.79 (s), 28.69 (s).

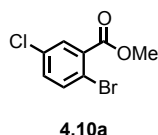
2-(3-Aminopropyl)-4,5-difluoro-*N*-(5-nitrothiazol-2-yl)benzamide hydrochloride (4.9)



General procedure **G** was used to deprotect **4.9d** (276 mg, 0.624 mmol). Sublimation yielded 131 mg of the title compound. 55%. Light orange powder. ^1H NMR (800 MHz, DMSO- d_6) δ 13.55 (s, 1H), 8.60 (s, 1H), 7.75 (dd, J = 10.8, 8.1 Hz, 1H), 7.47 (dd, J = 11.6, 7.8 Hz, 1H), 2.70 – 2.67 (m, 2H), 2.64 (dq, J = 12.0, 5.8 Hz, 2H), 1.75 (p, J = 7.7

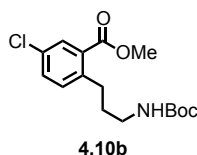
Hz, 2H). ^{13}C NMR (201 MHz, DMSO- d_6) δ 166.96 (s), 162.27 (s), 151.23 (dd, J = 251.4, 12.5 Hz), 147.44 (dd, J = 246.1, 13.0 Hz), 142.78 (d, J = 67.7 Hz), 139.44 (dd, J = 6.9, 3.9 Hz), 129.42 (d, J = 5.2 Hz), 119.66 (d, J = 17.6 Hz), 119.05 (d, J = 19.3 Hz), 38.62 (s), 29.26 (s), 28.98 (s). LCMS: t_R = 2.94; m/z = 343.1. HRMS m/z calc. for $\text{C}_{13}\text{H}_{13}\text{N}_4\text{O}_3\text{F}_2\text{S}$ (M+H), 343.0676; found, 343.0672.

Methyl 2-bromo-5-chlorobenzoate (4.10a)



General procedure **D** was used to esterify 2-bromo-5-chlorobenzoic acid (500 mg, 2.12 mmol) with acetyl chloride (7.06 mL) in MeOH (35.3 mL). Extraction of the reaction mixture yielded 526 mg of the title compound. 99%. Clear oil. ^1H NMR (300 MHz, CDCl_3) δ 7.67 (d, J = 2.4 Hz, 1H), 7.47 (d, J = 8.5 Hz, 1H), 7.23 – 7.12 (m, 1H), 3.85 (s, 3H).

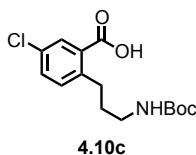
Methyl 2-(3-((*tert*-butoxycarbonyl)amino)propyl)-5-chlorobenzoate (4.10b)



General procedure **A** was used to couple **4.10a** (526 mg, 2.22 mmol) and *tert*-butyl *N*-allyl carbamate (450 mg, 2.89 mmol). Purified by flash chromatography (15 % EtOAc/hexanes) to yield 207 mg of the title compound. 30%. Clear oil. ^1H NMR (300 MHz, CDCl_3) δ 7.84 – 7.79 (m, 1H), 7.38 – 7.29 (m, 1H), 7.15 (d, J = 8.2 Hz, 1H), 4.32

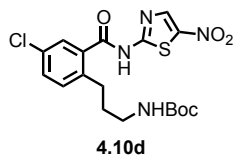
(s, 1H), 3.85 (s, 3H), 3.16 – 3.04 (m, 2H), 2.94 – 2.84 (m, 2H), 1.85 – 1.67 (m, 2H), 1.40 (s, 9H). ^{13}C NMR (75 MHz, CDCl_3) δ 169.56, 156.33, 142.52, 132.58, 132.23, 130.85, 129.44, 127.86, 71.10, 52.40, 32.46, 32.23, 28.60.

2-(3-((*tert*-Butoxycarbonyl)amino)propyl)-5-chlorobenzoic acid (4.10c)



General procedure **C** was used to saponify **4.10b** (207 mg, 0.63 mmol). Extraction of the reaction mixture yielded 197 mg of the title compound. 99%. Clear oil. ^1H NMR (300 MHz, CDCl_3) δ 7.97 (s, 1H), 7.29 (dd, J = 58.7, 8.0 Hz, 2H), 4.85 (s, 1H), 4.39 (s, 3H), 3.15 (m, 2H), 3.04 – 2.93 (m, 2H), 1.81 (m, 2H), 1.43 (s, 9H).

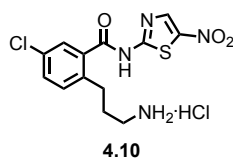
***tert*-Butyl (3-(4-chloro-2-((5-nitrothiazol-2-yl)carbamoyl)phenyl)propyl)carbamate (4.10d)**



General procedure **F** was used to couple **4.10c** (197 mg, 0.64 mmol) to 2-amino-5-nitrothiazole (140 mg, 0.97 mmol). Purified by flash chromatography (35 % EtOAc/hexanes) to yield 103 mg of the title compound. 37%. Light yellow solid. ^1H NMR (497 MHz, CDCl_3) δ 12.35 (s, 1H), 7.74 (s, 1H), 7.49 (d, J = 6.6 Hz, 1H), 7.32 (t, J = 7.2 Hz, 1H), 7.22 (d, J = 7.4 Hz, 1H), 3.10 (p, J = 6.5 Hz, 2H), 2.78 (q, J = 6.7, 6.2 Hz,

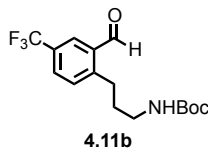
2H), 1.85 – 1.70 (m, 2H), 1.33 (s, 9H). ^{13}C NMR (125 MHz, CDCl_3) δ 167.01, 162.46, 140.75, 140.01, 133.58, 132.69, 132.47, 127.89, 77.29, 50.17, 45.00, 32.29, 29.95, 28.60.

2-(3-Aminopropyl)-5-chloro-*N*-(5-nitrothiazol-2-yl)benzamide hydrochloride (4.10)



General procedure **G** was used to deprotect **4.10d** (103 mg, 0.234 mmol). Sublimation yielded 75 mg of the title compound. 85%. Light yellow powder. ^1H NMR (800 MHz, DMSO-d_6) δ 13.64 (s, 1H), 8.70 (s, 1H), 7.76 (d, $J = 2.3$ Hz, 1H), 7.60 (dd, $J = 8.3, 2.4$ Hz, 1H), 7.44 (d, $J = 8.3$ Hz, 1H), 2.75 (dt, $J = 13.9, 7.1$ Hz, 2H), 2.48 (p, $J = 1.8$ Hz, 2H), 1.82 (p, $J = 7.7$ Hz, 2H). ^{13}C NMR (201 MHz, DMSO-d_6) δ 167.41, 162.08, 142.73, 139.34, 134.07, 132.18, 131.50, 130.80, 128.70, 70.75, 38.53, 29.10, 28.88. LCMS: $t_R = 3.15$; $m/z = 341.0$. HRMS m/z calc. for $\text{C}_{13}\text{H}_{14}\text{N}_4\text{O}_3\text{SCl}$ ($\text{M}+\text{H}$), 341.0475; found, 341.0468.

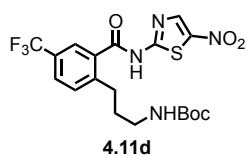
***tert*-Butyl (3-(2-formyl-4-(trifluoromethyl)phenyl)propyl)carbamate (4.11b)**



General procedure **A** was used to couple 2-bromo-5-(trifluoromethyl) benzaldehyde (500 mg, 1.98 mmol) and *tert*-butyl *N*-allyl carbamate (404 mg, 2.57 mmol). Purified by flash chromatography (15% - 20% EtOAc/hexanes) to yield 527 mg of the title compound. 80%. Clear and colorless oil. $R_f = 0.42$ (20 % EtOAc in hexanes; Ninhydrin/ Δ). ^1H

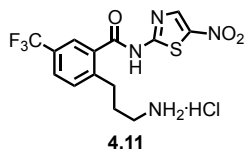
NMR (300 MHz, CDCl₃) δ 10.19 (s, 1H), 8.00 (s, 1H), 7.67 (d, J = 8.0 Hz, 1H), 7.15 (d, J = 7.6 Hz, 1H), 4.94 (t, J = 4.4 Hz, 1H), 3.14 (dt, J = 6.3, 6.3 Hz, 3H), 3.07 (t, J = 7.7 Hz, 3H), 1.62 – 1.51 (m, 2H), 1.37 (s, J = 6.6 Hz, 9H). ¹³C NMR (75 MHz, CDCl₃) δ 191.18 (s), 156.29 (s), 148.44 (s), 134.03 (s), 131.98 (s), 130.13 (d, J = 2.9 Hz), 129.45 (d, J = 3.0 Hz), 127.04 (q, J = 272.1 Hz), 125.26 (q, J = 57.8 Hz), 79.28 (s), 40.24 (s), 32.35 (s), 32.11 (s), 28.50 (s).

***tert*-Butyl (3-(2-((5-nitrothiazol-2-yl)carbamoyl)-4-(trifluoromethyl)phenyl)propyl)carbamate (**4.11d**)**



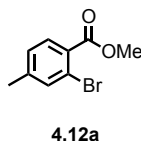
General procedure **I** was performed to oxidize aldehyde **4.11b** (237 mg, 0.842 mmol) to 2-(3-((*tert*-butoxycarbonyl)amino)propyl)-5-fluorobenzoic acid **4.11c** and immediately submitted to the conditions described in general procedure **F**. Purified by flash chromatography (40% EtOAc/hexanes) to yield 156 mg of the title compound. 44% over 2 steps. Yellow gel. R_f = 0.79 (50 % EtOAc in hexanes; KMnO₄). ¹H NMR (300 MHz, CDCl₃) δ 12.77 (s, 1H), 7.87 – 7.74 (m, J = 8.6 Hz, 2H), 7.71 (s, 1H), 7.55 (d, J = 8.0 Hz, 1H), 4.88 (s, J = 12.2 Hz, 1H), 3.14 (q, J = 6.5 Hz, 2H), 2.89 (t, J = 7.5 Hz, 2H), 1.87 (dt, J = 7.1, 6.8 Hz, 2H), 1.33 (s, 9H). ¹³C NMR (75 MHz, CDCl₃) δ 167.24 (s), 162.46 (s), 156.45 (s), 146.29 (s), 143.61 (s), 139.85 (s), 132.98 (s), 131.71 (s), 128.84 (s), 127.37 (q, J = 275.1 Hz), 125.02 (m), 79.63 (s), 40.16 (s), 31.62 (s), 30.80 (s), 28.48 (s).

2-(3-Aminopropyl)-N-(5-nitrothiazol-2-yl)-5-(trifluoromethyl)benzamide hydrochloride (4.11)



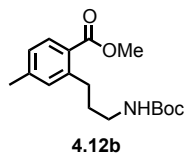
General procedure **G** was performed to deprotect **4.11d** (127 mg, 0.339 mmol) to yield 139 mg of the title product. Quant. Fluffy pineapple-yellow solid. ^1H NMR (500 MHz, DMSO- d_6) δ 13.78 (s, 1H), 8.72 (d, $J = 3.2$ Hz, 1H), 8.07 (s, 1H), 8.04 (s, 3H), 7.91 (d, $J = 8.0$ Hz, 1H), 7.66 (d, $J = 8.1$ Hz, 1H), 2.88 – 2.72 (m, 4H), 1.91 (dt, $J = 6.4$ Hz, 2H). ^{13}C NMR (126 MHz, DMSO- d_6) δ 167.80 (s), 162.50 (s), 145.53 (s), 143.02 (s), 142.55 (s), 133.50 (s), 131.63 (s), 128.51 (s), 127.26 (q, $J = 33.3$ Hz), 126.33 (s), 124.30 (q, $J = 272.5$ Hz), 38.77 (s), 29.91 (s), 28.98 (s). LCMS: $t_R = 3.29$; $m/z = 375.1$. HRMS m/z calc. for $\text{C}_{14}\text{H}_{14}\text{N}_4\text{O}_3\text{F}_3\text{S}$ (M+H), 375.0739; found, 375.0736.

Methyl 2-bromo-4-methylbenzoate (4.12a)



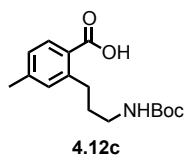
General procedure **D** was used to esterify 2-bromo-4-methylbenzoic acid (500 mg, 2.32 mmol) with acetyl chloride (7.73 mL) in MeOH (38.7 mL). Extraction of the reaction mixture yielded 494 mg of the title compound. 93%. Clear yellow oil. ^1H NMR (800 MHz, CDCl_3) δ 7.65 (d, $J = 7.8$ Hz, 1H), 7.41 (d, $J = 1.4$ Hz, 1H), 7.07 (dd, $J = 7.8, 1.6$ Hz, 1H), 3.84 (s, 3H), 2.27 (s, 3H). ^{13}C NMR (151 MHz, CDCl_3) δ 166.33, 143.60, 134.90, 131.42, 127.92, 121.77, 52.23, 21.00.

Methyl 2-(3-((*tert*-butoxycarbonyl)amino)propyl)-4-methylbenzoate (4.12b)



General procedure **A** was used to couple **4.12a** (494 mg, 2.16 mmol) and *tert*-butyl *N*-allyl carbamate (441 mg, 2.81 mmol). Purified by flash chromatography (15 % EtOAc/hexanes) to yield 734 mg of the title compound. 100%. Clear tan oil. R_f = 0.35 (20 % EtOAc in hexanes). ^1H NMR (300 MHz, CDCl_3) δ 7.58 (d, J = 7.9 Hz, 1H), 6.84 – 6.75 (m, 2H), 5.14 (t, J = 5.7 Hz, 1H), 3.63 (s, 3H), 2.95 (t, J = 6.5 Hz, 2H), 2.74 (t, J = 9.0 Hz, 2H), 2.11 (s, 3H), 1.58 (d, J = 5.0 Hz, 2H), 1.24 (s, 9H). ^{13}C NMR (75 MHz, CDCl_3) δ 167.59, 156.13, 144.11, 142.48, 131.81, 131.07, 126.69, 70.70, 51.57, 40.34, 33.68, 28.40, 26.51, 21.27.

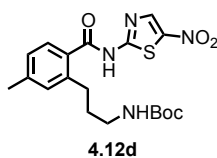
2-(3-((*tert*-Butoxycarbonyl)amino)propyl)-4-methylbenzoic acid (4.12c)



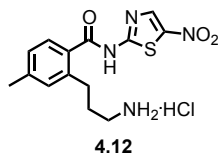
General procedure **C** was used to saponify **4.12b** (734 mg, 2.39 mmol). Extraction of the reaction mixture yielded 597 mg of the title compound. 85%. Oil. ^1H NMR (800 MHz, CDCl_3) δ 10.42 (s, 1H), 7.90 (d, J = 7.8 Hz, 1H), 7.02 (d, J = 8.7 Hz, 2H), 4.99 (s, 1H), 3.13 (t, J = 6.6 Hz, 2H), 2.97 (t, J = 7.7 Hz, 2H), 2.31 (s, 3H), 1.76 (d, J = 10.8 Hz, 2H),

1.40 (s, 8H). ^{13}C NMR (201 MHz, CDCl_3) δ 176.44, 156.30, 144.76, 143.38, 131.94, 126.84, 77.16, 40.36, 31.73, 28.38, 21.97, 21.38.

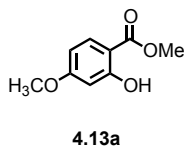
***tert*-Butyl (3-(5-methyl-2-((5-nitrothiazol-2-yl)carbamoyl)phenyl)propyl)carbamate (4.12d)**



General procedure **F** was used to couple **4.12c** (597 mg, 2.03 mmol) to 2-amino-5-nitrothiazole (443 mg, 3.05 mmol). Purified by flash chromatography (40 % EtOAc/hexanes) to yield 138 mg of the title compound. 16%. Yellow-orange solid. R_f = 0.50 (50 % EtOAc in hexanes; Ninhydrin/ Δ). ^1H NMR (600 MHz, DMSO- d_6) δ 13.46 (s, 1H), 7.53 (d, J = 7.8 Hz, 1H), 7.19 (d, J = 1.7 Hz, 1H), 7.15 (d, J = 6.5 Hz, 1H), 2.89 (q, J = 6.6 Hz, 2H), 2.73 (t, J = 6.2 Hz, 2H), 2.34 (s, 3H), 1.61 (p, J = 7.2 Hz, 2H), 1.34 (s, 9H).

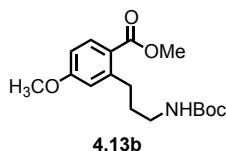
2-(3-Aminopropyl)-4-methyl-N-(5-nitrothiazol-2-yl)benzamide hydrochloride (4.12)

General procedure **G** was used to deprotect **4.12d** (138 mg, 0.33 mmol). Sublimation yielded 102 mg of the title compound. 91%. Light orange powder. ^1H NMR (600 MHz, DMSO- d_6) δ 13.49 (s, 1H), 8.67 (s, 1H), 7.94 (s, 3H), 7.56 (d, $J = 7.9$ Hz, 1H), 7.23 – 7.19 (m, 1H), 7.17 (d, $J = 7.9$ Hz, 1H), 2.80 – 2.76 (m, 2H), 2.74 (d, $J = 8.2$ Hz, 2H), 2.47 (p, $J = 1.8$ Hz, 2H), 1.92 – 1.68 (m, 2H). ^{13}C NMR (151 MHz, DMSO- d_6) δ 168.97, 162.73, 143.14, 142.35, 141.23, 131.42, 129.49, 127.25, 38.97, 30.05, 29.39, 21.50. LCMS: $t_R = 3.08$; $m/z = 321.1$. HRMS m/z calc. for $\text{C}_{14}\text{H}_{17}\text{N}_4\text{O}_3\text{S}$ (M+H), 321.1021; found, 321.1022.

Methyl 2-hydroxy-4-methoxybenzoate (4.13a)

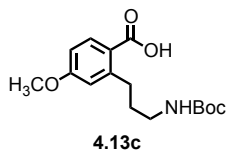
General procedure **E** was performed to esterify 2-hydroxy-4-methoxy benzoic acid (500 mg, 3.0 mmol) until complete by TLC analysis (16h, 20 % EtOAc/hexanes). Extracted to yield 524 mg of the title compound. 96%. Yellow liquid. ^1H NMR (300 MHz, CDCl_3) δ 10.93 (s, 1H), 7.65 – 7.59 (m, 1H), 6.38 – 6.31 (m, 2H), 3.82 (s, 3H), 3.72 (s, 3H). ^{13}C NMR (75 MHz, CDCl_3) δ 170.54, 165.72, 163.92, 131.35, 107.53, 105.53, 100.78, 55.52, 52.05.

Methyl 2-(3-((*tert*-butoxycarbonyl)amino)propyl)-4-methoxybenzoate (4.13b)



General procedure **H** was performed with phenol **4.13a** (524 mg, 2.9 mmol) and the crude product was taken on without further purification. General procedure **A** was performed to couple the reaction residue to *tert*-butyl-*N*-allyl carbamate (593 mg, 3.77 mmol). Purified by flash chromatography (15% EtOAc/hexanes) to yield 500 mg of the title compound. 53%. Light yellow oil. $R_f = 0.27$ (20 % EtOAc in hexanes; Ninhydrin/ Δ). ^1H NMR (300 MHz, CDCl_3) δ 7.86 (d, $J = 9.4$, 1H), 6.70 – 6.66 (m, 2H), 4.98 – 4.86 (m, 1H), 3.79 (s, 3H), 3.76 (s, 3H), 3.11 (t, $J = 6.4$, 2H), 2.94 – 2.87 (m, 2H), 1.58 – 1.52 (m, 2H), 1.39 (s, 9H). ^{13}C NMR (75 MHz, CDCl_3) δ 167.43, 162.59, 156.29, 146.94, 133.46, 121.27, 116.42, 111.48, 79.00, 70.85, 55.42, 51.79, 40.41, 32.36, 28.60, 26.60, 22.20.

2-(3-((*tert*-Butoxycarbonyl)amino)propyl)-4-methoxybenzoic acid (4.13c)

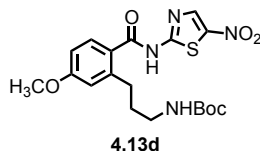


General procedure **C** was performed at 50–70 °C (7h) to saponify **4.13b** (500 mg, 1.55 mmol). Extracted to yield 333 mg of the title compound. 77%. Off-white solid. ^1H NMR (300 MHz, CDCl_3) δ 11.71 (s, 1H), 8.06 (d, $J = 9.3$ Hz, 1H), 6.76 (dd, $J = 6.8$, 1.9 Hz, 2H), 4.88 (s, 1H), 3.83 (s, 3H), 3.18 (q, $J = 6.6$ Hz, 2H), 3.05 (t, $J = 6.2$ Hz, 2H), 1.76 –

1.50 (m, 2H), 1.45 (s, 9H). ^{13}C NMR (75 MHz, CDCl_3) δ 172.14 , 163.23 , 156.44 , 147.93 , 134.63 , 120.43 , 116.70 , 111.61 , 79.30 , 55.56 , 40.55 , 32.44 , 31.86 , 28.65 .

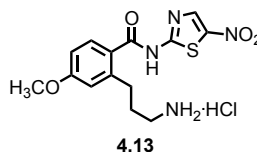
***tert*-Butyl (3-(5-methoxy-2-((5-nitrothiazol-2-yl)carbamoyl)phenyl)carbamate**

(4.13d)



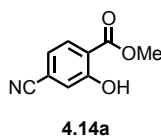
General procedure **F** was used to couple 2-amino-5-nitrothiazole (239 mg, 1.65 mmol) to **4.13c** (339 mg, 1.10 mmol). Purified by flash chromatography (40% EtOAc/hexanes) to yield 80 mg of the title compound. 17%. Yellow solid. R_f = 0.32 (50 % EtOAc in hexanes; Ninhydrin/ Δ). ^1H NMR (600 MHz, DMSO-d_6) δ 13.38 (s, 1H), 8.69 (s, 1H), 7.66 (d, J = 12.0 Hz, 1H), 6.94 (s, 1H), 6.92 (d, J = 12.0 Hz, 1H), 6.80 (t, J = 6.0 Hz, 1H), 3.83 (s, 3H), 2.92 (q, J = 6.0 Hz, 2H), 2.78 (t, J = 6.0 Hz, 2H), 1.64 (p, J = 12.0, 6.0 Hz, 2H), 1.35 (s, 9H). ^{13}C NMR (151 MHz, DMSO-d_6) δ 168.45, 162.88, 162.13, 156.01, 147.95, 145.08, 143.18, 131.53, 124.23, 116.51, 111.49, 77.83, 55.88, 40.27, 31.83, 30.76, 28.70.

2-(3-Aminopropyl)-4-methoxy-*N*-(5-nitrothiazol-2-yl)benzamide hydrochloride
(4.13)



General procedure **G** was performed to deprotect **4.13d** (75 mg, 0.17 mmol). Sublimation yielded 70.3 mg of the title compound. 100%. ¹H NMR (600 MHz, DMSO-d₆) δ 13.40 (s, 1H), 8.66 (s, 1H), 7.95 (s, 3H), 7.68 (d, *J* = 8.6 Hz, 1H), 6.96 (d, *J* = 2.6 Hz, 1H), 6.91 (dd, *J* = 8.6, 2.6 Hz, 1H), 3.80 (s, 3H), 2.82 (t, *J* = 7.5 Hz, 2H), 2.77 – 2.69 (m, 2H), 1.85 (p, *J* = 12.0, 6.0 Hz, 2H). ¹³C NMR (151 MHz, DMSO-d₆) δ 170.92, 162.87, 162.30, 144.25, 131.86, 124.02, 116.75, 111.67, 56.00, 38.90, 30.31, 29.29. LCMS: *t_R* = 3.01; *m/z* = 337.1. HRMS *m/z* calc. for C₁₄H₁₇N₄O₄S (M+H), 337.0971; found, 337.0976.

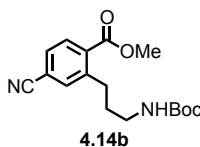
Methyl 4-cyano-2-hydroxybenzoate (4.14a)



Methyl-4-iodo salicylate (750 mg, 2.7 mmol) was dissolved in DMF (0.4 M) and CuCN (580 mg, 6.5 mmol) was added. The reaction was heated to reflux at 140 °C until complete by TLC analysis (2 h). The reaction was cooled to r.t. and dissolved in neat H₂O. The resulting mixture was diluted with EtOAc (100x the volume of reaction) and filtered to remove solid byproduct, then washed with 10% Na₂CO₃ (2 x 100x the volume

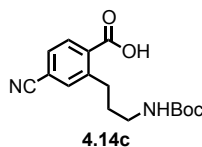
of reaction). The organic layer was dried over Na₂SO₄, filtered and evaporated. Purified by flash chromatography (10% EtOAc/hexanes) to yield 240 mg of the title compound. 50%. Off-white solid. R_f = 0.28 (10 % EtOAc in hexanes). ¹H NMR (300 MHz, DMSO-d₆) δ 10.77 (s, 1H), 7.84 (d, J = 8.2 Hz, 1H), 7.43 (d, J = 1.6 Hz, 1H), 7.34 (dd, J = 8.1, 1.6 Hz, 1H), 3.87 (s, 3H). ¹³C NMR (75 MHz, DMSO-d₆) δ 167.84, 159.25, 132.09, 123.14, 121.74, 119.90, 118.45, 117.02, 53.45.

Methyl 2-(3-((*tert*-butoxycarbonyl)amino)propyl)-4-cyanobenzoate (4.14b)



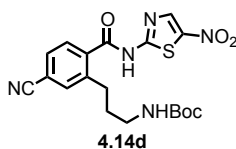
General procedure **H** was performed with phenol **4.14a** (230 mg, 1.3 mmol) and the crude product was taken on without further purification. General procedure **A** was performed to couple the reaction residue to *tert*-butyl-*N*-allyl carbamate (266 mg, 1.69 mmol). Purified by flash chromatography (15% EtOAc/hexanes) to yield 280 mg of the title compound. 68%. Light tan oil. R_f = 0.13 (20 % EtOAc in hexanes; Ninhydrin/ Δ). ¹H NMR (300 MHz, CDCl₃) δ 7.88 (d, J = 8.0 Hz, 1H), 7.54 – 7.42 (m, 2H), 4.86 (d, J = 6.1 Hz, 1H), 3.87 (s, 3H), 3.12 (q, J = 6.5 Hz, 2H), 2.99 – 2.86 (m, 2H), 1.57 (ddq, J = 12.7, 9.2, 5.8, 5.1 Hz, 2H), 1.38 (s, 9H). ¹³C NMR (75 MHz, CDCl₃) δ 166.74, 156.23, 144.87, 134.55, 133.69, 131.43, 129.69, 118.10, 115.66, 79.27, 52.74, 40.31, 31.80, 28.59, 26.42.

2-(3-((*tert*-Butoxycarbonyl)amino)propyl)-4-cyanobenzoic acid (4.14c)



General procedure **C** was performed to saponify **4.14b** (280 mg, 0.9 mmol). Extraction of the reaction mixture yielded 215 mg of the title compound. 78%. Oil. ^1H NMR (300 MHz, CDCl_3) δ 10.44 (s, 1H), 8.03 (d, J = 8.3 Hz, 1H), 7.53 (d, J = 6.8 Hz, 2H), 4.92 (s, 1H), 3.10 (dq, J = 40.1, 8.5, 7.6 Hz, 4H), 1.69 – 1.54 (m, 2H), 1.49 – 1.41 (m, 9H). ^{13}C NMR (75 MHz, CDCl_3) δ 170.98, 169.97, 158.51, 156.62, 145.23, 134.55, 133.77, 132.08, 130.57, 129.80, 118.22, 115.84, 79.88, 40.53, 31.81, 28.62, 26.54 .

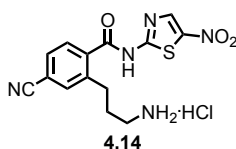
***tert*-Butyl (3-(5-cyano-2-((5-nitrothiazol-2-yl)carbamoyl)phenyl)propyl)carbamate (4.14d)**



General procedure **F** was performed to couple **4.14c** (215 mg, 0.7 mmol) to 2-amino-5-nitrothiazole (152 mg, 1.05 mmol). Purified by flash chromatography (40% EtOAc/hexanes) to yield 75 mg of the title compound. 25%. Light yellow solid. R_f = 0.30 (50 % EtOAc in hexanes; Ninhydrin/ Δ). ^1H NMR (600 MHz, DMSO-d_6) δ 13.75 (s, 1H), 8.71 (s, 1H), 7.91 (d, J = 1.6 Hz, 1H), 7.85 (dd, J = 7.9, 1.6 Hz, 1H), 7.79 (d, J = 7.9 Hz, 1H), 6.82 (t, J = 5.7 Hz, 1H), 2.89 (q, J = 6.5 Hz, 2H), 2.76 – 2.70 (m, 2H), 1.64 (p, J = 7.0 Hz, 2H), 1.33 (s, 9H). ^{13}C NMR (151 MHz, DMSO-d_6) δ 167.96, 162.05,

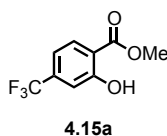
156.01, 142.98, 142.77, 142.59, 137.30, 134.15, 130.22, 129.73, 118.65, 114.16, 77.87, 40.52, 31.44, 30.01, 28.66.

2-(3-Aminopropyl)-4-cyano-*N*-(5-nitrothiazol-2-yl)benzamide hydrochloride (4.14).



General procedure **G** was performed to deprotect **4.14d** (52 mg, 0.12 mmol). Sublimation yielded 43 mg of the title compound. 100%. Off-white solid. ^1H NMR (600 MHz, DMSO- d_6) δ 13.82 (s, 1H), 8.73 (s, 1H), 8.00 (s, 3H), 7.96 (d, J = 1.5 Hz, 1H), 7.90 (dd, J = 8.0, 1.6 Hz, 1H), 7.84 (d, J = 7.9 Hz, 1H), 2.83 (t, J = 6.0 Hz, 2H), 2.76 (dt, J = 8.0, 6.0 Hz, 2H), 1.88 (p, J = 6.0 Hz, 2H). ^{13}C NMR (151 MHz, DMSO- d_6) δ 167.92, 162.16, 142.98, 142.73, 141.74, 137.27, 134.08, 130.54, 130.03, 118.60, 114.32, 38.67, 29.49, 28.80. LCMS: t_R = 2.94; m/z = 332.1. HRMS m/z calc. for $\text{C}_{14}\text{H}_{14}\text{N}_5\text{O}_3\text{S}$ (M+H), 332.0817; found, 332.0812.

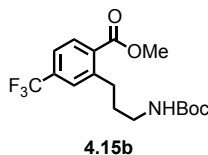
Methyl 2-hydroxy-4-(trifluoromethyl)benzoate (4.15a)



General procedure **E** was performed to esterify 4-trifluoromethyl salicylic acid (500 mg, 2.43 mmol) until complete by TLC analysis (3 h, 20 % EtOAc/hexanes; KMnO_4). Extracted to yield 303 mg of the title compound. 57%. ^1H NMR (300 MHz, CDCl_3) δ 10.87 (s, 1H), 7.89 (dd, J = 8.2, 0.8 Hz, 1H), 7.20 (dt, J = 1.5, 0.6 Hz, 1H), 7.07 (ddd, J =

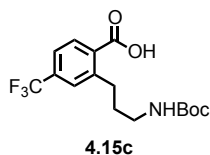
8.2, 1.8, 0.7 Hz, 1H), 3.96 (s, 3H). ^{13}C NMR (75 MHz, CDCl_3) δ 169.86 (s), 161.67 (s), 137.01 (q, $J = 32.8$ Hz), 130.91 (s), 123.36 (q, $J = 273.2$ Hz), 115.62 (d, $J = 3.2$ Hz), 115.09 (d, $J = 3.6$ Hz), 52.85 (s).

Methyl 2-(3-((*tert*-butoxycarbonyl)amino)propyl)-4-(trifluoromethyl)benzoate
(4.15b)



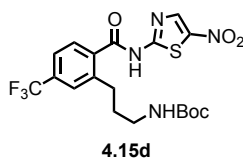
General procedure **H** was performed with phenol **4.15a** (303 mg, 1.4 mmol) and the crude product was taken on without further purification. General procedure **A** was performed to couple the reaction residue to *tert*-butyl-*N*-allyl carbamate (286 mg, 1.82 mmol). Purified by flash chromatography (15% EtOAc/hexanes) to yield 330 mg of the title compound. 65%. Light yellow oil. $R_f = 0.41$ (20 % EtOAc in hexanes; Ninhydrin/ Δ). ^1H NMR (300 MHz, CDCl_3) δ 7.90 (d, $J = 8.0$ Hz, 1H), 7.51 – 7.37 (m, 2H), 4.90 (s, 1H), 3.87 (d, $J = 3.4$ Hz, 3H), 3.15 (q, $J = 6.4$ Hz, 2H), 2.96 (dq, $J = 9.1$, 4.5, 3.5 Hz, 2H), 1.79 – 1.73 (m, 2H), 1.40 (s, 9H). ^{13}C NMR (75 MHz, CDCl_3) δ 167.11 (s), 156.25 (s), 144.70 (s), 133.65 (q, $J = 32.8$ Hz), 132.83 (s), 131.36 (s), 128.01 (q, $J = 286.8$ Hz), 127.79 (d, $J = 3.1$ Hz), 122.99 (d, $J = 3.1$ Hz), 79.19 (s), 52.53 (s), 40.40 (s), 31.94 (s), 31.72 (s), 28.55 (s).

2-(3-((*tert*-Butoxycarbonyl)amino)propyl)-4-(trifluoromethyl)benzoic acid (4.15c**)**



General procedure **C** was used to saponify **4.15b** (312 mg, 0.86 mmol). Extracted to yield 252 mg of the title compound. 84%. Oil. ^1H NMR (300 MHz, CDCl_3) δ 11.85 (s, 1H), 8.06 (d, $J = 8.5$ Hz, 1H), 7.49 (d, $J = 7.1$ Hz, 2H), 4.95 (s, 1H), 3.19 (h, $J = 6.5$ Hz, 2H), 3.06 (p, $J = 6.3$ Hz, 2H), 1.91 – 1.75 (m, 2H), 1.43 (s, 9H). ^{13}C NMR (75 MHz, CDCl_3) δ 170.98 (s), 156.67 (s), 145.20 (s), 132.83 (q, $J = 22.4$ Hz), 132.10 (s), 127.83 (s), 123.77 (q, $J = 272.8$ Hz), 123.07 (s), 79.83 (s), 40.62 (s), 31.90 (s), 28.55 (s).

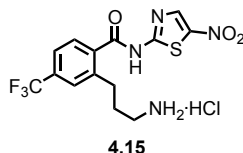
***tert*-Butyl(3-(2-((5-nitrothiazol-2-yl)carbamoyl)-5-(trifluoromethyl)phenyl)propyl) carbamate (**4.15d**)**



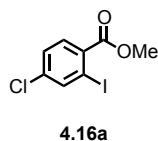
General procedure **F** was used to couple 2-amino-5-nitrothiazole (160 mg, 1.1 mmol) to **4.15c** (252 mg, 0.73 mmol). Purified by flash chromatography (40% EtOAc/hexanes) to yield 274 mg of the title compound. 79%. Light yellow solid. $R_f = 0.71$ (50 % EtOAc in hexanes; Ninhydrin/ Δ). ^1H NMR (600 MHz, DMSO-d_6) δ 13.71 (s, 1H), 8.85 – 8.43 (m, 1H), 7.84 (d, $J = 8.0$ Hz, 1H), 7.80 (s, 1H), 7.76 (d, $J = 8.0$, 1H), 6.82 (t, $J = 5.5$ Hz, 1H), 2.93 (q, $J = 6.4$ Hz, 2H), 2.81 (dq, $J = 10.3, 4.4, 3.5$ Hz, 2H), 1.68 (dq, $J = 13.0, 6.8$ Hz, 2H), 1.36 (s, 9H). ^{13}C NMR (151 MHz, DMSO-d_6) δ 168.23 (s), 162.14 (s), 156.03 (s), 142.98 (s), 142.78 (s), 136.90 (s), 131.67 (q, $J = 31.8$ Hz), 129.82 (s), 127.16 (d, $J = 3.8$

Hz), 124.24 (q, $J = 272.4$ Hz), 123.26 (d, $J = 3.3$ Hz), 77.86 (s), 40.55 (s), 31.70 (s), 30.26 (s), 28.66 (s).

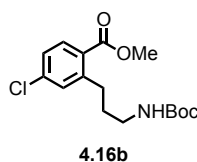
2-(3-Aminopropyl)-N-(5-nitrothiazol-2-yl)-4-(trifluoromethyl)benzamide hydrochloride (4.15)



General procedure **G** was performed to deprotect **4.15d** (264 mg, 0.56 mmol). Sublimation yielded 212 mg of the title compound. 92%. Light yellow powder. ^1H NMR (600 MHz, DMSO- d_6) δ 13.77 (s, 1H), 8.72 (s, 1H), 8.00 (s, 3H), 7.87 (d, $J = 8.0$ Hz, 1H), 7.83 (d, $J = 1.7$ Hz, 1H), 7.78 (dd, $J = 8.1, 1.7$ Hz, 1H), 2.89 (t, $J = 7.7$ Hz, 2H), 2.83 – 2.71 (m, 2H), 1.89 (p, $J = 6.0$ Hz, 2H). ^{13}C NMR (151 MHz, DMSO- d_6) δ 168.18 (s), 162.29 (s), 142.97 (s), 142.70 (s), 141.98 (s), 136.87 (s), 131.80 (q, $J = 31.9$ Hz), 130.13 (s), 127.15 (d, $J = 3.7$ Hz), 124.21 (q, $J = 272.9$ Hz), 123.60 (d, $J = 3.7$ Hz), 38.80 (s), 29.77 (s), 29.20 (s). LCMS: $t_R = 3.22$; $m/z = 375.1$. HRMS m/z calc. for $\text{C}_{14}\text{H}_{14}\text{N}_4\text{O}_3\text{SF}_3$ (M+H), 375.0739; found, 375.0737.

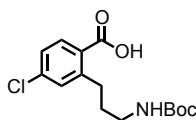
Methyl 4-chloro-2-iodobenzoate (4.16a)

General procedure **D** was used to esterify 4-chloro-2-iodobenzoic acid (500 mg, 1.77 mmol) with acetyl chloride (5.6 mL) in MeOH (28.33 mL). Extraction of the reaction mixture yielded 520 mg of the title compound. 99%. Clear yellow oil. ^1H NMR (300 MHz, CDCl_3) δ 7.95 (d, J = 1.9 Hz, 1H), 7.72 (d, J = 8.4 Hz, 1H), 7.33 (dd, J = 8.4, 2.0 Hz, 1H), 3.88 (s, 3H). ^{13}C NMR (75 MHz, CDCl_3) δ 165.98, 141.05, 138.30, 133.14, 131.99, 128.38, 94.87, 52.82, 42.13.

Methyl 2-(3-((*tert*-butoxycarbonyl)amino)propyl)-4-chlorobenzoate (4.16b)

General procedure **A** was used to couple **4.16a** (458 mg, 1.54 mmol) and *tert*-butyl *N*-allyl carbamate (316 mg, 2.01 mmol). Purified by flash chromatography (20 % EtOAc/hexanes) to yield 332 mg of the title compound. 66%. Clear oil. ^1H NMR (300 MHz, CDCl_3) δ 7.77 (d, J = 8.3 Hz, 1H), 7.20 – 7.10 (m, 2H), 4.89 (s, 1H), 3.82 (s, 3H), 3.15 – 3.03 (m, 2H), 2.94 – 2.82 (m, 2H), 1.81 – 1.64 (m, 2H), 1.39 (s, 9H). ^{13}C NMR (75 MHz, CDCl_3) δ 167.14, 156.24, 146.15, 138.36, 132.54, 131.11, 127.68, 126.44, 79.10, 52.26, 40.39, 31.78, 31.66.

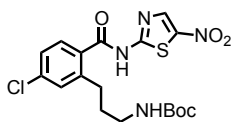
2-(3-((*tert*-Butoxycarbonyl)amino)propyl)-4-chlorobenzoic acid (4.16c)



4.16c

General procedure **C** was used to saponify **4.16b** (332 mg, 1.01 mmol). Extraction of the reaction mixture yielded 256 mg of the title compound. 81%. Oil. ^1H NMR (300 MHz, CDCl_3) δ 10.39 (s, 1H), 7.95 (d, J = 8.2 Hz, 1H), 7.23 (d, J = 9.2 Hz, 2H), 4.89 (s, 1H), 3.17 (s, 2H), 3.05 – 2.96 (m, 2H), 1.86 – 1.75 (m, 2H), 1.43 (s, 9H). ^{13}C NMR (75 MHz, CDCl_3) δ 171.12, 156.51, 146.83, 139.02, 133.42, 131.23, 126.58, 79.59, 40.57, 31.89, 31.79, 28.64.

***tert*-Butyl (3-(5-chloro-2-((5-nitrothiazol-2-yl)carbamoyl)phenyl)propyl)carbamate (4.16d)**

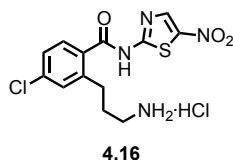


4.16d

General procedure **F** was used to couple **4.16c** (256 mg, 0.816 mmol) to 2-amino-5-nitrothiazole (178 mg, 1.22 mmol). Purified by flash chromatography (30-45 % EtOAc/hexanes) to yield 176 mg of the title compound. 49%. Light yellow solid. R_f = 0.40 (40 % EtOAc in hexanes; Ninhydrin/ Δ). ^1H NMR (500 MHz, $\text{DMSO}-d_6$) δ 13.61 (s, 1H), 8.71 (s, 1H), 7.65 (d, J = 8.5 Hz, 1H), 7.50 (s, 1H), 7.44 (d, J = 8.2 Hz, 1H), 2.90 (d, J = 5.5 Hz, 2H), 2.74 (t, J = 7.1 Hz, 2H), 1.67 – 1.59 (m, 2H), 1.34 (s, 9H). ^{13}C NMR

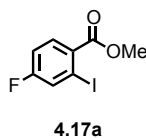
(75 MHz, DMSO-d₆) δ 168.53, 156.21, 144.49, 143.28, 142.74, 136.71, 131.79, 131.14, 130.63, 126.58, 78.06, 41.53, 31.87, 30.41, 28.89.

2-(3-Aminopropyl)-4-chloro-N-(5-nitrothiazol-2-yl)benzamide hydrochloride (4.16)



General procedure **G** was used to deprotect **4.16d** (176 mg, 0.40 mmol). Sublimation yielded 115 mg of the title compound. 76%. Light yellow powder. ¹H NMR (600 MHz, DMSO-d₆) δ 13.63 (s, 1H), 8.69 (s, 1H), 7.93 (s, 1H), 7.68 (d, *J* = 8.3 Hz, 1H), 7.54 – 7.52 (m, 1H), 7.46 (dd, *J* = 8.3, 2.2 Hz, 1H), 2.82 – 2.78 (m, 2H), 2.75 (dq, *J* = 12.0, 5.9 Hz, 2H), 1.85 (p, *J* = 7.7 Hz, 2H). ¹³C NMR (151 MHz, DMSO-d₆) δ 170.75, 165.03, 145.94, 145.55, 145.05, 139.23, 134.01, 133.75, 132.97, 129.25, 41.33, 32.22, 31.61. LCMS: *t_R* = 3.08; *m/z* = 341.1. HRMS *m/z* calc. for C₁₃H₁₄N₄O₃SCl (M+H), 342.0475; found, 341.0473.

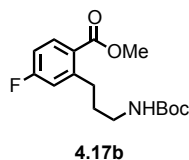
Methyl 4-fluoro-2-iodobenzoate (4.17a)



General procedure **D** was used to esterify 4-fluoro-2-iodobenzoic acid (500 mg, 1.88 mmol) with acetyl chloride (6.27 mL) in MeOH (31.33 mL). Extraction of the reaction mixture yielded 378 mg of the title compound. 72%. Clear oil. ¹H NMR (300 MHz, CDCl₃) δ 7.81 (dd, *J* = 8.7, 5.9 Hz, 1H), 7.67 (dd, *J* = 8.2, 2.5 Hz, 1H), 7.10 – 7.02 (m,

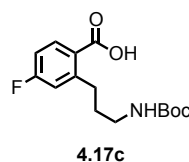
1H), 3.87 (s, 3H). ^{13}C NMR (75 MHz, CDCl_3) δ 165.88 (s), 163.60 (d, $J = 258.0$ Hz), 132.93 (d, $J = 8.7$ Hz), 130.84 (s), 128.84 (d, $J = 23.7$ Hz), 115.34 (d, $J = 21.2$ Hz), 94.85 (s), 52.74 (s).

Methyl 2-(3-((*tert*-butoxycarbonyl)amino)propyl)-4-fluorobenzoate (4.17b)



General procedure **A** was used to couple **4.17a** (378 mg, 1.35 mmol) and *tert*-butyl *N*-allyl carbamate (276 mg, 1.75 mmol). Purified by flash chromatography (20 % EtOAc/hexanes) to yield 296 mg of the title compound. 70%. Clear oil. $R_f = 0.41$ (20 % EtOAc in hexanes; Ninhydrin/ Δ). ^1H NMR (300 MHz, CDCl_3) δ 7.90 (dd, $J = 8.4, 6.2$ Hz, 1H), 6.94 – 6.90 (m, 1H), 6.90 – 6.85 (m, 1H), 4.86 (s, 1H), 3.84 (s, 3H), 3.14 (q, $J = 6.2$ Hz, 2H), 3.00 – 2.89 (m, 2H), 1.77 (dd, $J = 14.7, 7.4$ Hz, 2H), 1.41 (s, 9H). ^{13}C NMR (75 MHz, CDCl_3) δ 166.81 (d, $J = 37.4$ Hz), 164.88 (d, $J = 253.7$ Hz), 161.91 (s), 156.27 (s), 147.68 (d, $J = 8.2$ Hz), 133.73 (d, $J = 9.2$ Hz), 117.84 (d, $J = 21.2$ Hz), 113.30 (d, $J = 21.5$ Hz), 79.19 (s), 52.19 (s), 40.39 (s), 32.24 (s), 31.86 (s), 28.60 (s).

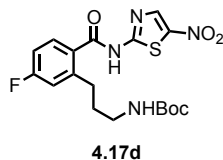
2-(3-((*tert*-Butoxycarbonyl)amino)propyl)-4-fluorobenzoic acid (4.17c)



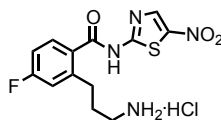
General procedure **C** was used to saponify **4.17b** (296 mg, 0.95 mmol). Extraction of the reaction mixture yielded 229 mg of the title compound. 81%. Oil. ^1H NMR (300 MHz,

CDCl_3) δ 10.25 (s, 1H), 8.09 – 8.00 (m, 2H), 6.93 (t, J = 8.9 Hz, 1H), 4.91 (s, 1H), 3.27 – 2.89 (m, 4H), 1.91 – 1.65 (m, 2H), 1.42 (s, 9H).

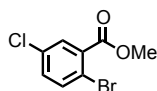
***tert*-Butyl (3-(5-fluoro-2-((5-nitrothiazol-2-yl)carbamoyl)phenyl)propyl)carbamate**
(4.17d)



General procedure **F** was used to couple **4.17c** (229 mg, 0.770 mmol) to 2-amino-5-nitrothiazole (167 mg, 1.16 mmol). Purified by flash chromatography (30 % EtOAc/hexanes) to yield 173 mg of the title compound. 53%. Light yellow solid. R_f = 0.42 (40 % EtOAc in hexanes; Ninhydrin/ Δ). ^1H NMR (600 MHz, DMSO-d_6) δ 13.55 (s, 1H), 8.71 (s, 1H), 7.73 – 7.70 (m, 1H), 7.28 (dd, J = 10.2, 2.5 Hz, 1H), 7.22 (td, J = 8.5, 2.6 Hz, 1H), 2.92 (q, J = 6.6 Hz, 2H), 2.80 – 2.75 (m, 2H), 1.65 (p, J = 7.0 Hz, 2H), 1.35 (s, 9H). ^{13}C NMR (151 MHz, DMSO-d_6) δ 168.29 (s), 163.98 (d, J = 249.2 Hz), 162.49 (s), 156.02 (s), 145.56 (d, J = 8.4 Hz), 143.08 (s), 142.53 (s), 131.79 (d, J = 9.1 Hz), 129.20 (s), 117.42 (d, J = 21.4 Hz), 113.30 (d, J = 21.7 Hz), 79.65 (s), 39.93 (s), 31.56 (s), 30.36 (s), 28.68 (s).

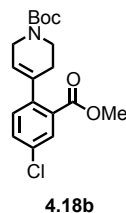
2-(3-Aminopropyl)-4-fluoro-N-(5-nitrothiazol-2-yl)benzamide hydrochloride (4.17)**4.17**

General procedure **G** was used to deprotect **4.17d** (173 mg, 0.41 mmol). Sublimation yielded 146 mg of the title compound. 99%. Light orange powder. ^1H NMR (800 MHz, DMSO- d_6) δ 13.60 (s, 1H), 8.71 (s, 1H), 7.76 (dd, J = 8.6, 5.8 Hz, 1H), 7.33 (dd, J = 10.1, 2.6 Hz, 1H), 7.25 (td, J = 8.4, 2.6 Hz, 1H), 2.86 – 2.82 (m, 2H), 2.77 (dq, J = 11.9, 5.8 Hz, 2H), 1.88 (p, J = 7.7 Hz, 2H). ^{13}C NMR (201 MHz, DMSO- d_6) δ 168.13 (s), 164.05 (d, J = 249.3 Hz), 162.47 (s), 144.73 (d, J = 8.5 Hz), 143.07 (s), 142.54 (s), 132.13 (d, J = 9.2 Hz), 129.05 (d, J = 2.6 Hz), 117.48 (dd, J = 21.6, 7.0 Hz), 113.65 (d, J = 21.7 Hz), 38.79 (d, J = 10.3 Hz), 29.88 (s), 28.98 (s). LCMS: t_R = 2.86; m/z = 325.1. HRMS m/z calc. for $\text{C}_{13}\text{H}_{14}\text{N}_4\text{O}_3\text{SF}$ ($\text{M}+\text{H}$), 325.0771; found, 325.0769.

Methyl 2-bromo-5-chlorobenzoate (4.18a)**4.18a**

General procedure **D** was used to esterify 2-bromo-5-chlorobenzoic acid (500 mg, 2.12 mmol) with acetyl chloride (7.06 mL) in MeOH (35.3 mL). Extraction of the reaction mixture yielded 526 mg of the title compound. Quant. Clear oil. ^1H NMR (300 MHz, CDCl_3) δ 7.67 (d, J = 2.4 Hz, 1H), 7.47 (d, J = 8.5 Hz, 1H), 7.23 – 7.12 (m, 1H), 3.85 (s, 3H).

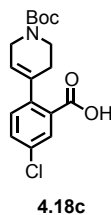
***tert*-Butyl 4-(4-chloro-2-(methoxycarbonyl)phenyl)-5,6-dihydropyridine-1(2*H*)-carboxylate (4.18b)**



General procedure **B** was used to couple **4.10a** (529 mg, 2.12 mmol) to *N*-Boc-1, 2, 3, 6-tetrahydropyridine-4-boronic acid pinacol ester (655 mg, 2.12 mmol). Purified by flash chromatography (10 % EtOAc/hexanes) to yield 77 mg of the title compound. 10%. Oil. R_f = 0.49 (20 % EtOAc in hexanes; Ninhydrin/ Δ). ^1H NMR (300 MHz, Chloroform- d) δ 7.81 (d, J = 2.3 Hz, 1H), 7.41 (dd, J = 8.2, 2.3 Hz, 1H), 7.13 (d, J = 8.2 Hz, 1H), 5.50 (tt, J = 3.0, 1.4 Hz, 1H), 4.01 (q, J = 2.8 Hz, 2H), 3.84 (s, 3H), 3.62 (t, J = 5.5 Hz, 2H), 2.30 (tt, J = 5.3, 2.5 Hz, 2H), 1.49 (s, 9H). ^{13}C NMR (75 MHz, CDCl_3) δ 166.90, 156.01, 142.61, 137.42, 133.13, 131.91, 131.21, 130.75, 130.23, 121.94, 79.80, 52.51, 43.61, 40.72, 30.31, 28.62.

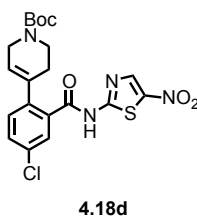
2-(1-(*tert*-Butoxycarbonyl)-1,2,3,6-tetrahydropyridin-4-yl)-5-chlorobenzoic acid

(4.18c)



General procedure **C** was used to saponify **4.18b** (77 mg, 0.22 mmol). Extraction of the reaction mixture yielded 62 mg of the title compound. 83%. Yellow oil. ^1H NMR (300 MHz, Chloroform- d) δ 9.33 (s, 1H), 7.94 (d, J = 2.1 Hz, 1H), 7.45 (ddd, J = 8.2, 2.3, 1.0 Hz, 1H), 7.15 (d, J = 8.2 Hz, 1H), 5.52 (t, J = 2.1 Hz, 1H), 4.02 (q, J = 2.6 Hz, 2H), 3.62 (t, J = 5.4 Hz, 2H), 2.33 (s, 2H), 1.49 (s, 9H). ^{13}C NMR (75 MHz, CDCl_3) δ 170.46, 155.42, 143.29, 137.50, 133.26, 132.61, 131.49, 130.93, 129.90, 121.69, 80.23, 43.64, 40.75, 30.39, 28.62.

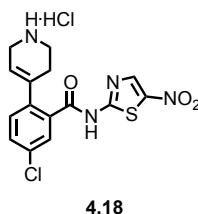
***tert*-Butyl 4-(4-chloro-2-((5-nitrothiazol-2-yl)carbamoyl)phenyl)-5,6-dihydropyridine-1(2*H*)-carboxylate (4.18d)**



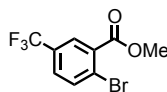
General procedure **F** was used to couple **4.18c** (62 mg, 0.18 mmol) to 2-amino-5-nitrothiazole (39.2 mg, 0.27 mmol). Purified by flash chromatography (35 %

EtOAc/hexanes) to yield 55 mg of the title compound. 66%. Light yellow solid. R_f = 0.64 (50 % EtOAc in hexanes; Ninhydrin/ Δ). ^1H NMR (600 MHz, DMSO- d_6) δ 13.57 (s, 1H), 8.68 (s, 1H), 7.75 (d, J = 2.3 Hz, 1H), 7.62 (dd, J = 8.3, 2.3 Hz, 1H), 7.42 (d, J = 8.3 Hz, 1H), 5.62 (s, 1H), 3.83 (q, J = 2.8 Hz, 2H), 3.43 (t, J = 5.6 Hz, 2H), 2.31 (s, 2H), 1.38 (s, 9H). ^{13}C NMR (151 MHz, DMSO) δ 167.54, 161.63, 153.78, 142.64, 142.15, 140.16, 134.46, 131.56, 130.95, 130.28, 128.02, 124.47, 79.17, 28.03.

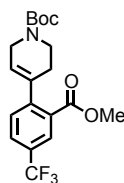
5-Chloro-*N*-(5-nitrothiazol-2-yl)-2-(1,2,3,6-tetrahydropyridin-4-yl)benzamide hydrochloride (4.18)



General procedure **G** was used to deprotect **4.18d** (44 mg, 0.09 mmol). Sublimation yielded 36.1 mg of the title compound. Quant. Orange solid. ^1H NMR (600 MHz, DMSO- d_6) δ 13.67 (s, 1H), 9.21 (s, 2H), 8.71 (d, J = 1.2 Hz, 1H), 7.82 (d, J = 2.3 Hz, 1H), 7.69 – 7.66 (m, 1H), 7.41 – 7.37 (m, 1H), 5.64 (dt, J = 3.3, 1.7 Hz, 1H), 3.61 (d, J = 4.2 Hz, 2H), 3.18 (q, J = 6.1, 4.7 Hz, 2H), 2.50 (d, J = 2.4 Hz, 2H). ^{13}C NMR (151 MHz, DMSO) δ 167.14, 161.71, 142.58, 142.19, 139.23, 134.58, 133.41, 132.06, 131.19, 130.35, 128.40, 120.34, 41.09, 40.06, 25.43. LCMS: t_R = 3.29; m/z = 365.1. HRMS m/z calc. for $\text{C}_{15}\text{H}_{14}\text{N}_4\text{O}_3\text{SCl}$ ($\text{M}+\text{H}$), 365.0475; found, 365.0469.

Methyl 2-bromo-5-(trifluoromethyl)benzoate (4.19a)**4.19a**

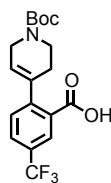
General procedure **I** was performed to oxidize 2-bromo-5-(trifluoromethyl)-benzaldehyde (750 mg, 2.96 mmol). The benzoic acid (718 mg, 2.67 mmol) was then esterified following general procedure **E** until complete by TLC analysis (24h). Purified by flash chromatography (15 % EtOAc/hexanes) to yield 524 mg of the title compound. 69%. Colorless oil. R_f = 0.65 (20 % EtOAc in hexanes). ^1H NMR (300 MHz, Chloroform- d) δ 8.01 (d, J = 2.2 Hz, 1H), 7.75 (d, J = 8.4 Hz, 1H), 7.52 (m, 1H), 3.92 (d, J = 0.6 Hz, 3H). ^{13}C NMR (75 MHz, CDCl_3) δ 165.35 (s), 135.34 (s), 132.88 (s), 130.20 (s), 129.76 (s), 128.72 (q, J = 62.25 Hz), 126.02 (s), 125.30 (s), 52.96 (s).

***tert*-Butyl 4-(2-(methoxycarbonyl)-4-(trifluoromethyl)phenyl)-5,6-dihydropyridine-1(2*H*)-carboxylate (4.19b)****4.19b**

General procedure **B** was used to couple **4.19a** (152.5 mg, 0.97 mmol) to *N*-Boc-1, 2, 3, 6-tetrahydropyridine-4-boronic acid pinacol ester (300 mg, 0.97 mmol). Purified by flash chromatography (15 % EtOAc/hexanes) to yield 160 mg of the title compound. 43%. Colorless oil. R_f = 0.40 (20 % EtOAc in hexanes; Ninhydrin/ Δ). ^1H NMR (300 MHz,

Chloroform-d) δ 8.12 – 8.08 (m, 1H), 7.69 (m, 1H), 7.37 – 7.28 (m, 1H), 5.57 – 5.52 (m, 1H), 4.03 (q, J = 2.8 Hz, 2H), 3.87 (d, J = 0.8 Hz, 3H), 3.64 (t, J = 5.5 Hz, 2H), 2.32 (td, J = 5.1, 2.4 Hz, 2H), 1.48 (s, 9H). ^{13}C NMR (75 MHz, CDCl_3) δ 166.92 (s), 155.12 (s), 147.76 (s), 137.52 (s), 130.62 (s), 130.11 (s), 130.01 (s), 129.57 (s), 128.03 (d, J = 111 Hz), 122.53 (s), 79.96 (s), 52.69 (s), 43.67 (s), 40.68 (s), 30.22 (s), 28.69 (s).

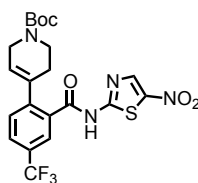
2-(1-(*tert*-Butoxycarbonyl)-1,2,3,6-tetrahydropyridin-4-yl)-5-(trifluoromethyl)benzoic acid (4.19c)



4.19c

General procedure **C** was used to saponify **4.19b** (160 mg, 0.42 mmol). Extraction of the reaction mixture yielded 133 mg of the title compound. 85%. Yellow oil. ^1H NMR (300 MHz, Chloroform-d) δ 9.43 (s, 1H), 8.23 (d, J = 2.1 Hz, 1H), 7.80 – 7.66 (m, 1H), 7.35 (d, J = 7.9 Hz, 1H), 5.67 – 5.48 (m, 1H), 4.06 (q, J = 2.8 Hz, 2H), 3.66 (t, J = 5.5 Hz, 2H), 2.44 – 2.31 (m, 2H), 1.49 (s, 9H). ^{13}C NMR (75 MHz, CDCl_3) δ 170.19 (s), 155.56 (s), 148.35 (s), 137.61 (s), 130.89 (s), 130.16 (s), 129.72 (s), 129.44 (s), 128.68 (q, J = 90.75 Hz), 122.23 (s), 80.50 (s), 43.72 (s), 40.76 (s), 30.29 (s), 28.69 (s).

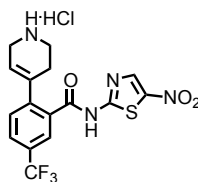
***tert*-Butyl 4-(2-((5-nitrothiazol-2-yl)carbamoyl)-4-(trifluoromethyl)phenyl)-5,6-dihydropyridine-1(2*H*)-carboxylate (**4.19d**)**



4.19d

General procedure **F** was used to couple **4.19c** (133 mg, 0.36 mmol) to 2-amino-5-nitrothiazole (78.4 mg, 0.54 mmol). Purified by flash chromatography (40 % EtOAc/hexanes) to yield 104 mg of the title compound. 60%. Yellow-orange gel. R_f = 0.54 (50 % EtOAc in hexanes; Ninhydrin/ Δ). ^1H NMR (600 MHz, DMSO- d_6) δ 13.65 (s, 1H), 8.69 (s, 1H), 8.05 (d, J = 1.8 Hz, 1H), 7.92 (dd, J = 8.3, 1.9 Hz, 1H), 7.63 (d, J = 8.1 Hz, 1H), 5.71 (s, 1H), 3.86 (q, J = 2.8 Hz, 2H), 3.46 (t, J = 5.6 Hz, 2H), 2.39 – 2.31 (m, 2H), 1.38 (s, 9H). ^{13}C NMR (75 MHz, Chloroform- d) δ 170.19 (s), 155.56 (s), 148.35 (s), 137.61 (s), 130.89 (s), 130.16 (s), 129.72 (s), 129.44 (s), 128.01 (dd, J = 32.2, 1.6 Hz), 122.23 (s), 80.50 (s), 43.72 (s), 40.76 (s), 30.29 (s), 28.69 (s).

***N*-(5-nitrothiazol-2-yl)-2-(1,2,3,6-tetrahydropyridin-4-yl)-5-(trifluoromethyl) benzamide hydrochloride (4.19)**



4.19

General procedure **G** was used to deprotect **4.19d** (94.1 mg, 0.18 mmol). Sublimation yielded 78 mg of the title compound. Quant. Dark orange powder. ^1H NMR (600 MHz, DMSO- d_6) δ 13.69 (s, 1H), 9.26 (s, 2H), 8.65 (d, J = 1.4 Hz, 1H), 8.07 (t, J = 1.5 Hz, 1H), 7.91 (dt, J = 8.2, 1.6 Hz, 1H), 7.54 (d, J = 8.1 Hz, 1H), 5.67 (td, J = 3.3, 1.6 Hz, 1H), 3.58 (s, 2H), 3.20 – 3.10 (m, 2H), 2.50 (m, 2H). ^{13}C NMR (151 MHz, DMSO) δ 167.23 (s), 161.87 (s), 144.44 (s), 142.51 (s), 142.12 (s), 134.68 (s), 132.60 (s), 129.61 (s), 128.04 (s), 126.80 (q, J = 339.75 Hz), 41.03 (s), 40.06 (s), 25.32 (s). LCMS: t_R = 3.44; m/z = 399.1. HRMS m/z calc. for $\text{C}_{16}\text{H}_{14}\text{N}_4\text{O}_3\text{SF}_3$ ($\text{M}+\text{H}$), 399.0739; found, 399.0727.

References

1. Ballard, T. E.; Wang, X.; Olekhnovich, I.; Koerner, T.; Seymour, C.; Salamoun, J.; Warthan, M.; Hoffman, P. S.; Macdonald, T. L. Synthesis and Antimicrobial Evaluation of Nitazoxanide-Based Analogues: Identification of Selective and Broad Spectrum Activity. *ChemMedChem* **2011**, *6*, 362-377.
2. Warren, C. A.; van Opstal, E.; Ballard, T. E.; Kennedy, A.; Wang, X.; Riggins, M.; Olekhnovich, I.; Warthan, M.; Kolling, G. L.; Guerrant, R. L.; Macdonald, T. L.; Hoffman, P. S. Amixicile, a Novel Inhibitor of Pyruvate:Ferredoxin Oxidoreductase, Shows Efficacy against *Clostridium difficile* in a Mouse Infection Model. *Antimicrob. Agents Chemother.* **2012**, *56*, 4103-4111.
3. Ballard, T. E.; Wang, X.; Olekhnovich, I.; Koerner, T.; Seymour, C.; Hoffman, P. S.; Macdonald, T. L. Biological activity of modified and exchanged 2-amino-5-nitrothiazole amide analogues of nitazoxanide. *Bioorg. Med. Chem. Lett.* **2010**, *20*, 3537-3539.
4. Kamatani, A.; Overman, L. E. A Suzuki Coupling Method for Directly Introducing a Protected β -Aminoethyl Group into Arenes and Alkenes. Convenient Synthesis of Phenethyl and Homoallylic Amines. *J. Org. Chem.* **1999**, *64*, 8743-8744.
5. Guo, W.; Li, J.; Fan, N.; Wu, W.; Zhou, P.; Xia, C. A simple and effective method for chemoselective esterification of phenolic acids. *Synth. Commun.* **2005**, *35*, 145-152.
6. Wieber, G. M.; Hegedus, L. S.; Akemark, B.; Michalson, E. T. Palladium (II)-assisted carboacylation of enamides to produce functionalized. beta.-amino acids. Synthesis of relays to (. -.)-thienamycin. *J. Org. Chem.* **1989**, *54*, 4649-4653.